NASA Tech Briefs

National Aeronautics and Space Administration

April 1988
Volume 12 Number 4

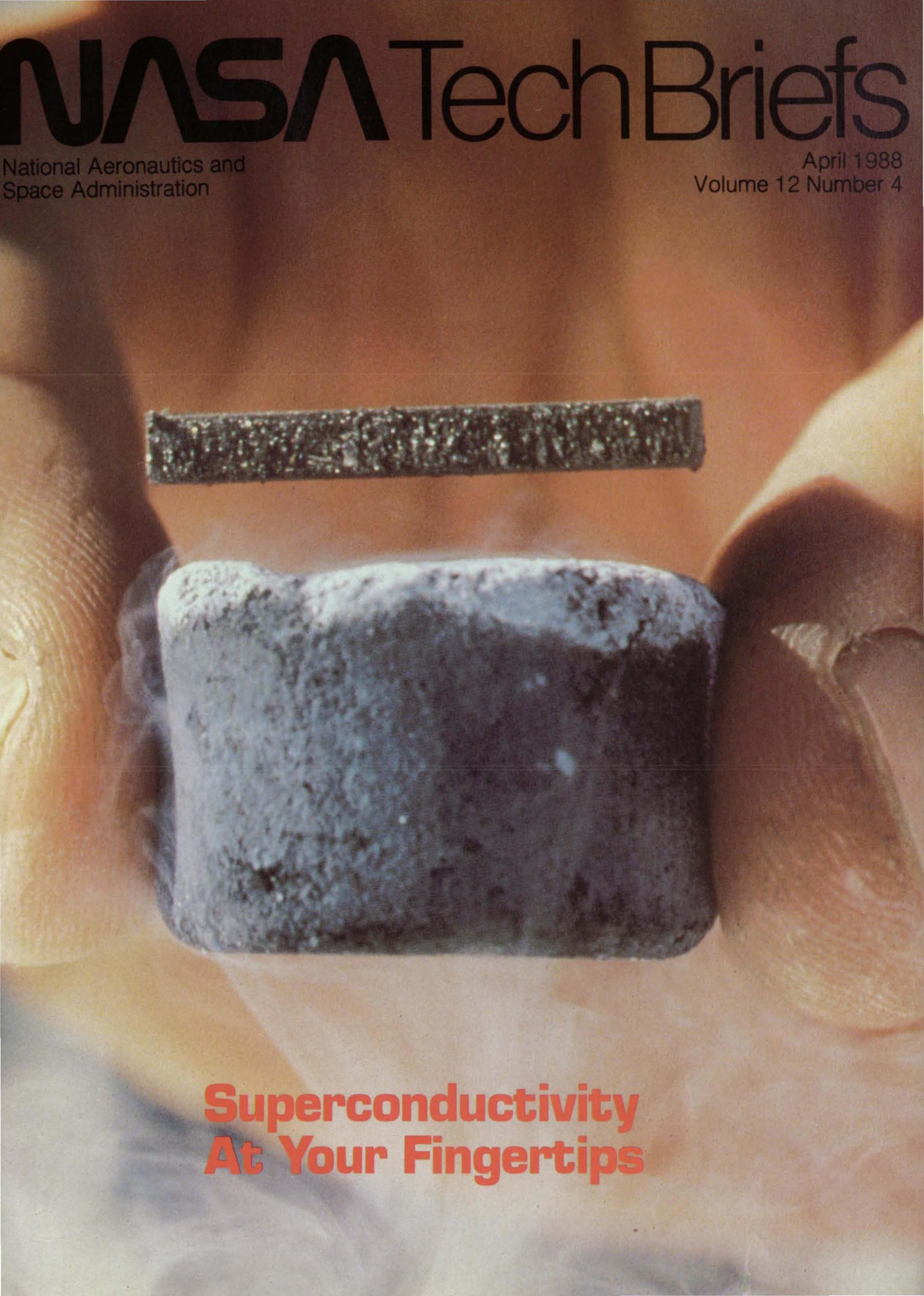

Superconductivity At Your Fingertips

The New 4180 Plug-In

SPEED TRIALS.

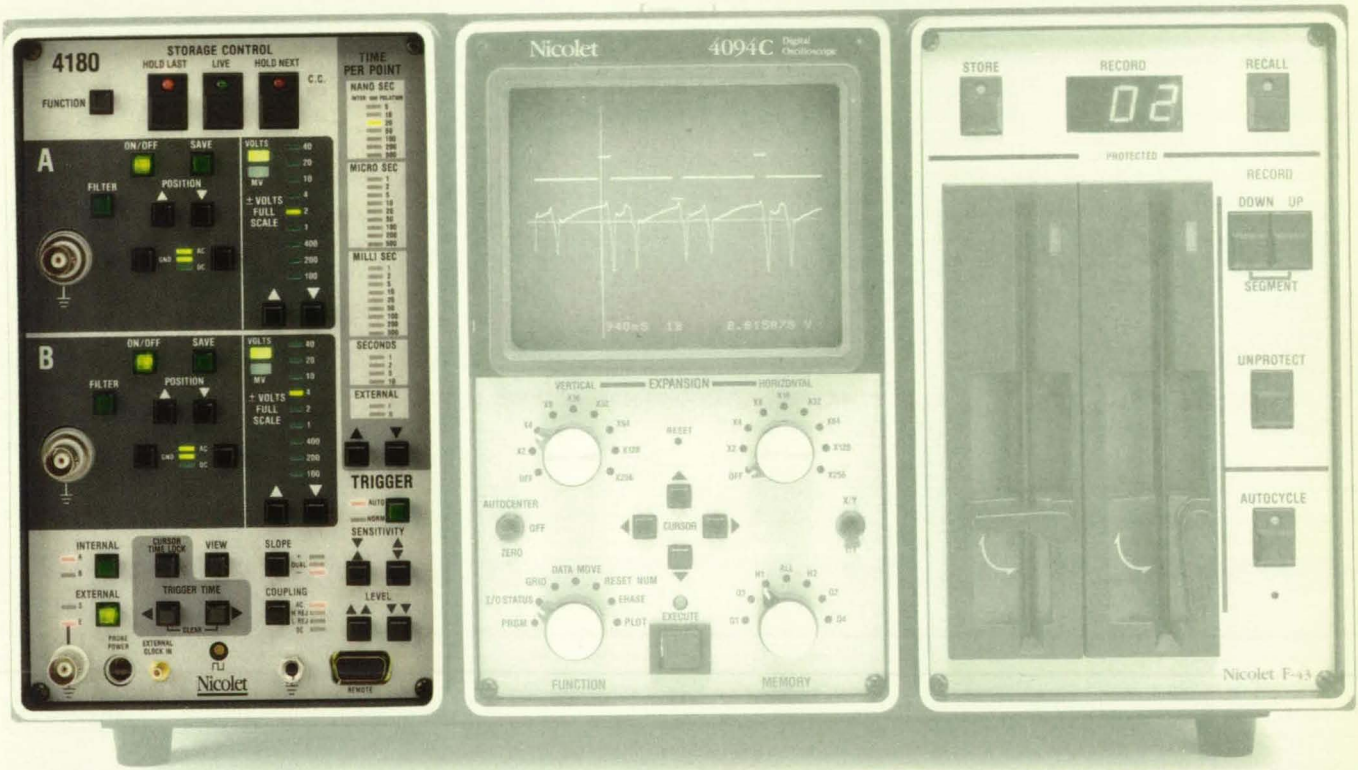

- ***Multi-channel: two or four channel configurations.***
- ***Unmatched single-shot capabilities.***
- ***High speed, 200 MHz digitizing.***
- ***100 MHz analog input bandwidth.***
- ***Real-time math functions.***

- ***For your Free Speed Trial call: 800-356-3090 or 608-273-5008***

Nicolet Test Instruments Division
P.O. Box 4288
5225-2 Verona Road
Madison, WI 53711-0288

Nicolet Digital Oscilloscopes

Speed. Using the latest designs in ADC technology, your input signal can be digitized at speeds up to 200 MHz (5ns per data point) and saved for analysis. The wide band input amplifiers allow signals up to the 100 MHz Nyquist limit to be input without distortion. Sophisticated trigger setup displays allow you to accurately set the level, sensitivity, and slope to make one-shot transients easy to catch; eliminating the usual hit or miss guesswork. For multi-channel applications two 4180's can operate together in one mainframe producing a four channel scope with no degradation in speed or performance.

Real-Time Math. In addition to the extensive post-processing capabilities in the mainframe, the 4180 has several useful routines which present computed results as live, real-time displays: *FFT, MAX/MIN, A+B, A−B, A×B, A/B,* and *AVERAGING.*

Nicolet
INSTRUMENTS OF DISCOVERY

Circle Reader Action No. 350

How does Heath Tecna prevent in-process distortion of the V-22's 40′ graphite longerons?

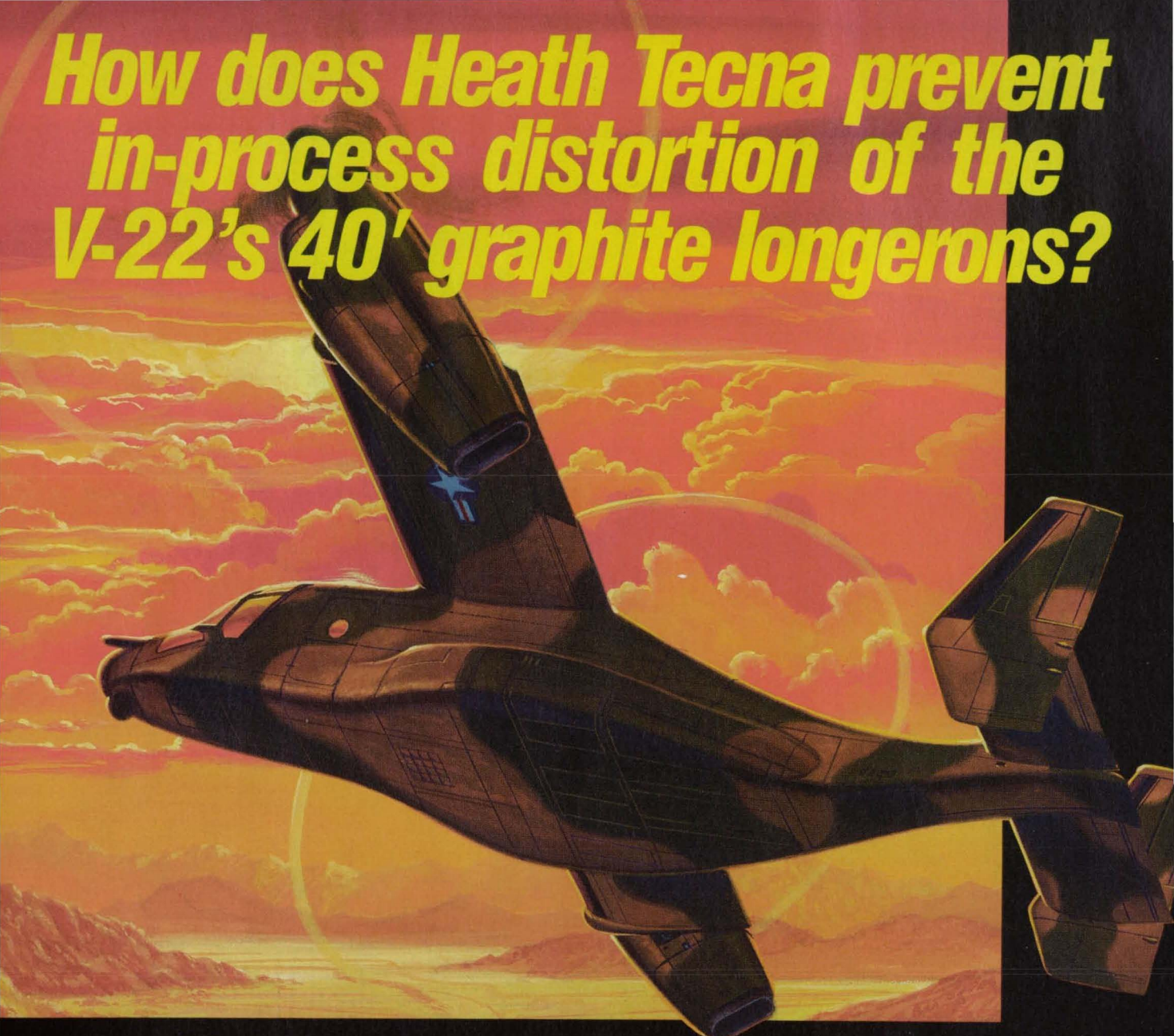

Hummingbird with talons.

Combine the high-altitude speed of a turbofan with the vertical lift power of a helicopter and you have the V-22 Osprey. A revolutionary bird requiring innovative builders.

Osprey's lightweight high strength begins with an advanced composites skeleton, with all-graphite longerons from Heath Tecna...highly-stressed, close tolerance, primary structures.

Go with the flow.

Mission: Control complex contours across remarkable dimensions (up to 40 feet long, yet under 200 mils thick and just 3″–4″ wide).

Challenge: Manage expansion and contraction during high pressure/temperature curing, which under the unyielding duress of an extremely rigid tool, could produce distorted shapes or internal voids.

Our answer: Discipline movement rather than attempt to eradicate it. Fabricate the layup mold of graphite composite similar to that of the longeron, so that the tool flexes across the same narrow range and at the same rate as the product itself.

Using material properties, rather than fighting them, resulted in closer tolerances and greater structural integrity.

Less paper, more loft.

Movement of paperwork behind the project was similarly disciplined. Transmittal of loft contours from Boeing required no paper. We translated the data from magnetic tape into Euclid surfaces and numerically-controlled CAM language. Result? Precise design control. And faster communications.

Big machines, better talent.

Heath Tecna had the resources to assign 80 employees to the FSD contract, including 21 tool makers at peak fabrication. And unique in-plant equipment, such as autoclaves up to 16′ wide and 43′ long, further distinguished us as an ideal member of the tiltrotor Osprey team.

Aide to Design Engineers

Call VP/Jim Martenson with your challenge, 206/872-7500 ext.116. Or circle the reader service number. We'll send a pocket slide guide comparing properties of composites with those of metal alloys.

Designers and fabricators of advanced composite structures ...for over 20 years.

HEATH TECNA AEROSPACE CO.

A CIBA-GEIGY Company

Technology that takes design capabilities to a whole new plane.

Advanced Composite Systems

Design Freedom. Like no other carbon fiber supplier, we can help you design beyond the limits of today's technology. Our advances in thermoplastic prepregs, for example, offer a whole new world of materials solutions for both aircraft and aerospace applications.

Advanced Properties. Our thermoplastic composite systems offer distinct new advantages. They're reformable. Require no refrigeration. Offer superior toughness in high temperature situations. And require a minimum of manufacturing time.

Strategic Advantages. We're currently the only U.S. based fully integrated manufacturer of carbon fibers. From precursor to prepregs we offer the security of totally domestic production at our Greenville, South Carolina plant. So if domestic fiber is as important to you as it is to us, evaluate our fibers for your next project.

Multidimensional Commitment. We are dedicated to all areas of composites technology: precursor, carbon fibers, and thermoset and thermoplastic resins. We've been on the leading edge of research and development for composites since the early 1960's. Our domestic plants are state-of-the-art, computer controlled facilities. And our technological support is second to none. Even one-on-one if that's what your project requires.

Call us. Ask questions. The earlier you involve us in the development process, the more solutions we can help you find. You can reach Amoco Performance Products, Customer Service at 1-800-222-2448.

We can help even your most advanced designs take off.

THE ALL AMERICAN SOLUTION

AMOCO

Amoco Performance Products

Circle Reader Action No. 336

NASA Tech Briefs

National Aeronautics and Space Administration

APRIL 1988
Volume 12 Number 4

ABP BPA

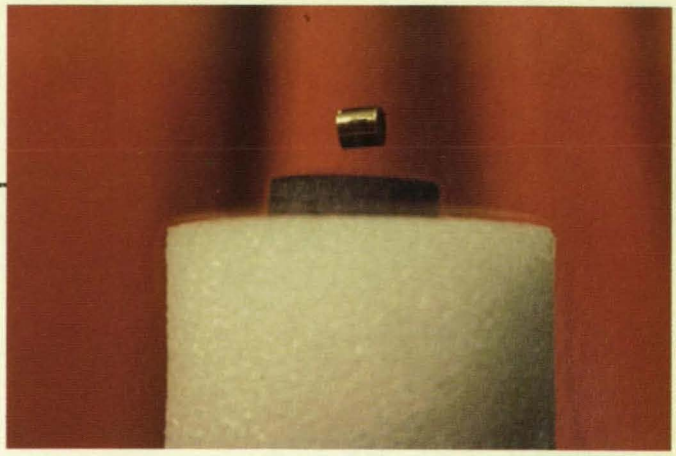

A rare earth magnet floats above a ceramic disk that has been cooled with liquid nitrogen to transform it into a superconducting state. The levitation arises from the strange electrical properties of the material. A magnetic field applied to a superconductor cannot penetrate it. If it could, it would create a current in the material, setting up an opposing magnetic force. Instead, the superconductor resists the magnetic field completely, which forces the magnet away. This phenomenon, known as the "Meissner Effect," may one day be used to suspend aircraft models during wind tunnel testing. See page 8.
Photo courtesy Fluoramics Inc., Upper Saddle River, NJ. Photography by George Stickles.

SPECIAL FEATURE

TECHNICAL SECTION

DEPARTMENTS

ON THE COVER—The discovery in 1986 of a new class of ceramic materials called high-temperature superconductors has galvanized the scientific community and spurred global competition for industrial applications. The superconductors lose all resistance to electricity at temperatures above 90 degrees Kelvin, a temperature easily reached using inexpensive liquid nitrogen rather than costly liquid helium. During the past year, NASA has begun studying potential superconductor applications to sensors, data and communications systems, and power and propulsion systems. What role will superconductors play in future space missions? Turn to page 8.
Photo courtesy HiTc Superconco, Lambertville, NJ.

NASA Tech Briefs, ISSN 0145-319X, USPS 750-070, copyright © 1988 in U.S., is published monthly except July/August and November/December (10x per year) by Associated Business Publications Co., Ltd. 41 E. 42nd St., New York, NY 10017-5391. The copyrighted information does not include the individual Tech Briefs which are supplied by NASA. Editorial, sales, production and circulation offices at 41 E. 42nd Street, New York, NY 10017-5391. Subscriptions for non-qualified subscribers in the U.S., Panama Canal Zone, and Puerto Rico, $75.00 for 1 year; $125.00 for 2 years; $200 for 3 years. Single copies $15.00. Remit by check, draft, postal or express orders. Other remittances at sender's risk. Address all communications for subscriptions or circulation to NASA Tech Briefs, 41 E. 42nd Street, New York, NY 10017-5391. Second-class postage paid at New York, NY and additional mailing offices.

POSTMASTER: please send address changes to NASA Tech Briefs, 41 E. 42nd Street, Suite 921, New York, NY 10017-5391.

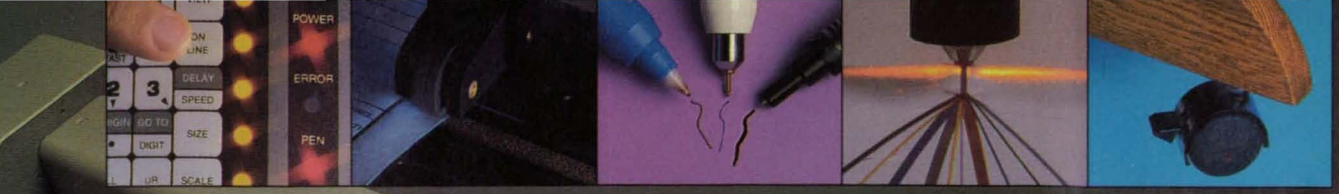

LP4000 with
Multi-pen Changer

Here's what to look for when you want great value

IOLINE plotters are designed to give you more flexibility and features for less cost than any other machine of their kind.

For example, our plotters draw not only on A through E sizes of media, but also plot on hundreds of in-between sizes from 1.5″×1.5″ up to 37″ wide roll stock. This saves you time and money by allowing you to make "check plots" on small, low-cost paper before committing to full-size media for final work.

It's easy also to set paper size, pen speed, micro-calibration, plot rotation—everything exactly as you want—by just tapping a few keys on the plotter's intelligent keypad. Plus, up to 3 sets of personalized defaults can be saved in its non-volatile memory.

They're fast, too. Our high-performance LP4000™ draws at speeds selectable up to 20 inches per second (ips) axially with .001″ resolution. For less demanding applications, our economical LP3700™ plots up to 10 ips axially with .0025″ resolution.

Another feature is compatibility. IOLINE plotters emulate both HP-GL and DM/PL plotter languages so they work with a host of software like AutoCAD, VersaCAD, and CADKEY, to name a few.

Furthermore, our Multi-pen Changer™ option holds up to 20 pens and, with our hyperBUFFER™ option, you can dramatically increase plotting throughput with intelligent vector sorting and compression buffering of up to 1MB of plot data.

Now here's the clincher: Our top-gun LP4000 costs just $5,495* less options. And there are other models priced even lower!

Why wait? Call us now at **1-206-775-7861.** Or, circle our reader service number and we'll gladly send you our brochure.

Remember, getting your money's worth—that's what IOLINE plotters are all about.

IOLINE™

LARGE-FORMAT PEN PLOTTERS

Circle Reader Action No. 472

IOLINE CORPORATION 19417-36TH AVE. W LYNNWOOD, WASH. 98036 (206) 775-7861 TELEX 4949856 IC UI FAX (206) 775-2818

LP4000, LP3700, Multi-pen Changer, and hyperBUFFER are trademarks of Ioline Corporation. AutoCAD is a registered trademark of Auto Desk Inc. VersaCAD is a registered trademark of T&W Systems. CADKEY is a registered trademark of MicroControl Systems, Inc. *Suggested U.S. List price.

AVAILABLE ON GSA CONTRACT

NASA Tech Briefs
National Aeronautics and Space Administration

ABP BPA

NASA Tech Briefs:

Published by ..... **Associated Business Publications**
Editor-in-Chief/Publisher ..... **Bill Schnirring**
Associate Publisher ..... **Frank Nothaft**
Associate Publisher ..... **Robin J. DuCharme**
Managing Editor ..... **R. J. Laer**
Associate Editor ..... **Joseph T. Pramberger**
Technical Advisor ..... **Dr. Robert E. Waterman**
Production Manager ..... **Rita Nothaft**
Traffic Manager ..... **James E. Cobb**
Circulation Director ..... **Anita Weissman**
Controller ..... **Neil B. Rose**
Awards Manager ..... **Evelyn Mars**
Reader Service Manager ..... **Arlene Berrios**

Technical Staff:
Briefs prepared for National Aeronautics and Space Administration by **Logical Technical Services Corp.**, NY, NY
Technical/Managing Editor ..... **Ted Selinsky**
Art Director ..... **Ernest Gillespie**
Administrator ..... **Elizabeth Texeira**
Chief Copy Editor ..... **Lorne Bullen**
Staff Editors ..... **Dr. James Boyd, Dr. Larry Grunberger, Jordan Randjelovich, George Watson, Oden Browne, Joseph Renzler, Dr. Theron Cole, Jr.**
Graphics ..... **Luis Martinez, Vernald Gillman, Charles Sammartano**
Editorial & Production ..... **Bill Little, Frank Ponce, Ivonne Valdes, Paul Marcus**

NASA:
NASA Tech Briefs are provided by the National Aeronautics and Space Administration, Technology Utilization Division, Washington, DC:
Administrator ..... **Dr. James C. Fletcher**
Assistant Administrator for Commercial Programs .... **James T. Rose**
Deputy Assistant Administrator (Programs) ..... **Henry J. Clarks**
Deputy Director TU Division (Publications Manager) .. **Leonard A. Ault**
Manager, Technology Utilization Office, NASA Scientific and Technology Information Facility ..... **Walter M. Helland**

Associated Business Publications
41 East 42nd Street, Suite 921, New York, NY 10017-5391
(212) 490-3999
President ..... **Bill Schnirring**
Executive Vice President ..... **Frank Nothaft**
Vice President Marketing ..... **Mark J. Seltman**

Advertising:
New York Office: (212) 490-3999 FAX (212) 986-7864
Sales Manager ..... **Robin DuCharme**
Regional Sales Manager (Mid-Atlantic & Midwest) ... **Michelle Larsen**
Marketing Research Manager ..... **Leo D. Kluger**
Advertising Coordination Manager ..... **Erving Dockery, Jr.**
Account Executives (Eastern MA, NH, ME, RI) ..... **Lee Arpin** at (617) 899-5613; **Bill Doucette** at (617) 278-7792
Account Executive (Western MA, CT, VT) ..... **George Watts** at (413) 596-4747
Account Executives (No. Calif., UT) ..... for Area Code 415—**Janice Richey King** and for Area Code 408—**Richard Cassidy** at (415) 656-3613
Account Executives (So. Calif., AZ, NV, NM) ..... for Area Codes 818/213/805—**Thomas Stillman** or **Dana Gindoff** and for Area Codes 619/714—**Leslie Alley** at (213) 541-4699

NTBM-Research Center
Project Director ..... **Mark J. Seltman**
Account Supervisor ..... **Lourdes Del Valle**

When the calls come from TDRSS, what will GE's experience in space mean to NASA's new ground terminal?

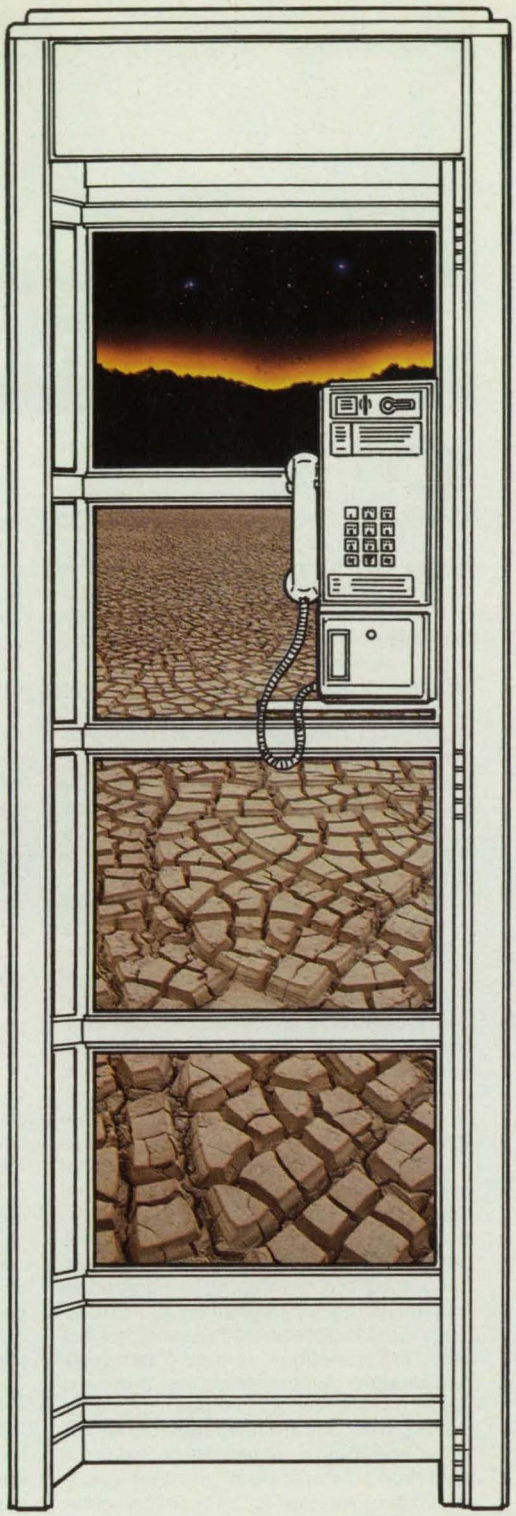

GE has been providing NASA with reliable space communications for more than 25 years.

Now there's a new challenge: In the desert near White Sands, New Mexico, NASA's Second TDRSS Ground Terminal (STGT) will soon be built to receive calls from space...

...*Critical* calls from space. And, that just happens to be a phase of space exploration where GE pioneered. That's why GE is competing to build STGT.

For instance, we were the earliest *user* of the first TDRSS. Through our involvement with Landsat, we have wide knowledge of TDRSS operational requirements.

Throughout our 25 years of experience, we've worked closely with the Goddard Space Flight Center. We've been a major NASA space network user. We are builders of satellites for NASA/NOAA. We build military and commercial satellites and subsystems. And we build and operate military, civilian, and commercial C^2 ground stations.

GE's corporate commitment to NASA continues with STGT. We understand the objectives of reliability, operability, maintainability *AND* low life cycle costs with 0.9999 availability.

STGT will play a key role in Earth/Space communications for years to come...and GE is committed to making 0.9999 availability a reality.

GE Aerospace

Ground Systems Department
Valley Forge, Pennsylvania

Circle Reader Action No. 583

STGT-2

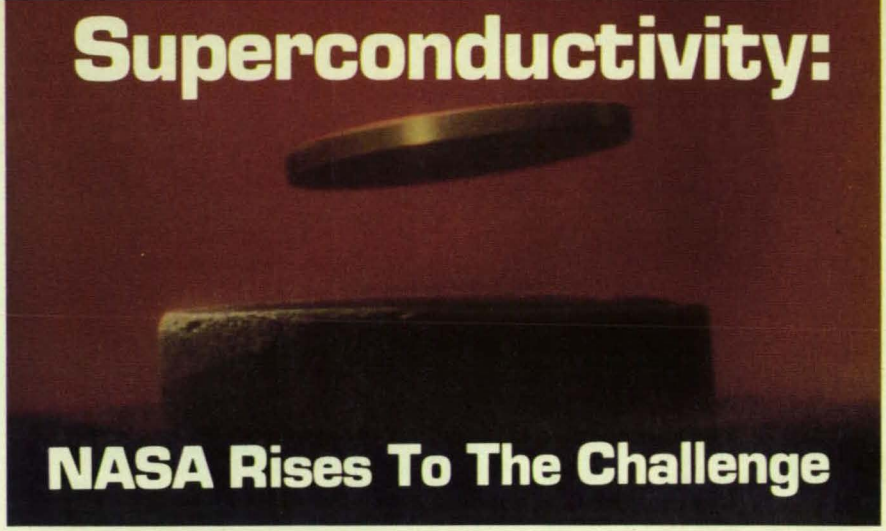

Superconductivity:

NASA Rises To The Challenge

Photo courtesy Fluoramics Inc. Photography by George Stickles.

Could high-temperature superconductors—ceramics that transmit electrical current without resistance—help power a manned mission to Mars? That's one possibility NASA is studying as part of an agency-wide effort to harness superconductivity for space use.

"There's been a lot of talk about how high-temperature superconductors are going to revolutionize everything from automobiles to dishwashers," said Dr. Martin Sokoloski, head of a coordinating group on superconductivity activities at NASA's Office of Aeronautics and Space Technology, "but what's been largely overlooked is the material's potential benefits for space. There are a variety of NASA-unique applications that could play an important role in future space missions."

Areas NASA has targeted for high-temperature superconductivity research include:

Sensors. NASA plans to use the new ceramics to improve the detection range of space-borne sensors. At NASA's Marshall Space Flight Center, research is focused on the development of ceramic thin-films for fabrication into a superconducting quantum interference device (SQUID), a highly sensitive magnetometer slated for use on future deep space gravity probes. A SQUID can measure weaker signals than traditional sensors because there is less background "noise" in its circuits, due to the free flow of electrons in the superconducting material.

Researchers at NASA's Jet Propulsion Laboratory are developing superconducting-insulating-superconducting (SIS) junctions for atmospheric remote sensing satellites. SIS junctions formed from high-temperature superconducting thin-films would be sensitive at ten times higher a frequency than current low-temperature versions, and could be radiatively cooled in the cold "room temperature" of outer space, eliminating the need for on-board cryogens. "That would mean lighter, more efficient satellites," said Dr. Carl Kukkonen, Director of the Center for Space Microelectronics Technology Directorate at Jet Propulsion Laboratories.

Power and Propulsion Systems. Both NASA's Lewis Research Center and the Department of Defense are studying the feasibility of using electrical power stored in superconducting coils to launch vehicles into orbit. Magnetic containment fields within the coils could store electricity by diverting it into endless loops, where it would circle forever, undiminished. If the amassed energy were discharged into a launching mechanism, it could conceivably propel a craft skyward. "High-temperature superconductors would reduce the energy requirements for an electromagnetic launcher because there would be no power loss during transmission," said Dr. Denis Connolly, Deputy Chief of Applied Research for the Lewis Center's Space Electronics Division.

Magnetic energy storage might also help extend mission duration, according to Dr. Charles Byvik, a Senior Research Physicist at NASA's Langley Research Center. "A superconducting magnetic energy storage system could generate ten times more energy than currently available from spacecraft batteries," he said. "The batteries we're now using are expensive and wouldn't provide the energy density required for long-duration manned flights, such as a Mars mission. Superconductivity could offer a cost-effective alternative."

Magnetic Suspension. Langley scientists want to use the strong magnetic field surrounding superconducting current to suspend and balance models in wind tunnels. "The traditional physical methods of suspension interfere with the flow field surrounding the model, which hampers our getting accurate test results," explained Dr. Byvik. "With magnetic levitation, we could eliminate this interference completely."

Space Shields. A high magnetic field created by a superconducting magnet and coil could be used to protect a spaceship from the intense heat of reentry, according to Dr. Connolly. "If we could arrange to generate this magnetic field around the front of the craft, it would act as a shield, keeping the hot ionizing gases at a distance."

A Long Road Ahead

Researchers must overcome a number of technical obstacles before any of these ideas reach fruition. High-temperature superconductors as they exist today can carry only small volumes of current, are too brittle to form into wires and other usable shapes, and lose their superconductive properties within a few months. In addition, there are problems unique to the space environment. "No one knows if these ceramics can handle the pressure in the high magnetic fields of space," said Dr. Eugene Urban, Chief of the Cryogenics Physics Branch at Marshall, "or if they can withstand bombardment by ionizing radiation."

"While we're excited about the potential for superconductors in space," said Dr. Urban, "we know there's a long, hard road ahead." □

First in a series of articles on Superconductivity.

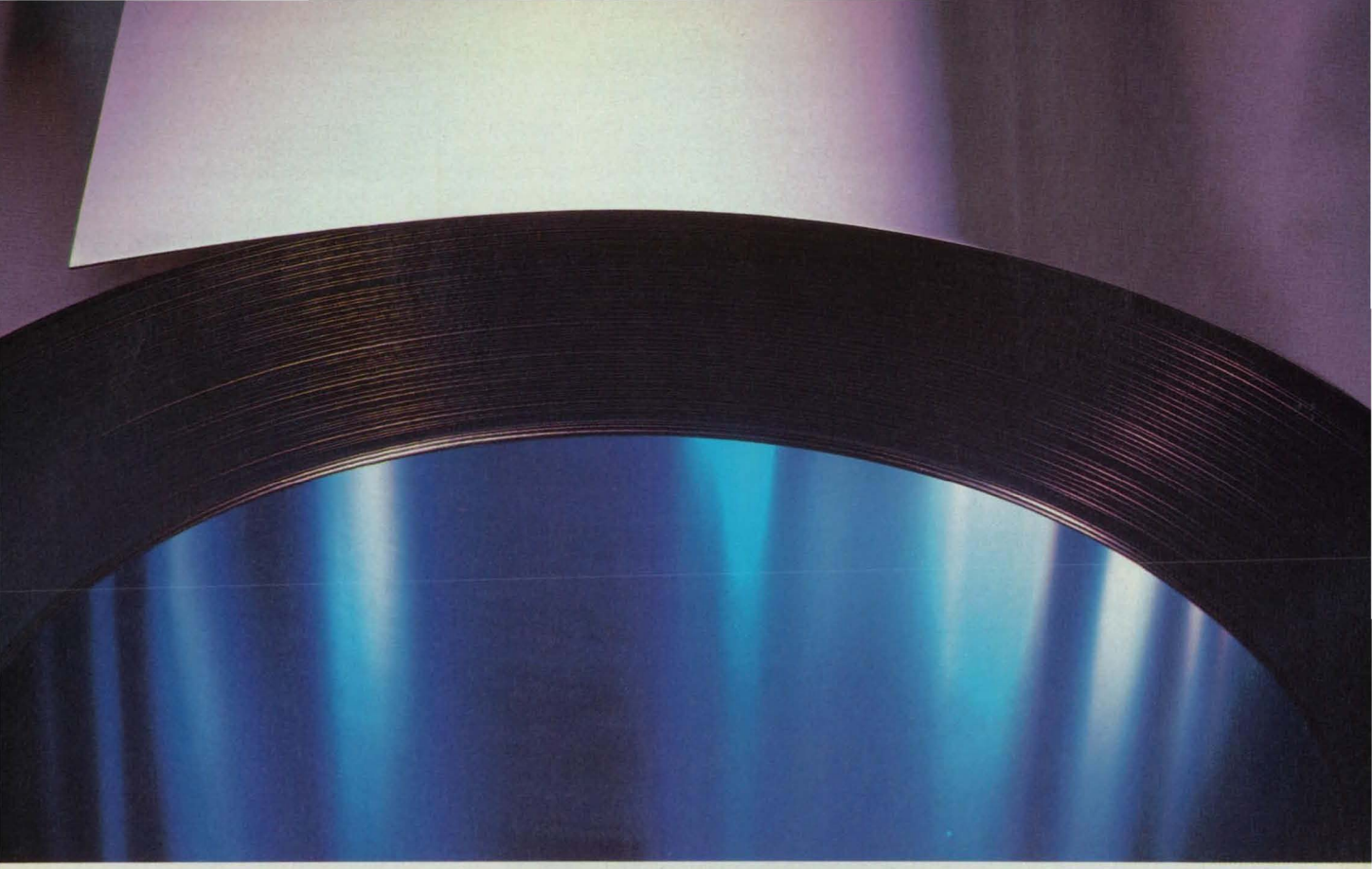

MORE HIGH-PERFORMANCE ALLOYS IN MORE FORMS. BECAUSE YOU KEEP FINDING MORE JOBS FOR THEM.

At Inco Alloys International, you'll find the world's widest selection of high-nickel alloys in the widest range of forms and sizes. Rod, bar, plate, sheet, strip, section, pipe, tubing, wire, and companion welding products. All from one full-line manufacturer, all available through a worldwide network of sales offices and distributor warehouses.

As the pioneers of nickel alloy technology, our scientists invented the alloys whose trademarks are synonymous with quality and performance —MONEL, INCONEL, INCOLOY, INCO, NIMONIC, BRIGHTRAY, and NILO.

These alloys offer superior corrosion resistance, high-temperature strength and other special properties for your most demanding applications, prolonging equipment life and preventing costly repair, replacement and downtime.

A single source for the properties and performance you need, in the forms you need, with the quality assurance and traceability you need, delivered where and when you need them. Inco Alloys International is the only name you need to know.

For a free copy of our "Quick Reference Guide," please write or call. In the U.S., Inco Alloys International, Inc., Huntington, West Virginia 25720. Telephone (304) 526-5388. Telex 886413. Telexfax (304) 526-5441. In Europe, Inco Alloys International Ltd., Wiggin Works, Hereford, England HR4 9SL. Telephone (0432) 272777. Telex 35101. Telefax (0432) 264030.

INCO ALLOYS INTERNATIONAL

New Product Ideas

New Product Ideas are just a few of the many innovations described in this issue of *NASA Tech Briefs* and having promising commercial applications. Each is discussed further on the referenced page in the appropriate section in this issue. If you are interested in developing a product from these or other NASA innovations, you can receive further technical information by requesting the TSP referenced at the end of the full-length article or by writing the Technology Utilization Office of the sponsoring NASA center (see page 12). NASA's patent-licensing program to encourage commercial development is described on page 12.

Rust Inhibitor and Fungicide for Cooling Systems

A mixture of benzotriazole, benzoic acid, and a fungicide prevents the growth of rust and fungus. This water-based cooling mixture made from readily available materials prevents the formation of metallic oxides and the growth of fungi in metallic pipes. The coolant is compatible with iron, copper, aluminum, and stainless steel. (See page 43).

Sublid Speeds Growth of Silicon Ribbon

A thermal barrier between the molten silicon and the lid of a susceptor and crucible allows a solidifying ribbon of silicon to be withdrawn faster. In one experimental system, the growth speed of a ribbon was increased by almost 50 percent. (See page 68).

Modified Withdrawal Slot Increases Silicon Production

A new shape for the slot through which single-crystal silicon ribbon is pulled from a melt increases productivity by 17.5 percent. The new configuration has made it easier to grow wider ribbons while maintaining uniform thickness and resulted in a record-size 17-m-long ribbon grown in a single pull. (See page 67).

Growing Wider Silicon Ribbons

Wider silicon ribbons can be grown by the dendritic-wed method with a proposed modification of the furnace lid by adding cross slots at the ends of the middle slot through which the ribbon is pulled. The modification would increase the size of the portion of the lid that limits the ribbon width by about 22 percent. (See page 66).

Dovetail Rotor Construction for Permanent-Magnet Motors

Rotor/stator-gap and eddy-current losses are reduced thanks to a new way of mounting magnets in permanent-magnet, electronically commutated, brushless dc motors. This change makes it possible to exploit the high torque and fast response characteristic of rare-earth-magnet motors. (See page 62).

Door Opens Four Ways

A proposed hinge system would allow a door to swing open on any of its four edges. The proposed system consists of four separable ball joints that resemble "pop-it" beads, one at each corner of the door. Made of molded plastic, the joints would be cheap to make and install. (See page 58).

NOVESPACE

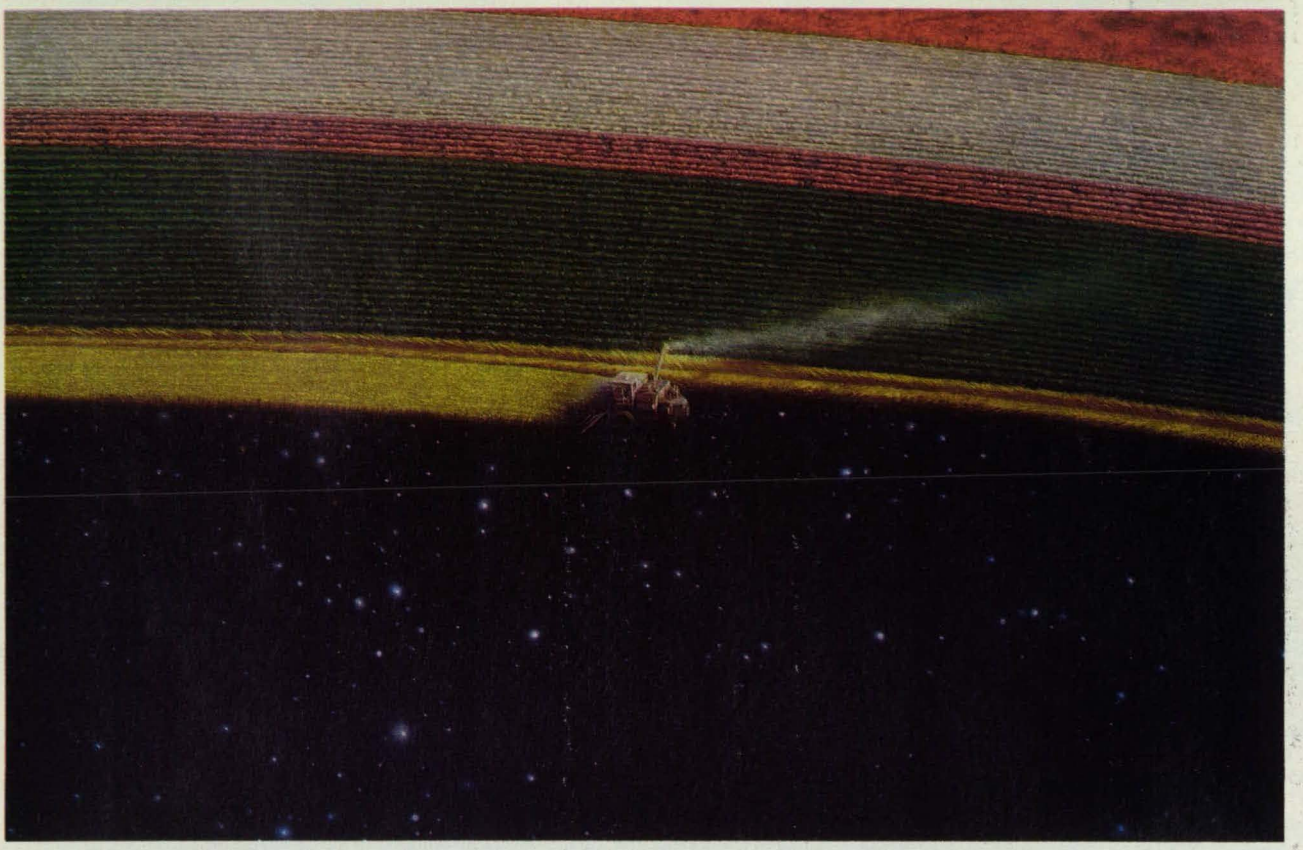

The Foremost Consultancy Company for the Transfer and Utilization of Space Technologies.

NOVESPACE main goal is to transfer technologies or products developed for space programs to non-space industries.
Therefore, **NOVESPACE**
Collects information about technologies or products available for transfer under the form of licenses or partnership agreements;
Edits a catalog of these technologies : MUTATIONS, published twice a year and sent to 20,000 executives around the world;
Is in touch with many innovative companies in France, in Europe; in Japan and in the USA;
Advises companies in negotiating agreements and in finding financial resources for transfers.

What we can do with your company :

We can look for the best partners or licensees in the European Community for your high-tech products.
We can work out marketing studies, financial schemes.
We can help in the negotiation of licensing, partnership or joint-venture agreements.
We can also propose you licenses for technologies, coming from several European aerospace companies, in sectors as varied as electronics, medical instrumentation, materials, optics, software etc.

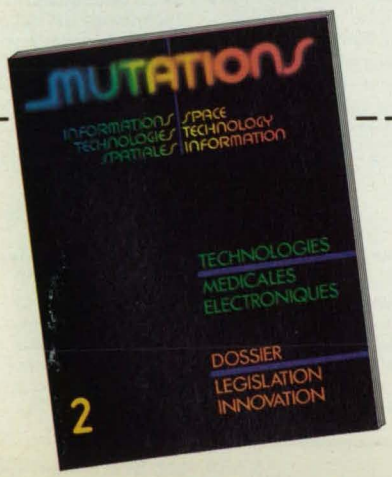

To receive more information about NOVESPACE and to get a free copy of our catalog « MUTATIONS », please fill this coupon.

NAME : _____ TITLE : _____

COMPANY NAME : _____

ADDRESS : _____

CITY : _____ COUNTRY / STATE : _____

ZIP CODE : _____ TEL NUMBER : _____

NOVESPACE

15, rue des Halles - 75001 PARIS - FRANCE - Tel. : 33 (1) 42.33.41.41 - Telex : 214 674

Circle Reader Action No. 554

HOW YOU CAN BENEFIT FROM NASA'S TECHNOLOGY UTILIZATION SERVICES

If you're a regular reader of TECH BRIEFS, then you're already making use of one of the low- and no-cost services provided by NASA's Technology Utilization (TU) Network. But a TECH BRIEFS subscription represents only a fraction of the technical information and applications/engineering services offered by the TU Network as a whole. In fact, when all of the components of NASA's Technology Utilization Network are considered, TECH BRIEFS represents the proverbial tip of the iceberg.

We've outlined below NASA's TU Network—named the participants, described their services, and listed the individuals you can contact for more information relating to your specific needs. We encourage you to make use of the information, access, and applications services offered by NASA's Technology Utilization Network.

How You Can Utilize **NASA's Industrial Applications Centers**—A nationwide network offering a broad range of technical services, including computerized access to over 100 million documents worldwide.

You can contact NASA's network of Industrial Applications Centers (IACs) for assistance in solving a specific technical problem or meeting your information needs. The "user friendly" IACs are staffed by technology transfer experts who provide computerized information retrieval from one of the world's largest banks of technical data. Nearly 500 computerized data bases, ranging from NASA's own data base to Chemical Abstracts and INSPEC, are accessible through the nine IACs located throughout the nation. The IACs also offer technical consultation services and/or linkage with other experts in the field. You can obtain more information about these services by calling or writing the nearest IAC. User fees are charged for IAC information services.

Aerospace Research Applications Center (ARAC)
Indianapolis Center for Advanced Research
611 N. Capitol Avenue
Indianapolis, IN 46204
Dr. F. Timothy Janis, Director
(317) 262-5036

Central Industrial Applications Center/NASA (CIAC)
Southeastern Oklahoma State U.
Station A, Box 2584
Durant, OK 74701
Dickie Deel, Acting Director
(405) 924-6822

North Carolina Science and Technology Research Center (NC/STRC)
Post Office Box 12235
Research Triangle Park, NC 27709
J. Graves Vann, Jr., Director
(919) 549-0671

NASA Industrial Applications Ctr. 823 William Pitt Union
University of Pittsburgh
Pittsburgh, PA 15260
Paul A. McWilliams, Exec. Director
(412) 648-7000

NASA/Southern Technology Applications Center
P. O. Box 24
Progress Ctr., One Progress Blvd.
Alachua, FL 32615
J. Ronald Thornton, Director
(904) 462-3913
(800) 354-4832 (FL only)
(800) 225-0308 (toll-free US)

NASA/UK Technology Applications Center
University of Kentucky
109 Kinkead Hall
Lexington, KY 40506-0057
William R. Strong, Director
(606) 257-6322

NERAC, Inc.
One Technology Drive
Tolland, CT 06084
Daniel U. Wilde, President
(203) 872-7000

Technology Application Center (TAC)
University of New Mexico
Albuquerque, NM 87131
Stanley A. Morain, Director
(505) 277-3622

NASA Industrial Applications Center (WESRAC)
University of Southern California
Research Annex
3716 South Hope Street, Room 200
Los Angeles, CA 90007
Radford G. King, Acting Director
(213) 743-8988
(800) 642-2872 (CA only)
(800) 872-7477 (toll-free US)

NASA/SU Industrial Applications Center
Southern University Department of Computer Science
Baton Rouge, LA 70813
John Hubbell, Director
(504) 771-2060

If you represent a public sector organization with a particular need, you can contact NASA's Application Team for technology matching and problem solving assistance. Staffed by professional engineers from a variety of disciplines, the Application Team works with public sector organizations to identify and solve critical problems with existing NASA technology. **Technology Application Team, Research Triangle Institute, P.O. Box 12194, Research Triangle Park, NC 27709. *Doris Rouse, Director,* (919) 541-6980**

How You Can Access Technology Transfer Services At NASA Field Centers:

Technology Utilization Officers & Patent Counsels—Each NASA Field Center has a Technology Utilization Officer (TUO) and a Patent Counsel to facilitate technology transfer between NASA and the private sector.

If you need further information about new technologies presented in *NASA Tech Briefs*, request the Technical Support Package (TSP). If a TSP is not available, you can contact the Technology Utilization Officer at the NASA Field Center that sponsored the research. He can arrange for assistance in applying the technology by putting you in touch with the people who developed it. If you want information about the patent status of a technology or are interested in licensing a NASA invention, contact the Patent Counsel at the NASA Field Center that sponsored the research. Refer to the NASA reference number at the end of the Tech Brief.

Ames Research Ctr.
Technology Utilization Officer: Laurance Milov
Mail Code 223-3
Moffett Field, CA 94035
(415) 694-6471
Patent Counsel: Darrell G. Brekke
Mail Code 200-11
Moffett Field, CA 94035
(415) 694-5104

Lewis Research Center
Technology Utilization Officer: Daniel G. Soltis
Mail Stop 7-3
21000 Brookpark Road
Cleveland, OH 44135
(216) 433-5567
Patent Counsel: Gene E. Shook
Mail Code 301-6
21000 Brookpark Road
Cleveland, OH 44135
(216) 433-5753

National Space Technology Laboratories
Technology Utilization Officer: Robert M. Barlow
Code GA-00
NSTL Station, MS 39529
(601) 688-1929

John F. Kennedy Space Center
Technology Utilization Officer: Thomas M. Hammond
Mail Stop PT-TPO-A
Kennedy Space Center, FL 32899
(305) 867-3017
Patent Counsel: James O. Harrell
Mail Code PT-PAT
Kennedy Space Center, FL 32899
(305) 867-2544

Langley Research Ctr.
Technology Utilization Officer: John Samos
Mail Stop 139A
Hampton, VA 23665
(804) 865-3281
Patent Counsel: George F. Helfrich
Mail Code 279
Hampton, VA 23665
(804) 865-3725

Goddard Space Flight Center
Technology Utilization Officer: Donald S. Friedman
Mail Code 702
Greenbelt, MD 20771
(301) 286-6242
Patent Counsel: R. Dennis Marchant
Mail Code 204
Greenbelt, MD 20771
(301) 286-7351

Jet Propulsion Lab.
Technology Utilization Mgr.: Norman L. Chalfin
Mail Stop 156-211
4800 Oak Grove Drive
Pasadena, CA 91109
(818) 354-2240
NASA Resident *Technology Utilization Officer: Gordon S. Chapman*
Mail Stop 180-801
4800 Oak Grove Drive
Pasadena, CA 91109
(818) 354-4849
Patent Counsel: Paul F. McCaul
Mail Code 180-801
4800 Oak Grove Drive
Pasadena, CA 91109
(818) 354-2734

George C. Marshall Space Flight Center
Technology Utilization Officer: Ismail Akbay
Code AT01
Marshall Space Flight Center,
AL 35812
(205) 544-2223
Patent Counsel: Leon D. Wofford, Jr.
Mail Code CC01
Marshall Space Flight Center,
AL 35812
(205) 544-0024

Lyndon B. Johnson Space Center
Technology Utilization Officer: Dean C. Glenn
Mail Code EA4
Houston, TX 77058
(713) 483-3809
Patent Counsel: Edward K. Fein
Mail Code AL3
Houston, TX 77058
(713) 483-4871

NASA Headquarters
Technology Utilization Officer: Leonard A. Ault
Code IU
Washington, DC 20546
(202) 453-1920
Assistant General Counsel for Patent Matters: Robert F. Kempf, Code GP
Washington, DC 20546
(202) 453-2424

A Shortcut To Software: **COSMIC®**— For software developed with NASA funding, contact COSMIC, NASA's Computer Software Management and Information Center. New and updated programs are announced in the Computer Programs section. COSMIC publishes an annual software catalog. For more information call or write: **COSMIC®**, 382 East Broad Street, Athens, GA 30602 *John A. Gibson, Dir.,* (404) 542-3265

If You Have a Question . . . **NASA Scientific & Technical Information Facility** can answer questions about NASA's Technology Utilization Network and its services and documents. The STI staff supplies documents and provides referrals. Call, write or use the feedback card in this issue to contact: **NASA Scientific and Technical Information Facility,** Technology Utilization Office, P.O. Box 8757, Baltimore, MD 21240-0757. *Walter M. Heiland, Manager,* (301) 859-5300, Ext. 242, 243

Check coupon for FREE BROCHURE "Fun with Superconductors"

FLUORAMICS, INC. IS PROUD TO ANNOUNCE

SUPERCONDUCTORS FOR SALE

HISTORY WAS MADE THIS YEAR AND YOU CAN BE PART OF IT!

Who would ever have expected that a black ceramic material would revolutionize the world of science and be the source of a whole new class of superconductors?

NOW FOR THE FIRST TIME IN THE HISTORY OF SCIENCE

When the first reports describing these amazing ceramic superconductors appeared, our research director followed them with great interest. The equipment and skills required fit our lab to a tee. Now, after months of intensive work, we would like to make the results of our efforts available. Experimentors who would like to evaluate the new superconductors but don't have the time, personnel or facilities to make them, can now go to work. A multitude of applications will no doubt appear. All you need is a bottle of Liquid Nitrogen and the usual electronic skills.

Good luck, we hope you get lots of patents and find dozens of applications for this new remarkable technology.

EACH SUPERCONDUCTOR TESTED BY THE SCIENTIST WHO MADE IT

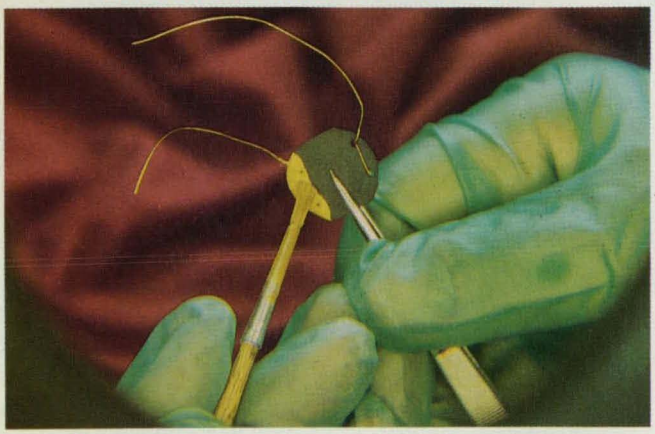

Each Fluoramics' superconductor is carefully drilled with 4 holes. Copper wire is threaded in place. Conductive silver paste is hand-painted to assure uniform area contact. Meissner levitation and transition curves are run on representative samples from each lot.

A ceramic with zero electrical resistance? See for yourself!

As the temperature is lowered, the superconductor's resistance drops slowly until about 90° kelvin (that's -280° below zero farenheit—very hot in the world of superconductors). Then it falls as if on a ride over Niagara Falls in a barrel . . . to zero ohms or nearly so (77° kelvin or -320° F Liquid Nitrogen Temperature).

A SPECTACULAR SIGHT! A small cobalt samarium magnet resting on its surface will magically float up and levitate at the same time, demonstrating the Meissner effect.

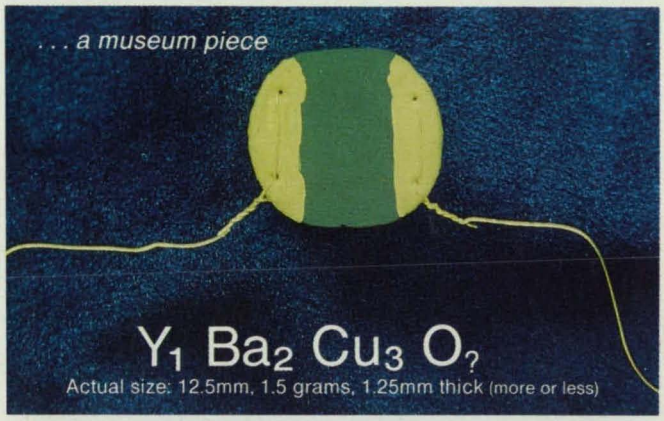

HERE'S WHAT YOU'LL SEE

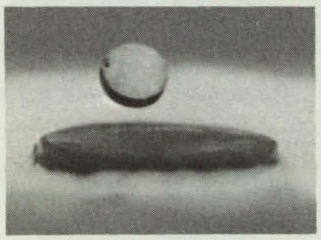

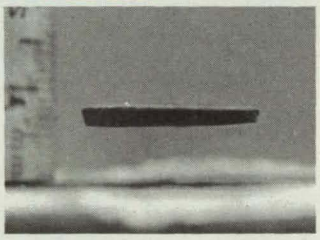

THE MEISSNER EFFECT

A rare earth magnet levitates over Fluoramics' superconductor that's been cooled with Liquid Nitrogen.

A superconductor floats ¼" or more over a nest of 4 magnets. It'll stay up about 30 seconds before it warms and settles.

TYPICAL SUPERCONDUCTOR TRANSITION CURVE
$Y_1\ Ba_2\ Cu_3\ O_?$ CERAMIC

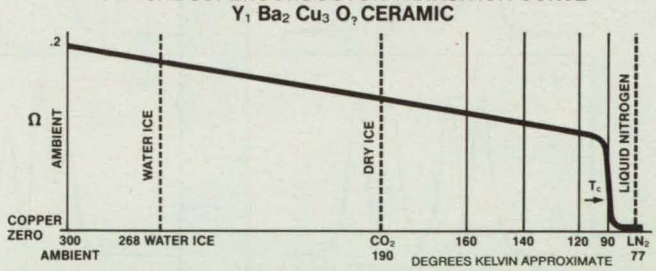

PLEASE SEND A.S.A.P.

TO ORDER:
CALL TOLL FREE
1-800-922-0075
OR SEND IN THE ORDER FORM BELOW

Limited Quantity

Laboratory test superconductors for the introductory price of . .

18K Gold Wire Painted Gold Electrodes	Copper Wire Painted Silver Electrodes	Rare Earth Magnets
____ (1) $100.00	____ (1) $ 95.00	____ (1) small disc $25.00 each
____ (2) $150.00	____ (2) $142.50	
____ (3) $170.00	____ (3) $165.50	
____ (2) $100.00	No electrode blanks for Meissner Effect	
____	FREE BROCHURE "Fun with Superconductors"	

Call for volume prices.

Fluoramics, Inc. N-188
103 Pleasant Avenue
Upper Saddle River, N.J. 07458

My check or money order for $ ____ is enclosed
Charge my credit card:
☐ Am.Express ☐ MasterCard ☐ Visa

Card No. _____
Exp. Date _____
P.O. # _____
Name _____
Address _____
City _____
State _____ Zip _____

(N.J. residents please add 6% sales tax.)

Circle Reader Action No. 541

See NASA Tech Briefs for our award-winning ads of 1986 and 1987 "TUFOIL, The Transistor of Lubrication"

Electronic Components & Circuits

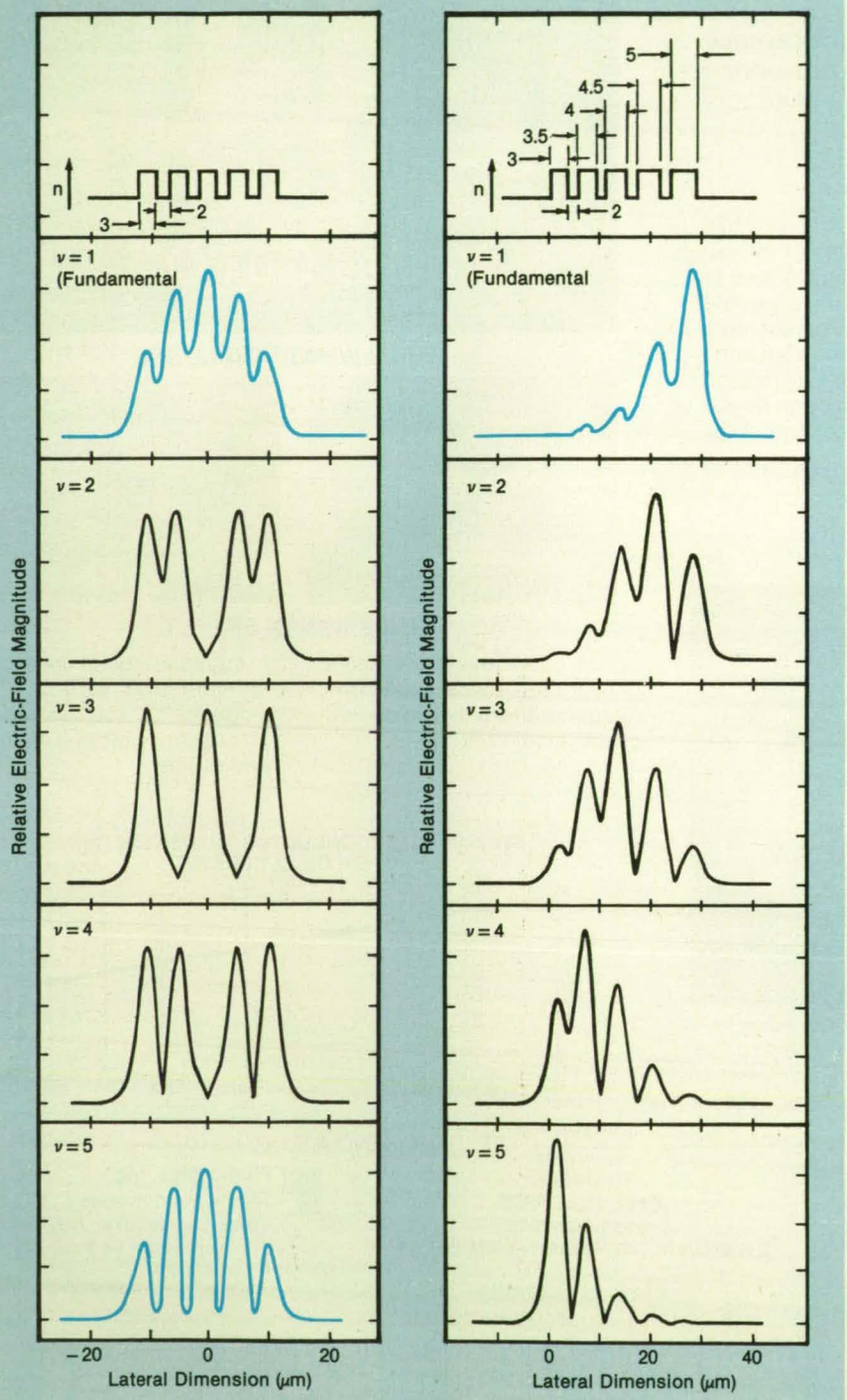

Note: ν = Supermode order.
Wavelength = 0.9 μm.
n = index of refraction = 3.4149 in diodes and 3.4118 between diodes.

Diode-Laser Array Suppresses Extraneous Modes

Diode parameters are varied to shape the output beam.

NASA's Jet Propulsion Laboratory, Pasadena, California

An array of phase-locked GaAs/GaAlAs diode lasers produces a light beam with one main radiation lobe. The physical parameters of the laser diodes differ from each other in a way that favors oscillation in the fundamental supermode while suppressing oscillation in the higher-order modes.

The term "supermode" denotes the electromagnetic mode of the array, as distinguished from the modes that each diode would exhibit if operated in isolation from the others. Oscillation in the fundamental supermode is necessary to obtain a diffraction-limited beam with one lobe and minimal spectral width.

Ordinarily, a phase-locked array of laser diodes produces several supermodes at once, resulting in a relatively broad far-field radiation pattern and a wide spectrum. The supermodes of higher order can be suppressed if the laser gain is varied among the diodes in a pattern that resembles the envelope of the near-field amplitude pattern of the fundamental supermode.

This strategy does not work, however, if the envelope of a higher supermode resembles that of the fundamental. In such a case, the gain pattern would favor both modes. By purposely making the diodes differ in width or spacing or both (see figure), one can introduce appreciable differences in pattern between the fundamental and higher supermodes. In this arrangement, a proper gain distribution will emphasize the fundamental supermode

In an **Array of Identical Laser Diodes** (left), the gain or amplitude pattern is similar in the fundamental and fifth-order supermodes. However, in an array of nonidentical diodes (right), the envelopes of the supermodes of higher order differ appreciably from that of the fundamental.

and the main radiation lobe. The gains of the individual laser diodes therefore are made independently adjustable. Another way to emphasize the fundamental supermode is to place a stripe contact above the position corresponding to the peak of the gain envelope in that mode.

This work was done by Elyahou Kapon, Chris P. Lindsey, Joseph Katz, Shlomo Margalit, and Amnon Yariv of Caltech for **NASA's Jet Propulsion Laboratory**. *For further information, Circle 10 on the TSP Request Card.*

In accordance with Public Law 96-517, the contractor has elected to retain title to this invention. Inquiries concerning rights for its commercial use should be addressed to

Edward Ansell,
Director of Patents and Licensing
Mail Stop 301-6
California Institute of Technology
1207 East California Boulevard
Pasadena, CA 91125

Refer to NPO-16465, volume and number of this NASA Tech Briefs *issue, and the page number.*

Multiple-Feed Design for DSN/SETI Antenna

Frequency bands are changed with little interruption of operation.

NASA's Jet Propulsion Laboratory, Pasadena, California

A modification of the feedhorn mounting on an existing 34-m-diameter antenna in the Deep Space Network (DSN) would enable the antenna to be shared by the Search for Extra-Terrestrial Intelligence (SETI) program with minimal interruption of DSN spacecraft tracking. The modified antenna concept may also be useful in terrestrial communication systems that require frequent changes of operating frequencies.

Seven feedhorns, each covering a 1.4-to-1 frequency range, are required to cover the 1- to 10-GHz frequency range, which is of interest in the SETI program. There appears to be no practical way to mount all seven horns simultaneously without causing undesirable asymmetries in the radiation pattern of the antenna. For-

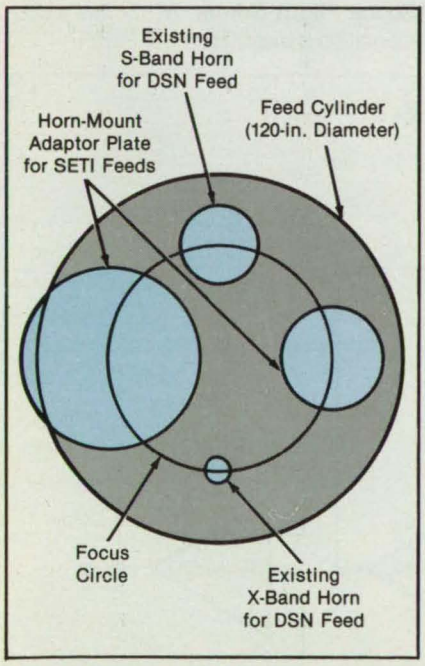

The **Modified Feedcone of the Antenna** would include modular adapter plates to enable the mounting of one or two of seven different SETI feedhorns at one time without interfering with two permanently mounted S-and X-band feedhorns used for DSN. One SETI feedhorn could be in use while the second was being installed, maintained, or tested.

tunately, SETI plans call for using only one frequency band at a time, perhaps for several weeks or months continuously.

For the modified system, the feedcone would be converted to a cylinder 120 in. (3.05 m) in diameter, large enough to contain the feedcones in use and to eliminate unnecessary lengths of waveguides. At any given time, one or two out of the seven SETI plug-in feedhorn-and-waveguide assemblies would be mounted. The two existing DSN feedhorns and their associated waveguides would be permanently mounted (see figure).

Switching between DSN and SETI feedhorns would take only a few minutes. The DSN and SETI feed systems would be independent of each other so that modifications to one would not affect the other, an important consideration in guaranteeing the operational integrity of the DSN. The phase centers of all the horns would be located on a circle centered on the axis of the main reflector paraboloid. This circular arrangement enables the use of a rotating subreflector to switch from horn to horn without shifting the aim of the antenna. (Such a subreflector system has been used successfully in a 64-m antenna.)

Calculations of gain divided by system noise temperature, a figure of merit, show that best performance would occur at 3.24 GHz and 90-degree antenna elevation. The expected degradation from that level of performance is less than 3 dB for each of the seven feedhorns at elevations of 20 degrees or higher.

This work was done by S. D. Slobin and D. A. Bathker of Caltech for **NASA's Jet Propulsion Laboratory**. *For further information, Circle 23 on the TSP Request Card. NPO-16883*

Electrically-Isolating Analog Amplifier

Signals can be transmitted between units at different ground potentials.

Goddard Space Flight Center, Greenbelt, Maryland

An analog amplifier electrically isolates its input from its output through the use of optoelectronic components. Such a circuit may be useful in most spacecraft electronic systems, where there is a need to isolate signal grounds from power grounds. Similarly, in a typical power-conditioning circuit, there is a need to transfer a signal voltage from a circuit grounded to the supply voltage to a circuit grounded to the return of the supply voltage. Although differential amplifiers can be used for this purpose, constraints on dc impedance between grounds or limitations on common-mode voltages can restrain their use.

The circuit (see figure) includes a dual-phototransistor optoisolator (MCT6 or equivalent). The device must be selected for a matched pair. The incoming signal voltage is converted to a current (I_1) by operational amplifier IC_1 connected as a transconductance amplifier with transconductance determined by the inverse of resistor R_1.

The current I_1 is fed as an input to one of the phototransistors in the optoisolator, which in turn causes a current I_2 to flow through R_2 and establishes a voltage proportional to the incoming signal voltage. This voltage is then fed to a second operational amplifier (IC_2), which in turn drives a current I_3 into input of the second phototransistor in the optoisolator.

The output current of the second transistor, I_4, which is proportional to I_3, is then used to close the loop by comparison of the voltage induced by I_4 across resistor R_4 with that of the voltage across R_2. Because of the matching of the components in the optoisolator, the current I_3 equals the current I_1, and the corresponding voltage across R_3 equals the input voltage.

The voltage across R_3 can be buffered by a third operational amplifier (IC_3) to provide an output voltage with low impedance, directly proportional to the signal voltage, and the return of which is isolated from the input return, with impedance and voltage-isolation limits determined by the characteristics of the optoisolator.

This work was done by John Paulkovich and G. Ernest Rodriguez of **Goddard Space Flight Center**. *No further documentation is available. GSC-13150*

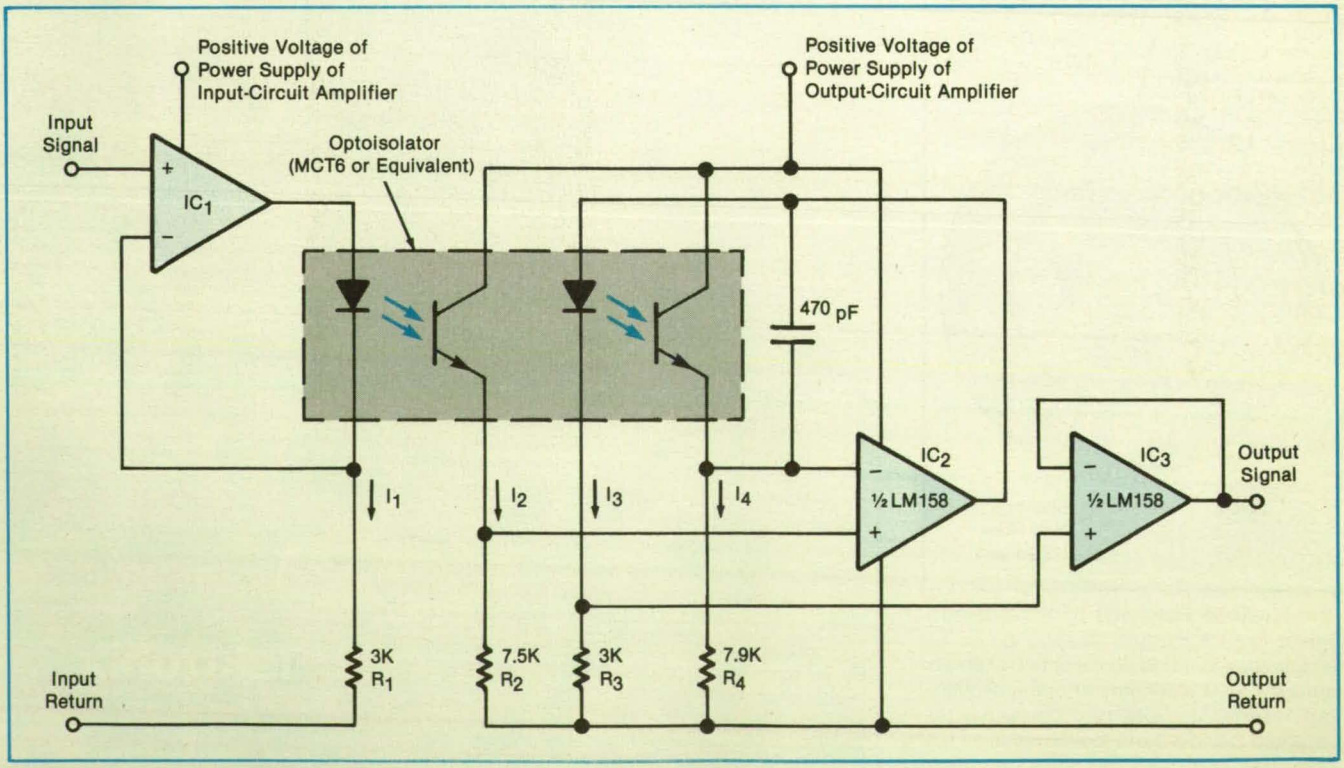

The **Analog Isolation Amplifier** uses a dual-transistor optoisolator to prevent the transmission of common-mode voltage from the input to the output.

Small, Optically-Driven Power Source

Power would be transmitted along fiber-optic cables.

NASA's Jet Propulsion Laboratory, Pasadena, California

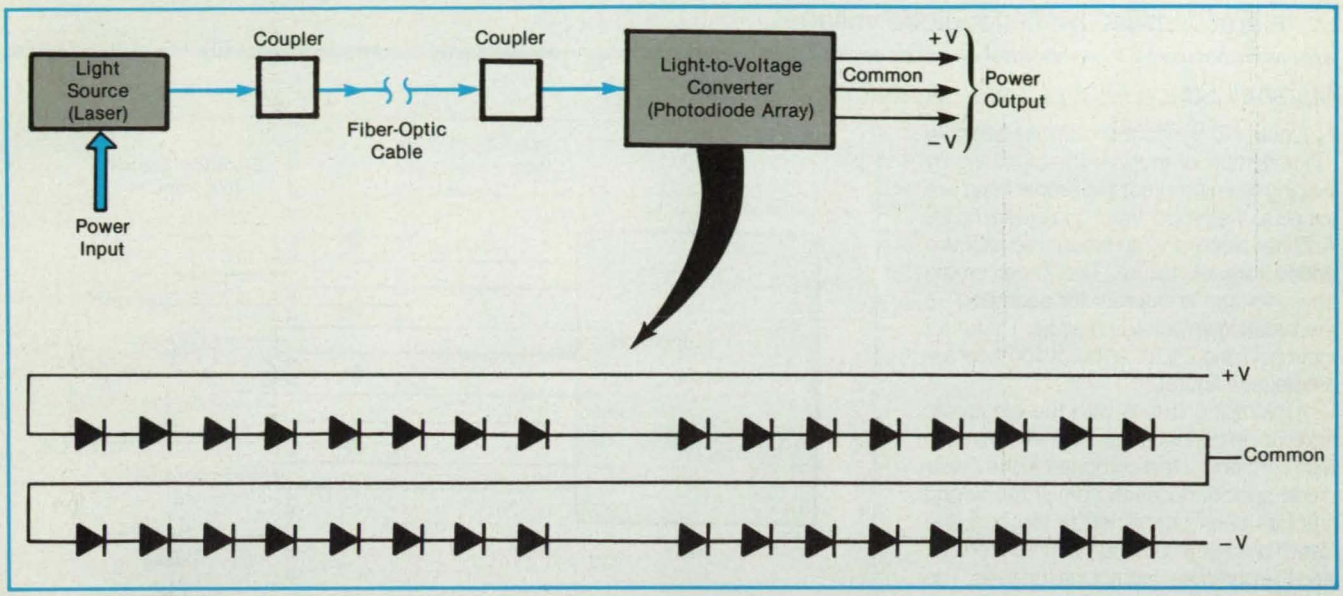

Figure 1. **Power Would Be Transmitted** as infrared light along a fiber-optic cable, then converted to electricity to supply a small electronic circuit. The power source and the circuit could thus remain electrically isolated from each other for safety or to reduce electromagnetic interference.

Arrays of AlGaAs/GaAs photodiodes undergoing development are expected to deliver 4 to 12 V at currents up to 1 mA under infrared illumination at a wavelength of 850 nm. The conversion efficiency of optical to electrical energy may be as high as 40 percent. In the intended application, the infrared light would be transmitted along optical fibers to the diode array (see Figure 1) to supply power to a small electronic circuit that has to be electrically isolated; for example, to an electric-field sensor in or near a source of high voltage.

An experimental version of the power-conversion device includes 32 AlGaAs/GaAs diodes connected in four strings of eight diodes each (see Figure 2). Even though it is more difficult to fabricate, GaAs is used because its higher energy-conversion efficiency at 850 nm enables the fabrication of a thin diode array that fits into a small package. The array was made according to standard integrated-circuit design rules, using standard glass photomasks for the photolithographic process.

The diode layers are grown by metal/organic chemical-vapor deposition. A semi-insulating GaAs wafer serves as the substrate and electrically isolates the diodes from each other. A thick layer of n-type GaAs is deposited on the substrate, followed by a thinner layer of p-type GaAs; these two layers form the p/n diode junction that converts the light to electricity. A thin layer of p-type AlGaAs is then deposited as a surface-passivation layer.

The layers are etched into individual

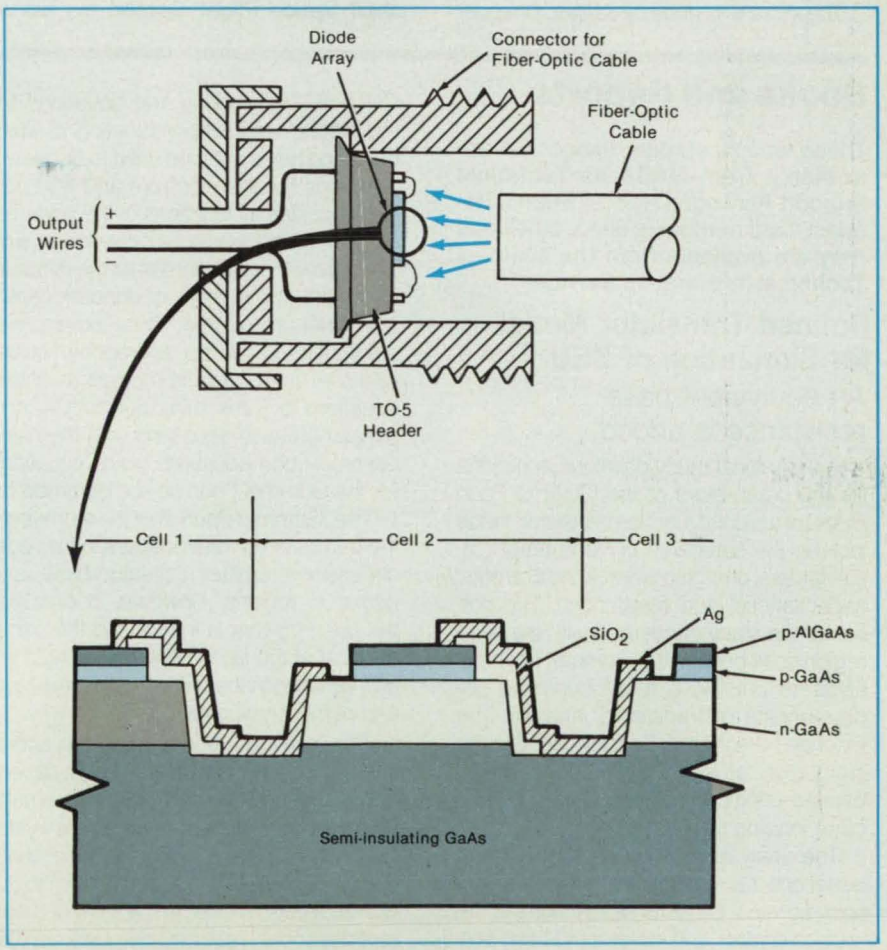

Figure 2. The **Array of Diodes** is made by standard integrated-circuit techniques and packaged for mounting at the end of the fiber-optic cable.

mesas, each of which will become a diode. A layer of SiO_2 is deposited by radio-frequency sputtering, then etched to remove all oxide except that on one side of the mesas. This oxide prevents the shorting of the diodes when the interconnecting metal (Ag) is evaporated onto the device. The metal is etched to form the interconnections. Finally, the device is mounted in a standard TO-5 package.

This work was done by Richard H. Cockrum and Ke-Li J. Wang of Caltech for **NASA's Jet Propulsion Laboratory**. *For further information, Circle 30 on the TSP Request Card.* *NPO-16827*

Checking Plumbing Connections Electrically

Ports are identified by Zener-diode voltages.

Marshall Space Flight Center, Alabama

Electronic verification circuits assist in the assembly of multiple-line plumbing by helping to ensure that the proper lines are joined to the proper input and output ports. A Zener diode and an electronic jack are added to each fixture. The Zener breakdown voltage is different for each port — the breakdown voltage may be 1 V for an input port and 2 V for an output port, for example (see figure).

A plumbing fixture with the electronic addition, in connecting a fluid line to a port, also connects a test computer to the Zener diode specific to each port. If the wrong line has been connected to the port, the Zener breakdown voltage will be incorrect, and the computer will not initiate tests. The application of the wrong flow or of flow in the wrong direction or at the wrong pressure is thus avoided, and damage to the system is prevented.

This work was done by Jerry L. Chappel of Rockwell International Corp. for **Marshall Space Flight Center**. *No further documentation is available.* *MFS-29289*

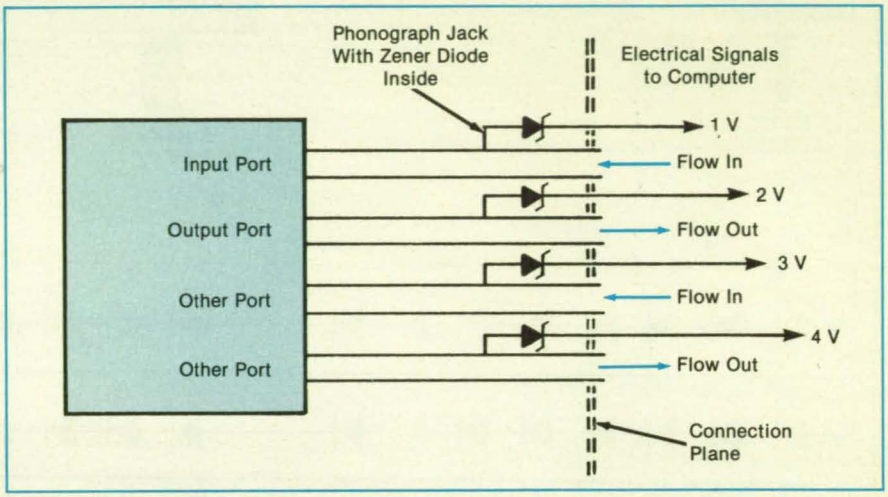

When a Fixture Makes a Fluid Connection, it also makes an electrical connection. The Zener breakdown voltage identifies the line, port, or valve to which a fluid line has been connected.

Books and Reports

These reports, studies, handbooks are available from NASA as Technical Support Packages (TSP's) when a Request Card number is cited; otherwise they are available from the National Technical Information Service.

Refined Transistor Model for Simulation of SEU

An equivalent base resistance is added.

A theoretical study develops equations for the parameters of the Gummel-Poon model of a bipolar junction transistor: these include the saturation current, amplification factors, charging times, knee currents, capacitances, and resistances. The portion of the study concerned with the base region goes beyond the Gummel-Poon analysis to provide a more complete understanding of transistor behavior. The extended theory is especially useful in the simulation of single-event upset (SEU) caused in logic circuits by cosmic rays or other ionizing radiation.

The analysis begins with the standard equations for the emitter, collector, and base-terminal currents as functions of the base-to-emitter and collector-to-base voltages, as well as of the model parameters: these are the basic equations of the Gummel-Poon model. The equations for the diffusion and recombination of electrons and holes are then used to derive expressions for the electron- and hole-current densities as functions of the voltages, some of the dimensions of the device, and of such material properties as the diffusion constants and number of donor/acceptor atoms per unit volume. These expressions are multiplied by the appropriate cross-sectional areas and combined to obtain equations for the terminal currents. A comparison of these equations with the basic Gummel-Poon equations yields equations for the Gummel-Poon device parameters.

The Gummel-Poon model represents the transistor as a stack of essentially-one-dimensional emitter, collector, base, and depletion regions. However, in practice, the base current is introduced through a terminal at the side, thereby causing a lateral variation in the base-to-emitter voltage and of the longitudinal current density.

The extended model treats the lateral variation by recognizing the two-dimensional nature of the problem in the formulation of the current-density equations for the base region. The solution to these equations is essentially a correction term to the Gummel-Poon model, in the form of a current-dependent resistance R_B between the portion of the base in the longitudinal emitter/base/collector region and the portion of the base in the lateral base/collector region where the base contact is attached.

The extended model improves the analysis of experimental SEU data in that it enables one to distinguish the effects of ions traveling through one region from the effects produced in another region, whereas the original Gummel-Poon model made no such distinction. To test the extended model, SEU cross sections were measured on a bipolar integrated-circuit chip irradiated with bromine ions at energies of 50 to 100 MeV. The two-dimensional correction is consistent with the observed cross sections as a function of ion energy. Apparently R_B serves to impede the flow of ion-induced charge from the base-contact region into the longitudinal current path, so that, for ions incident in the base-contact region, a higher energy is required to cause SEU.

This work was done by John A. Zoutendyk and Reuben Benumof of Caltech for **NASA's Jet Propulsion Laboratory**. *To obtain a copy of the report, "Theoretical Values of the Gummel-Poon Model of a Bipolar Junction Transistor" and of the accompanying explanatory note, "Modification of the Gummel-Poon Transistor Model to Enable the Accurate Simulation of Single-Event Upset (SEU) in Bipolar Integrated-Circuit Chips," Circle 41 on the TSP Request Card.* *NPO-16771*

The shortest distance between two points just became shorter.

DCS Announces its NEW Programmable Universal Demodulator.

DCS brings to existing, field-proven technology a new twist in innovative thinking.

The result is an FM demodulator that is a quantum leap beyond competition. For one thing, this computer controlled advance is menu-driven, with keypad entry, and stored formats. It can discriminate all 50 standard IRIG channels as well as non-standard configurations. And when you consider that the complete system is packed in a single housing and priced substantially below other units, you can understand our pride.

Innovation is not new at Data-Control Systems. For thirty years, we have been extending the leading edge in telemetry systems. Our specialty is solving problems. In fact, we've just shortened the shortest distance between two points.

DCS Universal FM Tunable Demodulator
Full 2 MHz bandwidth / Accuracy to 1 HZ / Programmable low pass filter / Tape speed compensation / Spectral display / All formats PBW, CBW-LP, CA / Large alphanumeric display / Multiple computer interfaces

Quanta Systems Corporation
Data-Control Systems
CompuDyne Defense
Electronics Group

1455 Research Boulevard
Rockville, MD 20850
(301) 279-8798
TWX (710) 828-9785

8291 Westminster Ave., Suite 150
Westminster, CA 92683
(714) 984-4471
TWX (910) 596-1802

Electronic Systems

Hardware, Techniques, and Processes

Noninterlaced-to-Interlaced Television-Scan Converter

Computer text and ordinary images are displayed together without text jitter.

NASA's Jet Propulsion Laboratory, Pasadena, California

A scan converter enables the superposition of alphanumerical text generated by a computer-driven video generator on a National Television System Committee (NTSC) standard interlaced-scan image. It is made of commercially available integrated circuits and operates in conjunction with an NTSC synchronizing-signal generator.

An NTSC picture nominally contains 525 horizontal lines transmitted in two alternating fields of 262½ lines each (see Figure 1a). Field 1 contains the odd-numbered lines, while field 2 contains the even-numbered lines.

On the other hand, the text video generators associated with computers produce identical, noninterlaced fields of 262 or 263 lines each. Thus, if the computer video output is used directly mastered by the NTSC synchronization, the identical text is projected alternately in the odd and even fields, causing the letters and numbers to move up and down by one line space at the frame rate of ~ 60 Hz (see Figure 1b). To prevent this motion, one can use either or both of two methods: one for exclusively mixing or superposing computer-generated images or another for mixing both computer images and NTSC interlaced images.

To superpose exclusively computer images in a system slaved to the NTSC standard, it becomes necessary to do the following:

- Postpone the vertical-drive pulse of field 2 so that it occurs at the time of the 263rd horizontal-drive pulse, so that field 2 starts exactly where field 1 did.
- Compensate for the shortage of field 2 that was left with only 262 lines (525 – 263 = 262) so that the scanning of the entire screen will be coincident to that of field 1. This is done by stealing one line to the vertical retrace (VR) prior to the vertical trace (VT) of field 2.

In this manner the visible part of both fields will be identical, both containing the same number of lines. Only the VT of both fields will differ in one line count. The simplified timing diagram in Figure 2 makes this clearer.

This diagram assumes a frame of 21 lines instead of 525. This "shorthand" NTSC frame does not affect the theory of operation of the circuit but makes the diagram more readable. In other words, anything said for the "shorthand" frame of 21 lines is applicable to a real NTSC frame of 525 lines. In both cases, one is concerned with only one horizontal line and with only one horizontal pulse.

The entire "shorthand" NTSC frame is composed of two fields, each containing 10½ lines, of which 3 correspond to the VR and 7½ to the VT on each field. In the "shorthand" modified frame, field 1 contains 11 lines, of which 3 are for the VR and 8 for the VT, while field 2 contains 10 lines, of which only 2 correspond to the VR and 8 to the VT.

In order to achieve the modified frame, an extra pulse is given to the horizontal counter. This pulse has the following two effects:

1. Because the VR is terminated at the count of three, the VR period is shortened to two NTSC horizontal pulses; and
2. The start of the display of the information of field 2 coincides with that of field 1.

The use of the extra pulse results in an NTSC master synchronization that is suitable for the mixing of a variety of images, without sacrifice of the advantage of the noninterlaced system. The noninterlaced system maintains the same field repeated every 1/60 second, in contrast to the NTSC standard, which repeats the same field every 1/30 second. The consequence is less flickering at the expense of approx-

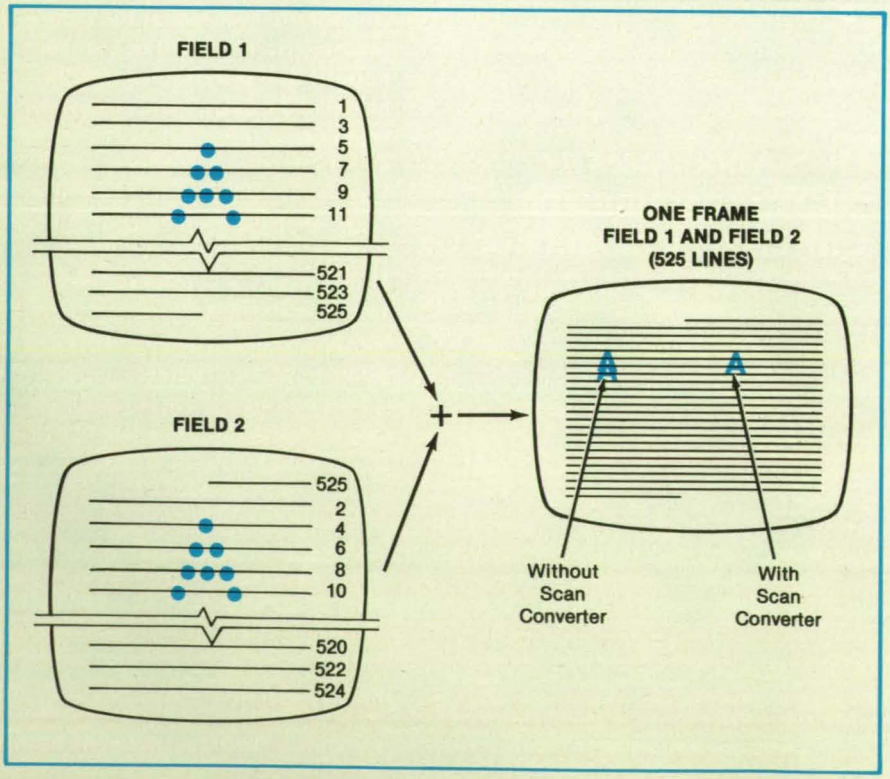

Figure 1. A **Standard Television Picture** is transmitted in two interlaced fields. Without the scan converter, the text image moves up and down by one line as the fields change. With the scan converter, the text image stands still.

MARK YOUR CALENDAR

for the world's most important commercial space conference and exposition in 1988:

SPACE

TECHNOLOGY
COMMERCE &
COMMUNICATIONS

November 1–4, 1988
George R. Brown Convention Center
Houston, Texas USA

THE EXHIBITS

The first annual **SPACE: Technology, Commerce & Communications** was held in November 1987 and featured 78 exhibitors from all over the world, including NASDA (Japan), Aeritalia, Prospace, Belgium Science Policy Office, Government of Canada, Pilkington, NASA, Rockwell International, Lockheed, McDonnell Douglas, General Dynamics, Ford Aerospace, Martin Marietta, Hercules Aerospace, Tracor Aerospace, Morton Thiokol, ISC Group, SPOT Image, IBM, Digital Equipment Corp., Honeywell, Sun Microsystems, U.S. Air Force, Hewlett Packard, Eaton Corp., Space Industries and more.

The 1988 exposition will feature technologies, new products, and service offerings from organizations worldwide.

THE CONFERENCE

The second annual four-day conference will address the opportunities, risks and potential for business in space, and will feature world renowned experts discussing technology advancements, new business prospects, government issues, and more. Last year's speakers included **Mr. Robert Anderson,** *Chairman and CEO, Rockwell International Corp.;* **Mr. Shigemichi Sonoyama,** *VP-NASDA;* **Mr. Aaron Cohen,** *Director, Johnson Space Center;* **Mr. J.R. Thompson,** *Director, Marshall Space Flight Center;* **Mr. Paul Holloway,** *Deputy Director, Langley Research Center;* **Major Gen. Robert Rankine,** *Air Force Systems Command;* **Mr. Richard Darman,** *Managing Director, Shearson Lehman Brothers;* and many more.

CO-SPONSORED BY: THE SPACE FOUNDATION

The conference and exhibition is co-sponsored by The Space Foundation, the nationwide organization promoting the business of space at monthly Space Business Roundtable meetings across the country.

FOR MORE INFORMATION mail coupon to:

SPACE: Technology, Commerce & Communications
c/o T.F. Associates, Inc.
79 Milk Street, Suite 1108, Boston, MA 02109 USA
Telephone (617) 292-6480; Telex 951417 TFAS

_____ My company may wish to exhibit. Please send information.
_____ Please send attendee information.
_____ I wish to submit a paper and am including a 1-page precis.

Name_____ Title_____

Company _____

Address_____

City_____ State_____ Zip_____ Telephone ( ) _____ Telex _____

NTB488

Circle Reader Action No. 409

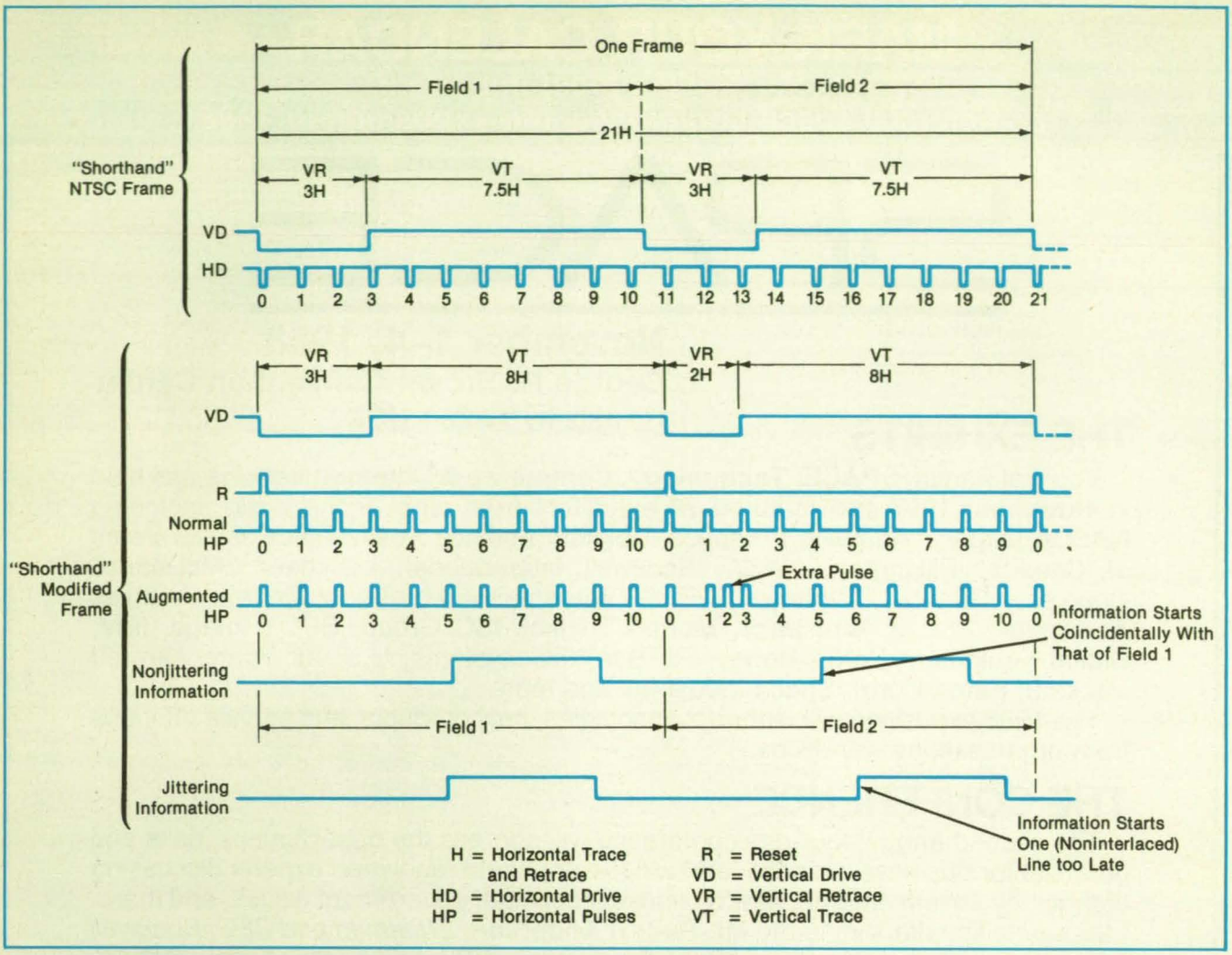

Figure 2. These **Timing Pulses** are those of a "shorthand" frame of 21 lines that is similar in principle to a standard 525-line frame.

imately half the number of horizontal lines.

In order to mix computer-generated images to NTSC interlaced images it becomes necessary to do the following:

- Let field 1 run with the standard 262.5 horizontal lines.
- Suppress, by means of a field detector, any portion of the computer-generated images during the interlaced scanning; that is, during the NTSC field 2.

In the interlaced scan, the vertical-drive pulse in field 2 occurs between two horizontal-drive pulses, whereas the vertical-drive pulse in field 1 starts simultaneously with a horizontal-drive pulse. The scan converter includes a field detector, which is made out of a timing circuit that opens a "window" of 10 μs at the beginning of each vertical-drive pulse of the interlaced-scan signal. If a horizontal-drive pulse is detected during this "window" (signifying field 1), the text video signal for field 1 is transmitted, and the vertical position of each horizontal line containing information is determined according to the line count starting from the reset shown in Figure 2.

If a horizontal-drive pulse is not detected during the "window" (signifying field 2) when mixing exclusively computer images, a video signal like that of field 1 is transmitted, but an extra pulse is sent to the horizontal-line counters during the VR of field 2. If computer images are to be mixed with NTSC images, only the computer information of field 1 will be included.

This work was done by Sergio Morales of Caltech for **NASA's Jet Propulsion Laboratory**. *For further information, Circle 165 on the TSP Request Card.*
NPO-16777

VLSI Architecture of a Binary Up/Down Counter

Identical stages contain relatively-few logic gates.

NASA's Jet Propulsion Laboratory, Pasadena, California

A new algorithm simplifies the design of a binary up/down counter. The new algorithm reduces the number of logic operations below that of other up/down counters. The design is regular, simple, and expandable: a counter that handles many bits can be made of identical cells, each containing relatively-few logic gates. Thus, the design is suitable for very-large-scale integrated circuits.

The input to the counter can have the value 1, 0, or -1. Equivalently, the input can be represented by signals on two bit lines, U and D: Signals to count up, count down, or not change would be represented by $(U = 1, D = 0)$, $(U = 0, D = 1)$, or $(U = D = 0)$, respectively. The new algorithm specifies the nth bit in the counter, as $A_n(t)$

$$= A_n(t-1) \oplus [(U \bullet P_n)\mathbf{U}(D \bullet Q_n)]$$

where A_n = the digit representing the $n-1$st power of 2, t = time in discrete units of a fundamental clock period,

$$P_n = \prod_{k=1}^{n-1} A_k,\ Q_n = \prod_{k=1}^{n-1} \bar{A}_k,$$

the bar over "A_k" denotes the complement of A_k, $\oplus$ denotes

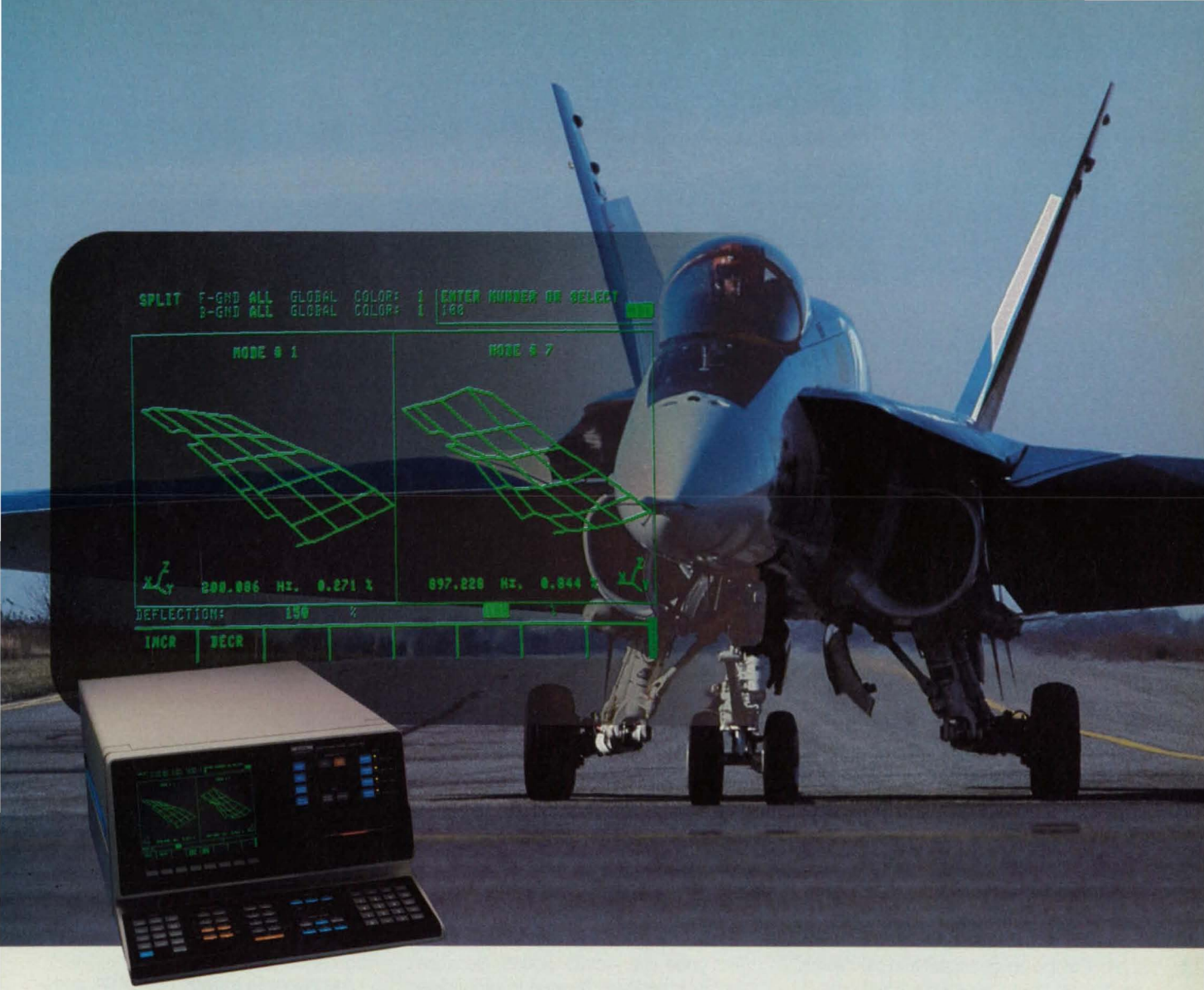

For critical structural test... a total solution

For mechanical design verification and vibration troubleshooting, the new 1202 Structural Analyzer does it all . . . from advanced FFT signal processing with zoom and integrated signal generation, to versatile modal analysis with interactive geometry and enhanced animation that simplifies the interpretation of complex structures. ONLY the 1202 does it all in a *single, user friendly,* portable, cost-effective package.

The 1202 is a complete 4-channel analysis system with integrated software for FFT signal processing, modal analysis, structural modification and forced response simulation. When combined with Schlumberger's 1250 series Frequency Response Analyzer, the 1202 can be expanded to 36 parallel channels for large complex projects. Fast graphics on a built-in display features unique hidden line animation of mode shapes, surface strain contours and flexible stack plots. Internal 20 Megabyte fixed drive with a 3-1/2 inch floppy backup, IEEE-488 and RS 232 are all standard.

All this capability is available, fully integrated, from one source. . . Schlumberger Instruments. Ask for our application oriented brochure for the full story.

Schlumberger Instruments

20 North Avenue, Burlington, MA 01803
Telephone: (617) 229-4825
Toll Free (outside MA): 1-800-225-5765

Schlumberger Technologies

Circle Reader Action No. 589

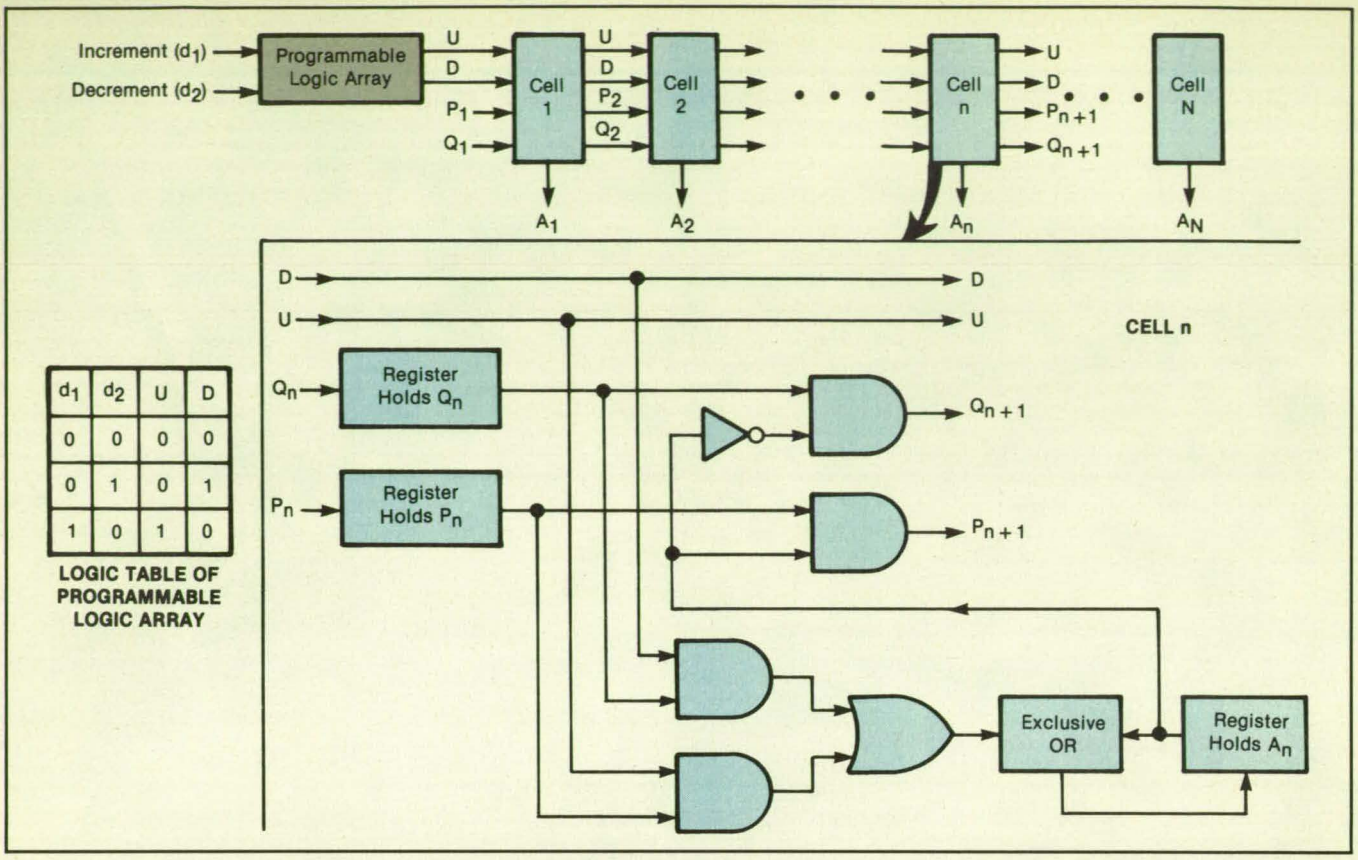

d_1	d_2	U	D
0	0	0	0
0	1	0	1
1	0	1	0

LOGIC TABLE OF PROGRAMMABLE LOGIC ARRAY

The **Binary Up/Down Counter** contains a simple "pipeline" array of identical cells. A programmable logic unit converts the increment and decrement input signals to the "U" and "D" signals required by the algorithm of the counter.

a logical "exclusive OR," **U** denotes logical "inclusive OR," and • denotes logical "and."

It is not necessary to compute the full product P_n and Q_n for each bit. Instead, the cell for each bit receives the product from the cell of the preceding bit and calculates the values from the recursive formulas $P_n = P_{n-1} \bullet A_{n-1}$ and $Q_n = Q_{n-1} \bullet \bar{A}_{n-1}$, except that $P_1 = Q_1 = 1$.

This algorithm can be executed by cells (one for each bit) in a simple "pipeline" configuration (see figure). The inputs to the nth cell are U, D, P_n, and Q_n, while the outputs are U, D, P_{n+1}, Q_{n+1}, and A_{n+1}. All the cells are identical except cell 1, the P and Q registers of which are wired to hold the values $P_1 = Q_1 = 1$ permanently.

The counter can increment or decrement once every clock period. Because one clock period is needed to propagate the calculation to each succeeding cell, the final value of the most significant bit in an N-bit counter is displayed N time units after the increment or decrement signal has been fed in; that is, the updated count "ripples" through the counter at the rate of 1 bit per clock period.

This work was done by In-Shek Hsu and Trieu-Kie Truong of Caltech and I. S. Reed of the University of Southern California for **NASA's Jet Propulsion Laboratory**. *For further information, Circle 43 on the TSP Request Card.*

This invention is owned by NASA, and a patent application has been filed. Inquiries concerning nonexclusive or exclusive license for its commercial development should be addressed to the Patent Counsel, NASA Resident Office-JPL [see page 12]. Refer to NPO-17205.

Canceling Electromagnetic Interference During Tests

An old technique solves a modern problem.

NASA's Jet Propulsion Laboratory, Pasadena, California

A simple amplitude-and-phase-cancellation technique removes strong electromagnetic interference from a received test signal, enabling the recovery of the relatively weak signal from the device under test. The technique is particularly useful in outdoor tests of devices for electromagnetic compatibility; in such tests, interfering signals often overwhelm those from the devices under test, thereby making the tests impossible to conduct or compromising the results.

The technique is based on destructive interference between the interfering component in the test signal and an oppositely polarized version of the interfering signal. As shown in the figure, an antenna is placed near the device under test; this antenna receives the test signal corrupted by the interfering signal. A second antenna is placed much farther from the device under test so that it receives a much weaker signal from the device under test, although it receives nearly the same interfering signal.

The signal from the first antenna is amplified and shifted in phase by 180°. The signal from the second antenna is fed through a variable attenuator that has been previously set so that the interference-signal outputs of both antenna circuits have equal amplitude. Thus, when the two signals are combined at the input terminal of a spectrum analyzer, the equal but opposite interference components cancel, leaving only the desired signal from the tested device. (A small device-signal component is present in the signal from the second antenna. This causes a slight reduction of the device signal at the input of the spectrum analyzer, but this reduction is easy to take into account at subsequent

COME FLY! WITH U.S.

MAY 13-22, 1988

Brown Field San Diego, California, USA

Finally, America's own International Aviation & Aerospace Trade Exposition & Air Show (Paris will never look the same).

Whatever your interest in flight, there is something for you at Air/Space America. If you're a manufacturer you'll meet qualifed buyers from around the world. If you're a buyer you can discuss your needs with leading manufacturers of electronic and avionic equipment, aircraft, and space vehicles. And, if you are an aerospace "buff," you're in for an unforgettable experience as you examine ultra-modern aircraft and space systems, and witness thrilling air shows and races.

Indeed, Air/Space America has something for everyone . . . an unprecedented opportunity for buyers and sellers to meet, plus the excitement of flight and space.

For further information, simply complete and mail the coupon, or write or call Dub Allen, Public Affairs Officer • Air/Space America 6110 Friars Road • Suite 204 San Diego, CA 92108-1004 USA (619) 294-8808

TO: Dub Allen • **Air/Space America** • 6110 Friars Rd., Suite 204 San Diego, California 92108-1004 USA

PLEASE RUSH ME INFORMATION ON:

❑ Attending ❑ Exhibiting ❑ Being a Volunteer

Name _____

Address _____

City/State/Zip _____

Phone ( ) _____

M/S _____

Circle Reader Action No. 591

stages of signal processing.)

The technique was verified in the test of a device transmitting at 59.75 MHz and subject to a strong interfering signal from a television station operating on channel 2. The first antenna was placed at a distance of 1 m from the device, while the second antenna was placed 17 m from the device. The interfering signal was so strong that the device signal could not be distinguished in the output of the near antenna. When the cancellation technique was employed, the device signal was clearly distinguishable.

This work was done by Paul A. Robinson, Jr., and Larry D. Edmonds of Caltech for **NASA's Jet Propulsion Laboratory**. *For further information, Circle 117 on the TSP Request Card.*

This invention is owned by NASA, and a patent application has been filed. Inquiries concerning nonexclusive or exclusive license for its commercial development should be addressed to the Patent Counsel, NASA Resident Office-JPL [see page 12]. Refer to NPO-17132.

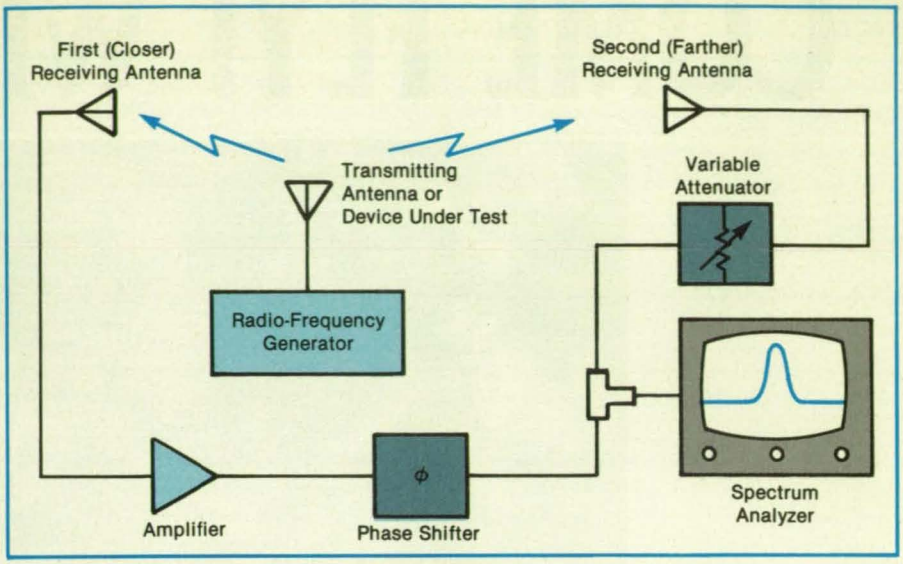

The **Common-Mode Interfering Signal** received by both antennas is canceled at the input of the spectrum analyzer, leaving only the signal from the device under test.

Books and Reports

These reports, studies, handbooks are available from NASA as Technical Support Packages (TSP's) when a Request Card number is cited; otherwise they are available from the National Technical Information Service.

Development of a Digital Flight-Control System

The feed-forward control path includes inversion of the model of the aircraft.

A report describes the concept, development, and tests of a digital flight-control system for a vertical-attitude-takeoff-and-landing aircraft. The report is, in effect, a summary of previous documents that discuss various aspects of the system and its development in greater detail. It should be of interest to flight-control specialists concerned with aircraft that must fly in a wide range of aerodynamic conditions.

The flight-control system is based in an airborne digital computer. It combines the control of attitude and thrust in a unified system for operation over the full coupled ranges of velocity, altitude, attitude, and acceleration. The system is based on a model-following concept in which several models of different complexity are used, including some that represent essentially all of the aerodynamic and propulsion details.

The feed-forward control path is split into a command section and a control section. The command section generates smooth, executable, and consistent acceleration-, velocity-, and position-command vectors in the reference inertial-axis system (north, east, and down) in response to corresponding rough trajectory-command inputs from an air-traffic-control system, from ground vectoring, from a trajectory stored in the computer, or generated by the pilot using a side-stick controller to command accelerations.

The control section of the feed-forward controller computes the thrust and moment controls needed to produce the total commanded acceleration. The series combination of the control section and the actual aircraft is essentially linear with decoupled axes when viewed from the command section. This is achieved by embedding an inverse of the force and moment model of the aircraft in the control section that determines the aircraft controls. The regulator feedback loop is closed around this approximate identity and hence can be easily designed by linear methods. It is called upon only to compensate for disturbances and for uncertainty in the model.

The model is inverted by applying an iterative Newton-Raphson trim procedure. Essentially, this procedure is a multivariable adaptation of Newton's method for finding the root of an equation by calculating a local derivative and using a linear extrapolation to find an approximation to the root in an iterative way. The trim procedure employs the force and moment equations in the coordinate system of the aircraft.

Computer-simulation tests were carried out over a range of flight conditions from vertical-attitude hover through transition to conventional flight at high subsonic speeds. The results show that the control system performs satisfactorily over a large part of the total range of conditions. The use of a vertical attitude-inertial-axis system (up, east, and north) for vertical-attitude hover maneuvers was quite satisfactory. No appreciable transients occurred, although the aircraft-attitude matrix was switched at three places in the control circuits simultaneously from one to the other reference-axis system. Because the switching point is not critical and could be anywhere between attitudes of 45° and 85°, a suitable hysteresis loop could prevent switching chatter when going through the switching region in either direction.

The response of the system to wind gusts was satisfactory for various reasonable combinations of wind magnitude and direction. However, trim failure could be induced by sufficiently severe disturbances.

Flight tests in a DHC-6 Twin Otter aircraft and in the Augmentor Wing Jet short-takeoff-and-landing research aircraft, both of which used multidimensional table look-up (instead of Newton-Raphson iteration) for model inversion, showed good agreement with numerical simulations. In a current flight-test program, the Newton-Raphson model-inversion technique has been used successfully to control a UH-1H helicopter over a complex trajectory in spite of strong nonlinear coupling between axes.

This work was done by G. Allan Smith and George Meyer of **Ames Research Center**. *To obtain a copy of the report, "Aircraft Automatic Digital Flight Control System With Inversion of the Model in the Feed-Forward Path," Circle 156 on the TSP Request Card.*

Inquiries concerning rights for the commercial use of this invention should be addressed to the Patent Counsel, Ames Research Center [see page 12]. Refer to ARC-11778.

You have to work with steppers and DC servos. So should your programmable motor controller.

In developing Klinger's MC4 motor control system, our engineers' had the dilemma of choosing between steppers or DC servos, or should they design two systems, one for each type.

Considering the specific application advantages of each motor, we decided the ideal controller should work equally well with both motor types and switching from one motor to the other should be easy and inexpensive.

That's precisely what we've accomplished with the MC4 system. Where a simple plug-in power card switches the system between motor types.

The MC4 is a powerful programmable motor control system capable of controlling up to four motors, interfacing with any host computer or, with its 8K of non-volatile memory, it can stand alone to operate on the production floor. You can even store up to 99 programs and locally access any 9 programs from front panel controls.

MINI-STEPPING YIELDS HIGH RESOLUTION AND HIGH VELOCITY.

Most stepping motors rotate 1.8 degrees per full step, a relatively large motion for extremely precise work. With each motor step, a small amount of shaft rebounding is possible, thus exciting vibrational noise.

Klinger's mini-step feature divides each full step by 10 and simultaneously increases the pulse rate by 10, resulting in less shaft rebounding and settling effect, higher resolution without sacrificing speed and virtually eliminating troublesome resonance.

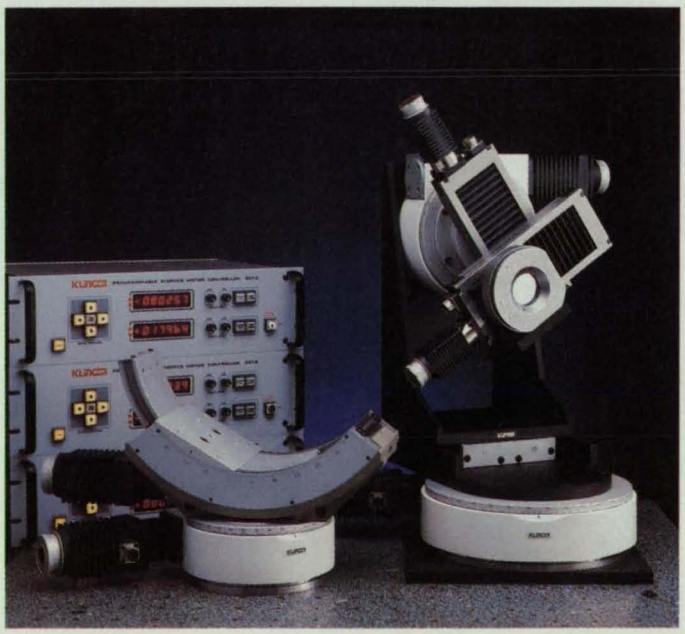

BUY ONE SUPERIOR CONTROLLER. NOT TWO.

You can't buy a better programmable motor controller than the Klinger MC4. And since you only have to buy one for both types of motors, you'll actually save time and money and not have to rewrite extensive software. Just slip in the modular drive card and you're ready to go.

To learn more about Klinger's programmable motor controllers, micropositioners and systems, send for our free micropositioning handbook. Write or call Klinger Scientific Corporation, 999 Stewart Avenue, Garden City, NY 11530. (516) 745-6800.

KLINGER SCIENTIFIC

Building better positioning systems, piece by perfect piece.

U.S.A. Headquarters: 999 Stewart Avenue, Garden City, NY 11530 (516) 745-6800.
Regional Offices: Northern California (415) 969-0247; Southern California (714) 999-5088. Worldwide distribution network: Contact Micro-Controle, Z.I. de St. Guenault, B.P. 144, 91005 Evry Cedex, France. Tel.33(1)64.97.98.98. FAX 33(1)60.79.45.61.

Circle Reader Action No. 368

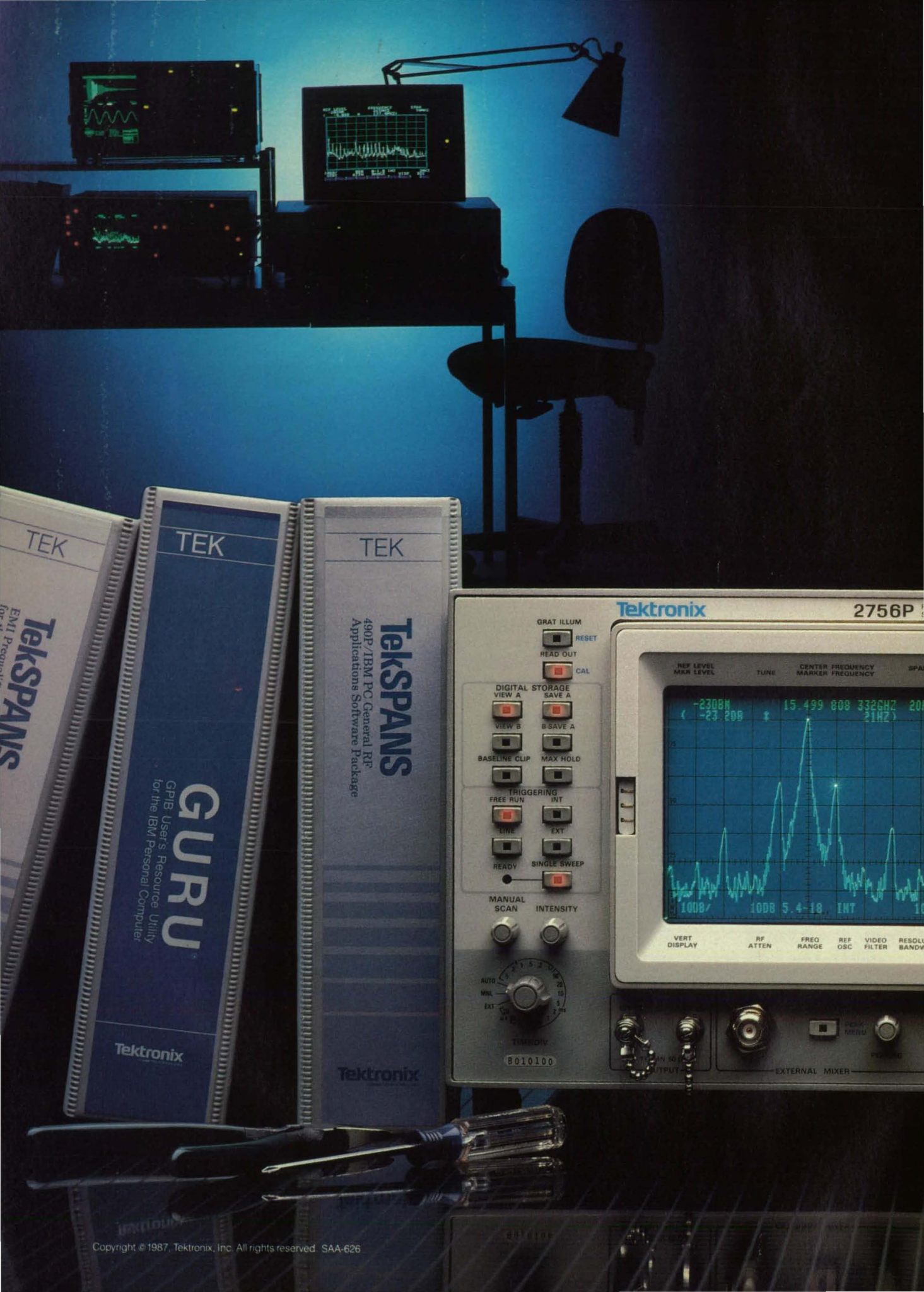

BUILT FOR THE BENCH.

The Tek 2750 Series of Laboratory Spectrum Analyzers. Configuration flexibility. Optioned to your application. From the powerful, fully programmable new 2756—at 325 GHz—to the VHF/UHF 2753, Tektronix sets a better-value standard in laboratory spectrum analysis.

Only Tek makes it so cost-effective to optimize spectrum analysis to your set of requirements and value criteria, whether your primary need is high-end performance—for research and development—or repeatability and throughput for manufacturing test.

You'll find a perfect fit for your bench, systems and budget needs. A choice of seven lab analyzers makes it possible for Tek to meet your needs precisely—at any frequency—with the right measure of economy and outstanding ease of use.

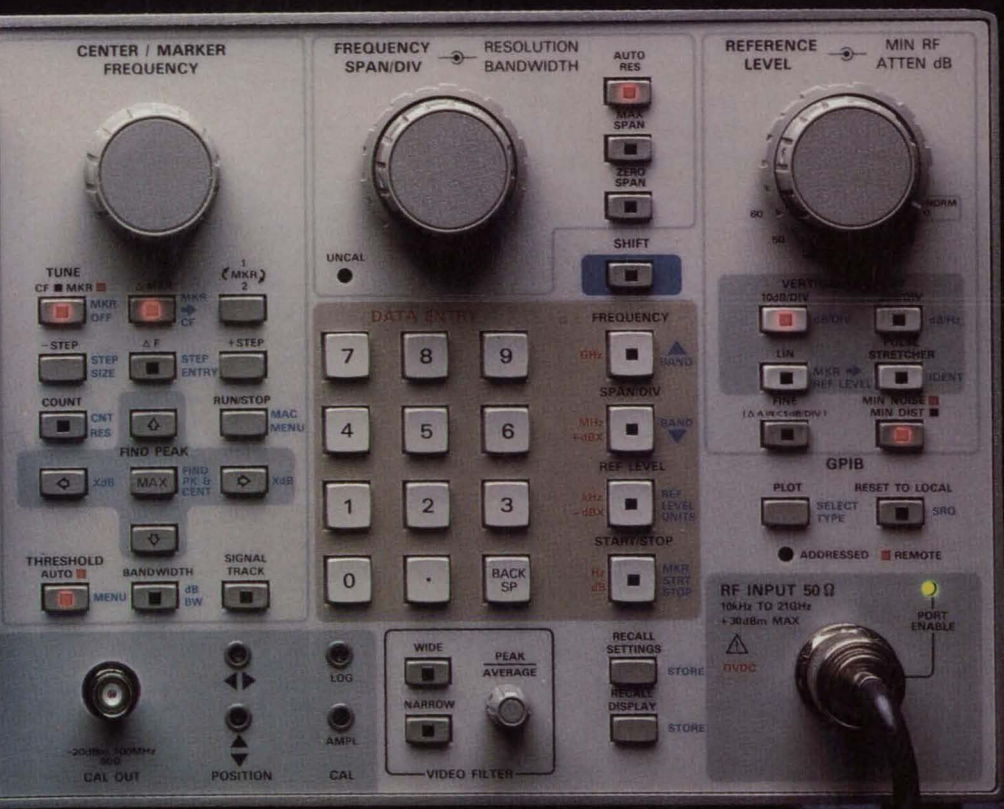

A built-in precision co ter, Macro programmi and signal processing intelligence are just a f ways to optimize the 2750 Series for your o use. Look at Tek featu like marker frequency accuracy of 10^{-9} and automatic signal track And with TekSPANS® software—available fo IBM PC, Tek and HP controllers—you can automate complex me surements, including EMI tests.

What you can count o is more performance the dollar than you've ever seen, including superior optionability: waveguide mixers, pr selectors, MATE com- patibility, 75-ohm inpu rackmount, computer packages and softwa for your system needs and more.

Get the facts! Discove the Tek value different before you make anot buy. Contact your Tek Sales Engineer or call direct: 1-800-TEK-SPE Ext. 23. In Oregon: 235-7315, Ext. 10.

TEKTRONIX 2750 SERIES LAB SPECTRU ANALYZERS

Tektronix

COMMITTED TO EXCELLEN

Circle Reader Action No.

Physical Sciences

Multiple-Diode-Laser Gas-Detection Spectrometer

Small concentrations of selected gases would be measured automatically.

NASA's Jet Propulsion Laboratory, Pasadena, California

A proposed multiple-laser-diode spectrometer would be part of a system for measuring automatically the concentrations of selected gases at the part-per-billion level. Intended for use during future exploration of Saturn's moon Titan, the spectrometer may be adaptable to such terrestrial uses as monitoring pollution or control of industrial processes.

The spectrometer would include an array of infrared tunable diode lasers, the frequencies of which vary with their input currents at rates of 200 to 2,000 MHz/mA. Each diode would operate at a wavelength selected in the range of 3 to 30 μm. Although the basic instrument concept calls for 11 lasers arranged in a circle (see figure), more or fewer could be used, and side-by-side or other arrangements might prove more suitable for some measurements.

A photodetector would be associated with each diode laser, and all the photodetectors and diodes would be mounted on a base cooled to a temperature of 80 K. The forward output light beam of each laser would travel through the atmosphere to a retroreflector at a distance of 20 cm, and the returned light would be measured by the associated photodetector. The backward output beam of each laser would pass through a reference cell (not shown in the figure) containing the molecular species to be measured by the laser/detector pair. This arrangement would provide absolute wavelength calibration.

The current in each laser diode would be swept repeatedly through a range that causes its output wavelength to sweep through a known portion of the absorption spectrum of the gas or gases to be detected. Each laser would be modulated at a different frequency so that ac detection techniques could be used to enable the simultaneous measurement of 11 or more gases.

The instantaneous output of each photodetector would give a measure of the absorption of the radiation in the atmosphere at the instantaneous wavelength. The photodetector output would be processed to identify the gas species from the variation of absorption with wavelength and the concentration of the species from the degree of absorption.

It is expected that the spectrometer can provide useful data even where peak absorptances are no greater than 0.01 percent. Volume mixing ratios as low as 10^{-9} should be measurable for most species of interest, including CH_4, CO, CO_2, HCN, C_2H_2, C_2N_2, C_2H_4, C_3H_4, C_2H_6, C_3H_8, C_3HN, and C_4H_2.

This work was done by Christopher R. Webster, Reinhard Beer, and Stanley P. Sander of Caltech for **NASA's Jet Propulsion Laboratory**. *For further information, Circle 65 on the TSP Request Card.*

Inquiries concerning rights for the commercial use of this invention should be addressed to the Patent Counsel, NASA Resident Office-JPL [see page 12]. Refer to NPO-17095.

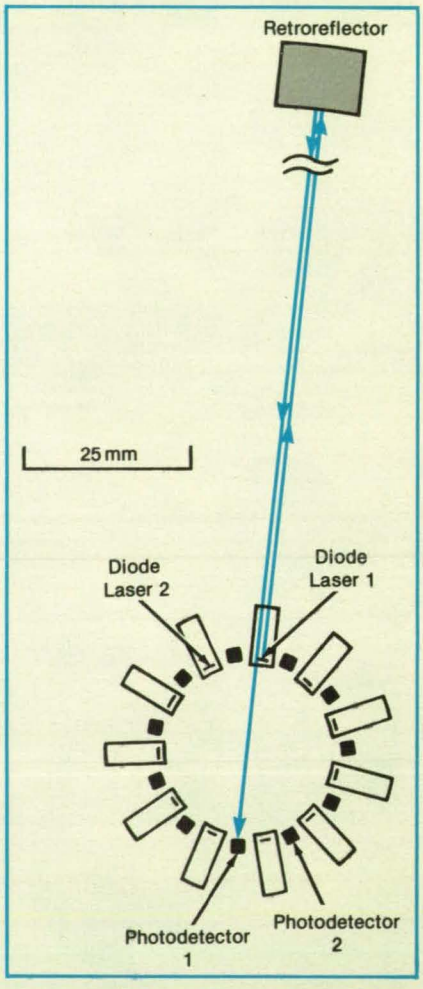

An **Array of Laser/Photodetector Pairs** would measure the infrared absorption spectrum of the atmosphere along the probing laser beams.

Multitemperature Cryogenic Radiative Cooler

Multiple radiator stages separated by V-groove shields protect a main cooler from parasitic heat radiation and offer usable cooling themselves.

NASA's Jet Propulsion Laboratory, Pasadena, California

A proposed cryogenic radiative cooler would achieve lower temperatures than previously possible with passive radiators in space. In addition, it would provide useful cooling power at several temperatures instead of just one. This device might be used on many planned future space missions that carry infrared detectors, or other science instruments, which must be

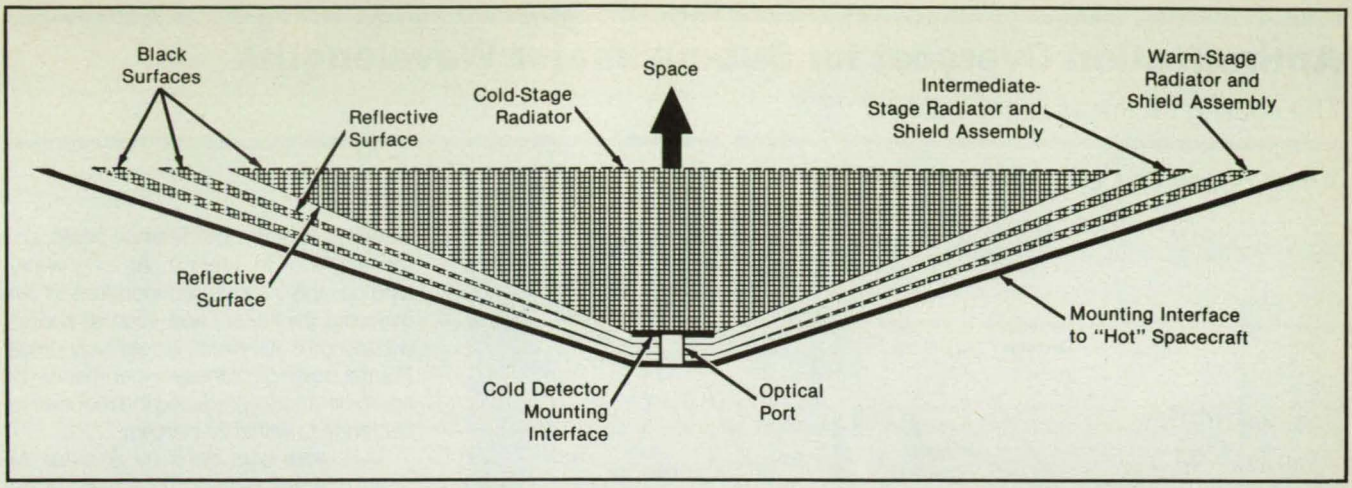

The **Cold-Radiator Stage** is protected by multiple shield assemblies that intercept radiation heat leaks from the warmer supporting structure and redirect it out to space. Each shield assembly has an effective cooling capacity of its own, enabling it to cool optical filters, for example.

cryogenically cooled to obtain adequate detector sensitivities.

The radiator would consist of several nested aluminum pyramids (see figure). The innermost pyramid is the cold stage of the radiator and would be painted black on its inner surface, allowing it to radiate heat from an infrared detector or other device placed near the vertex of the pyramid.

Surrounding the cold stage are two radiation shield assemblies. Each shield assembly consists of two aluminum pyramids, joined near their vertex. Each shield assembly protects the inwardly adjacent shield assembly from thermal radiation. The cavities between shield assemblies would have V-shaped cross sections with an included angle of about 1.5°. The side of each shield assembly that faces an adjacent shield assembly would be coated with a highly reflective, low-emissivity material such as vacuum-deposited gold. The outside surfaces of each shield assembly would thus intercept radiation from the warmer adjacent shield and reflect and redirect the radiation out to space through the cavity openings at the wide end.

The shields would thus reduce the leakage of heat from the surrounding structure, enabling the cold stage to cool to a lower temperature than would be otherwise possible. Moreover, each shield assembly would act as an intermediate radiator, having a cooling capacity of its own at temperatures between the coldest stage and the warm structure. This is achieved by either the use of a black aluminum plate at the top of each shield assembly, or by painting the inside walls of each shield assembly black.

Fiberglass bands, struts, or tubes would support the shields. These low thermal-conductance structural members would minimize conductive heat leaks to the radiator.

According to a computer model, the multistage V-groove radiator design can achieve temperatures as low as 60 K for the cooling of spaceborne infrared detectors with a 135 K intermediate stage temperature for cooling filters or optics, The 60 K cold-stage temperature is 15 K lower than that of any radiative cooler that has flown in space. These temperatures can be achieved with a reasonably small cooler, with a 450-cm^2 cold-stage area and a 400-cm^2 intermediate-stage area.

This work was done by Steven Bard of Caltech for **NASA's Jet Propulsion Laboratory**. *For further information, Circle 95 on the TSP Request Card.* *NPO-16957*

Optical Detection of Cryogenic Leaks

A conceptual system would identify leakage without requiring shutdown for testing.

Marshall Space Flight Center, Alabama

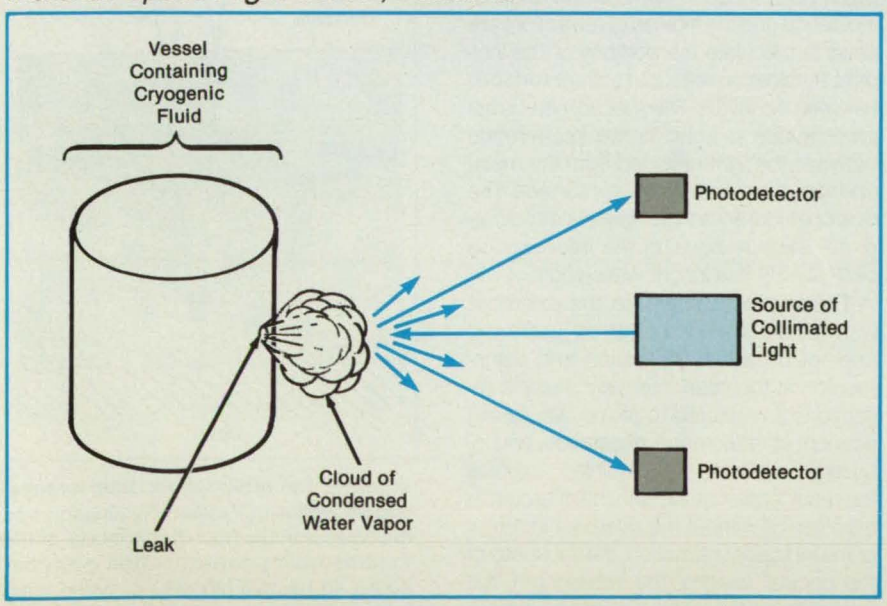

The **Fog Generated by a Leak of Cold Fluid** would be detected via light reflected from it.

A proposed device would detect and indicate leaks of cryogenic liquids automatically. The detector would make it unnecessary to shut the equipment down so that it can be checked for leakage by soap-bubble or helium-detection methods. It would not be necessary to mix special gases or other materials with the cryogenic liquid flowing through the equipment.

The leak detector would include a laser or other highly collimated bright source of light surrounded by a ring of photodetectors (see figure). A cryogenic leak condenses small drops of water and ice in the air in its vicinity. When struck by the light beam, the drops would reflect some of the light back toward the source, though not precisely along the beam axis. A portion of the reflected light would strike the ring of photodetectors.

This work was done by Lynn M. Wyett of Rockwell International Corp. for **Marshall Space Flight Center**. *No further documentation is available.* *MFS-29278*

Antireflection Overcoat for Submillimeter Wavelengths

The coating thickness is not critical.

Ames Research Center, Moffett Field, California

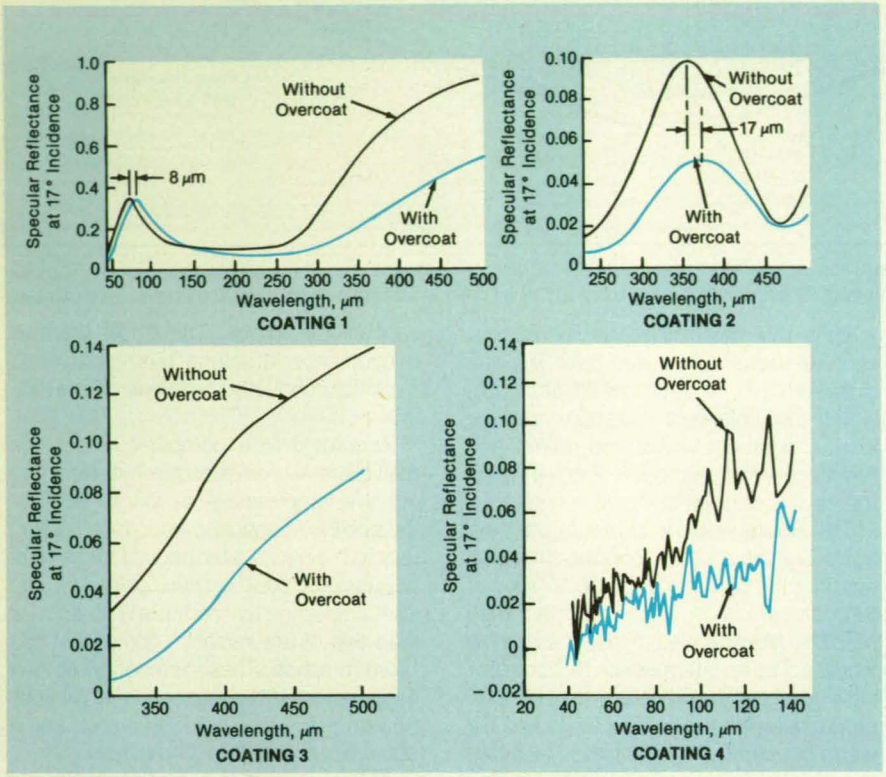

Figure 1. The **Specular-Reflectance Spectra** of four opaque coatings were measured at an angle of incidence of 17°, before and after spray application of an overcoat of polytetrafluoroethylene.

A polytetrafluoroethylene antireflection overcoat reduces the specular reflectance of an opaque baffle coating by a factor of nearly 2 at millimeter and infrared wavelengths. The overcoat is easily applied by spraying Teflon® Wet Lubricant (or equivalent) on the opaque coated surface. Although this technique makes it difficult to control the thickness of the overcoat, experimental and theoretical studies indicate that thickness has little effect because the antireflective property is based on creating a graded-index absorber.

In the experiments, the polytetrafluoroethylene lubricant was applied to four opaque coatings of various thicknesses and roughnesses, using heavy sprays in the effort to obtain thick overcoats. The specular-reflectance spectra of the surfaces were measured before and after spraying, so that changes could be attributed to the overcoats. As shown in Figure 1, these spectra indicate significant decreases in reflectance, and in two samples prominent spectral features are shifted to longer wavelengths.

A first-order analysis explains the essential features of the spectra. As shown in Figure 2, the incident radiation is considered to pass through a nonabsorbing overcoat, which has a small real index of refraction n_f, and into the opaque coating, which has a large index of refraction with real part n and imaginary part k (representing absorption). The Fresnel formulas (which express reflectance in terms of the angle of incidence and the indices of refraction) are used to calculate the portions of the incident illumination reflected at the interfaces between the layers. The spectral peak is apparently due to constructive interference between the light reflected from the metal and that reflected by the outer surface. The overcoat increases the optical-path difference, thereby causing the interference peak to shift to a longer wavelength.

The wavelength where the overcoat was tested is long enough to justify the neglect of diffuse reflection and transmission at the interfaces, and multiple reflections are ignored to first order. Taking account of reflectance, absorption, and interference effects, it is possible to express the ratio of reflectance with the overcoat to reflectance without the overcoat in terms of the indices of refraction, the thickness of the original coating, the wavelength, the thickness of the overcoat (or the shift in wavelength of the interference peak), and the angle of incidence. At long wavelengths, this ratio is independent of the overcoat thickness, and even at shorter wavelengths its effect is relatively small. For the coatings of these experiments, the first-order model predicted the reduced reflectance to within 26 percent.

This work was done by Sheldon M. Smith of **Ames Research Center**. *Further information may be found in NASA TM-88219 [N86-28730/NSP], "A Simple Antireflection Overcoat for Opaque Coatings in the Submillimeter Region."*

Copies may be purchased [prepayment required] from the National Technical Information Service, Springfield, Virginia 22161, Telephone No. (703) 487-4650. Rush orders may be placed for an extra fee by calling (800) 336-4700.

Inquiries concerning rights for the commercial use of this invention should be addressed to the Patent Counsel, Ames Research Center [see page 12]. Refer to ARC-11718.

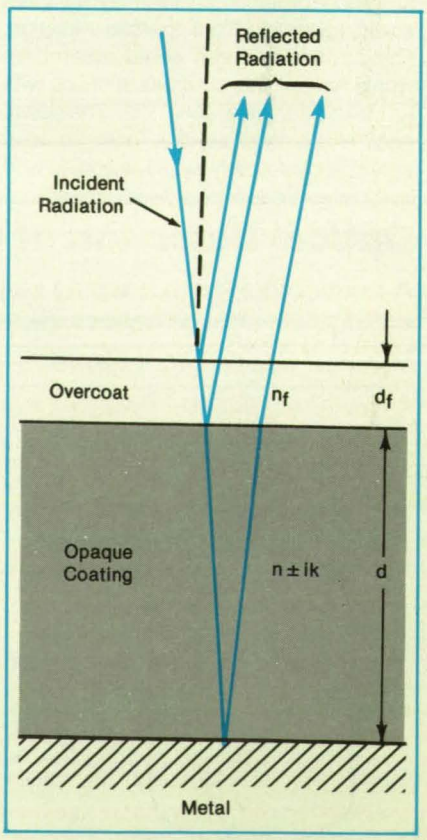

Figure 2. The **Attenuation, Interference, and Reflection** of incident illumination was analyzed with the help of this model of the nonabsorbing antireflection overcoat above an opaque (absorbing) baffle coating.

Standards for Bidirectional Reflectance and Transmittance

Sample-to-sample variations are reduced.

Marshall Space Flight Center, Alabama

Improved reference or standard samples for the measurement of the bidirectional reflectance or transmittance distribution functions are made by depositing single layers of spheres of the same size on flat surfaces (see figure). The new reference samples can be replicated easily and consistently, are durable with moderate care, and can be used to reconcile different measurement facilities.

The spheres, typically of glass or latex, can range in diameter from 0.1 to 500 μm. To make a reflectance standard, the spheres can be coated with gold, silver, or other highly reflective material. Transmittance samples can be made by using glass spheres with roughened surfaces.

A light beam is aimed at an unknown sample along a specified direction, and the transmitted or reflected radiance is measured along another specified direction. The measurement is repeated with a reference sample of the new type. Then the unknown sample can be characterized by $f_2 = f_1 V_2/V_1$, where f_2 and f_1 represent the bidirectional reflectance (or transmittance) distribution functions at the unknown and known samples, respectively, along the specified directions and V_2 and V_1 represent the reflected (or transmitted) radiances measured with the unknown and reference samples, respectively.

With the new standard reflectance samples, variations among and within each unit are less than those of conventional standard reflectance samples made of gold-plated sandpaper. The improved samples provide fairly uniform specular reflection in all directions. Also, unlike plated-sandpaper standards, they are not subject to random shadowing by adjacent microscopic surface features.

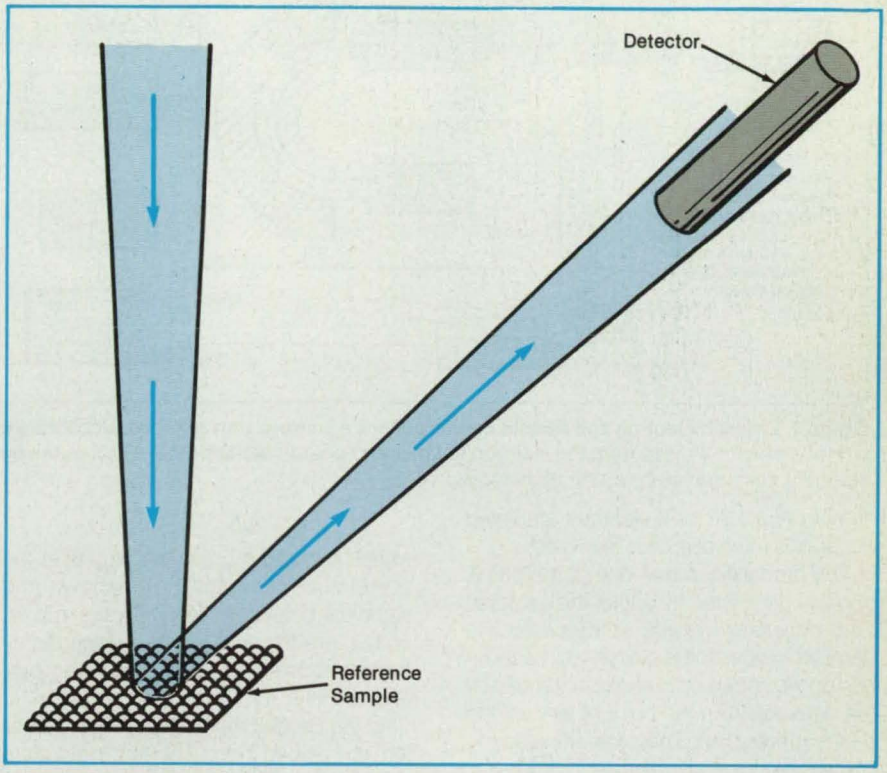

Spheres Packed on a Flat Surface are coated with reflective material and used as reflectance standards. Alternatively, translucent spheres can be used for transmittance measurements.

This work was done by William K. Witherow of **Marshall Space Flight Center**. *For further information, Circle 145 on the TSP Request Card.*

Inquiries concerning rights for the commercial use of this invention should be addressed to the Patent Counsel, Marshall Space Flight Center [see page 12]. Refer to MFS-28183.

Electron-Photon Coincidence Calibration of Photon Detectors

Absolute and relative detector efficiencies are measured.

NASA's Jet Propulsion Laboratory, Pasadena, California

An apparatus uses coincidence-counting techniques to measure the efficiency of an ultraviolet or vacuum ultraviolet detector at very low radiation intensity (in the photon-counting regime). A detector thus calibrated can be used to calibrate other detectors or to make absolute measurements of incident photon fluxes.

In the apparatus (see Figure 1) a beam of helium atoms (or any other atom) is struck perpendicularly by a beam of energetic (e.g., 100-eV) electrons. The atomic beam is made sparse enough so that it is nearly transparent to the 584-Å (21.2-eV) photons that are emitted when some of the helium atoms are struck by electrons. (Beams of other elements could also be used to measure efficiencies at other photon energies.) When an electron excites a 584-Å photon, it loses 21.2 eV of its energy, retaining 78.8 eV as it is scattered from the intersection of the beams. Photons and electrons of these and other energies are scattered in all directions.

Some of the 78.8-eV electrons continue along the original electron-beam direction, and some of the photons caused by these electrons are emitted perpendicularly to both beams toward either or both photon detectors. An electrostatic analyzer passes only the 78.8-eV electrons to an electron counter. Each electron-counting pulse is fed to the "start" input of a time-to-pulse-height converter.

The output pulses from either detector are fed through a delay line to the "stop" input of the associated time-to-pulse-height converter. The detector-output pulses that represent 584-Å photons are distinguished from those of other photons by their known correlation in time with the pulses of the causative 78.8-eV electrons scattered into the electrostatic analyzer.

The output of the time-to-pulse-height converter is fed to a pulse-height analyzer, the output of which includes a peak at the known correlation time. The measurement is continued during an interval long enough to satisfy the requirements of photon-counting statistics, and the number of counts N_c in this peak is recorded. The

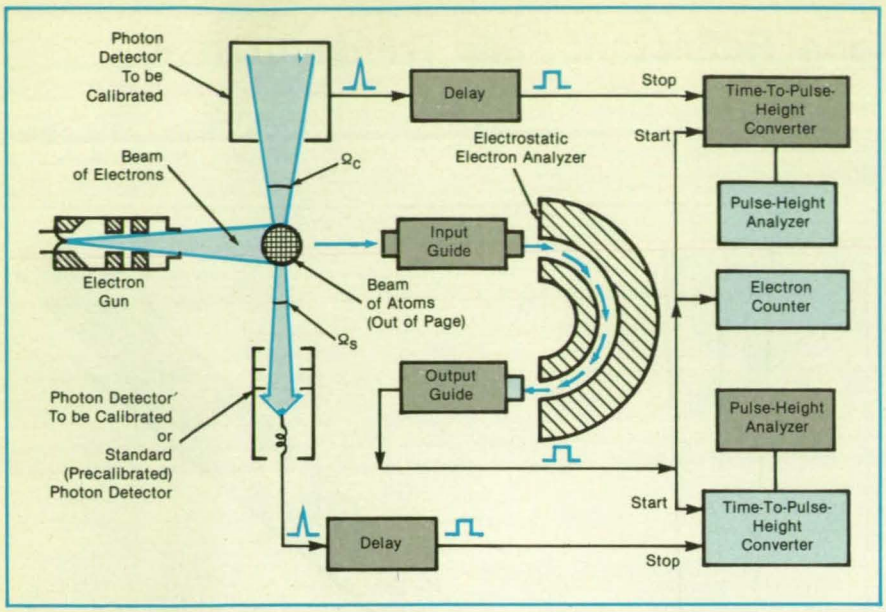

Figure 1. **Crossed Electron and Atomic Beams** generate photons that are used to calibrate a photon detector. Pulses from the electron counter and photon detector(s) are processed by standard coincidence-counting techniques.

number N_e of 78.8-eV electrons detected during this interval is also recorded.

The probability p that one of the 584-Å photons generated by one of the detected 78.8-eV electrons will scatter into the detector in question is calculated, based in part on the known solid angle subtended by the detector from the point of view of the beam intersection. Then the efficiency, η, of the detector is given by

$$\eta = N_c/pN_e$$

If the efficiency η_s of a detector (the standard detector) has already been measured, then it can be used to measure the efficiency η_u of an unknown detector in two ways. In the first, the measurement is made on the calibrating apparatus, without recording the electron count. The efficiency of the unknown detector is given by

$$\eta_u = \eta_s N_{cu}\Omega_s/N_{cs}\Omega_u$$

where N_{cu} and N_{cs} are the counts in the correlation peaks of the unknown and standard detectors, respectively, and Ω_s and Ω_u are the solid angles subtended by the standard and unknown detectors, respectively.

In the second method (see Figure 2), filters are placed in front of the detectors to pass only the 584-Å photons. Since the calibration of the standard detector is good for all 584-Å photons, it suffices to count all the photon pulses N_u and N_s put out by the unknown and standard detectors, respectively, without having to measure electrons or correlations. Then the efficiency of the unknown detector is given by

$$\eta_u = \eta_s N_u\Omega_s/N_s\Omega_u$$

This work was done by Santosh K. Srivastava of Caltech for **NASA's Jet Propulsion Laboratory**. *For further information, Circle 88 on the TSP Request Card.*

Inquiries concerning rights for the commercial use of this invention should be addressed to the Patent Counsel, NASA Resident Office-JPL [see page 12]. Refer to NPO-15644.

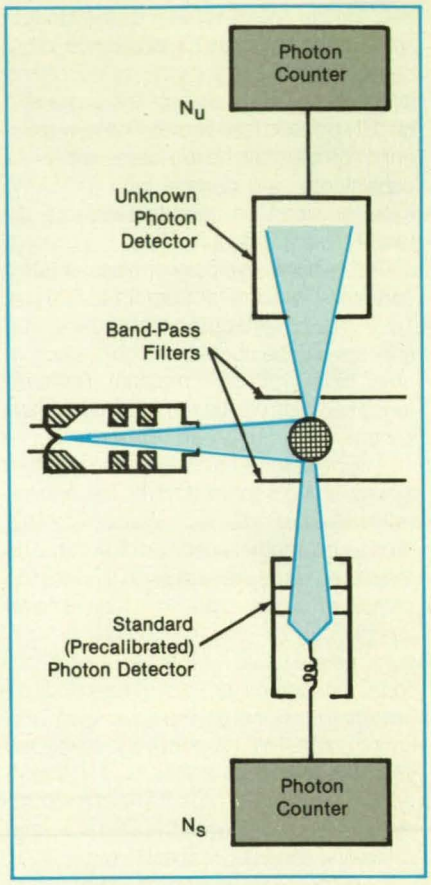

Figure 2. A **Standard Detector Is Used To Calibrate** an unknown detector. In this case, the photons are band-pass-filtered and the coincidence-counting circuitry is not used.

Books and Reports

These reports, studies, handbooks are available from NASA as Technical Support Packages (TSP's) when a Request Card number is cited; otherwise they are available from the National Technical Information Service.

Monitoring the Atmosphere by Diode-Laser Spectroscopy

Dilute constituents are detected with speed and accuracy.

A report describes the state of the art of tunable-diode-laser second-harmonic spectroscopy applied to measurements of the concentrations of trace constituents of the atmosphere. By a combination of temperature, composition, and drive-current tuning, the wavelengths of tunable diode lasers can be varied over the infrared range of 3 to 30 μm, which contains spectral lines of many of the molecules of interest in atmospheric research. Recent advances in fabrication have provided experimenters with quasi-single-mode diode lasers of relatively high power (0.1 to 10 mW) that operate at temperatures above 77 K; these lasers are readily adapted to compact, automatic, portable instruments.

In general harmonic spectroscopy, the infrared frequency of the laser-diode source is modulated, usually by modulating the diode current at a frequency of 1 to 5 kHz. The center infrared frequency might be scanned by slowly varying the dc component of the diode current, or the laser might be locked to a spectral line, depending on the requirements of the measurement.

In first- and second-harmonic spectroscopy, the laser signal that has traveled along a path in the atmosphere is detected by a phase-sensitive amplifier at the first or second harmonic of the modulating frequency, respectively. The second harmonic is the most useful one for the quantitative detection of molecules, because the peak values of its detection signature lie at the centers of the molecular spectral lines and its average baseline lies near a zero signal level. The first harmonic is useful in the line-locked mode because its detection signature has a steep zero crossing at the center of the spectral line that can be used as a negative feedback signal to control the diode current.

Because they are designed to detect laser-beam absorptions typically less than 1 percent, second-harmonic trace-gas detectors are inherently linear over wide dynamic ranges. When the second-harmonic signal is normalized by the beam energy, the linearity extends up to absorptions of 10

percent. This high linearity facilitates calibration and the analysis of measurement data.

In addition to exceptional sensitivity, second-harmonic spectroscopy offers high selectivity. For example, such small molecules as CO and NO_2 have isolated, strong spectral lines that are free of spectral interferences from the other constituents of the atmosphere. Because the spectral lines of diode lasers are typically less than one-tenth of the Doppler widths of near-infrared molecular absorption lines, nearby lines of fairly-abundant atmospheric molecules produce negligible interferences.

In a typical instrument, the laser beam is split into three paths: (1) through a reference cell, (2) through a local ambient region (to provide an instrument zero reference), and (3) through a multiple-reflection cell where it acquires the atmospheric information. The instrument is operated in both line-locked and scanning modes. In the line-locked mode, the reference cell provides a locking first-harmonic signature. In the scanning mode, the reference cell provides the reference spectral line(s) for the gas(es) sought.

Measurements taken with such instruments have yielded data on such important trace constituents as NO_2, NO, CO, O_3, H_2O_2, and HCl. As the interactions among weather, pollution, and photochemical processes come under increasing scrutiny, the broad tunability and speed of diode lasers will become increasingly valuable. It should be relatively easy to deploy instruments containing manifolds of lasers to satisfy the increasing demand for simultaneous measurements of multiple constituents.

This work was done by Max Loewenstein and James Podolske of **Ames Research Center**. *To obtain a copy of the report, "Diode Laser Harmonic Spectroscopy Applied to In Situ Measurements of Atmospheric Trace Molecules," Circle 157 on the TSP Request Card.*

Inquiries concerning rights for the commercial use of this invention should be addressed to the Patent Counsel, Ames Research Center [see page 12]. Refer to ARC-11775.

Effective-Mass Theory for Inhomogeneous Semiconductors

The effective masses of conduction electrons and holes should not depend on their positions.

A series of five papers present derivations in effective-mass theory for semiconducing materials of gradually varying spatial composition. In the first of a three-part series of papers entitled "Position-Dependent Effective Masses in Semiconductor Theory," the concept of spatially-varying effective masses is reviewed and shown to be unworkable. An extension of Bargmann's theorem is derived to show that the Hamiltonians representative of carriers with position-dependent masses are not invariant under a Galilean transformation. Furthermore, the approximation can give rise to many nonequivalent Hamiltonians as long as the concept of position-dependent effective mass is maintained.

The second paper considers a compound semiconductor that has a gradual spatial variation of composition. An effective-mass equation governing the dynamics of the motion of electrons or holes is derived using the Kohn-Luttinger representation and canonical transformations. It is shown that as long as the variation in chemical composition may be treated as a perturbation, the effective masses become independent of position.

The third paper shows that the effective masses depend on an average of the chemical composition over the entire crystal. In effect, the plane wave of an excited electron "samples" the entire crystal. Thus, a compound of nonuniform composition must be considered as a single quantum system, not as a collection of successive systems, each with its own effective mass.

The first of a pair of papers entitled "Forces Acting on Free Carriers in Semiconductors of Inhomogeneous Composition" shows that it is incorrect to apply the extended Wannier-Slater theorem using spatially changing effective masses. A perturbation method that begins with a model Hamiltonian representative of a homogeneous sample is then derived, and it is shown that the quasi-electric fields experienced by the carriers arise from positional changes of the potential energy just as in the classical case of deformation potentials.

The second paper of the pair shows that the quasi-electric fields due to spatial variations in chemical composition do not depend explicitly on the temperature, as had been believed. In extrinsic material, the quasi-electric field due to the majority carriers is almost completely screened out, irrespective of variations in the doping level, as long as there is no transition between *p*-type and *n*-type material. Therefore, the effective quasi-electric field experienced by the minority carriers under the conditions of low-level injection is determined solely by a variation of the bandgap energy with position.

This work was done by Oldwig Von Roos of Caltech for **NASA's Jet Propulsion Laboratory**, *Daniel Schechter of California State University, and Harry Mavroumatis of American University. To obtain a copy of the compendium, "Effective Mass Theory for Semiconductors of Variable, Position-Dependent Chemical Composition," Circle 83 on the TSP Request Card. NPO-16807*

Study of Large Telescopes

Design considerations for segmented mirrors are explored.

A document considers the selection of a suitable telescope for an advanced space laboratory. It analyzes and compares two- and four-mirror telescopes, both of which are practical and structurally similar. The document emphasizes the analysis of four-mirror telescope systems, since the design and performance characteristics of two-mirror telescopes are already well known. Three-mirror systems are not considered because their configuration is awkward, and the accessibility of their images is poor.

The criteria used to compare telescope designs include the residual aberrations as a function of the field angle and the effects of mirror misalignment on the quality of the image. The document notes that a Cassegrain configuration has the obvious advantages of a two-mirror configuration: it is simple and compact and requires only two reflections. However, it forms an image of good quality only on a highly curved focal surface. Even if rigorously corrected for spherical aberration, a Cassegrain telescope with a spherical primary mirror is essentially a zero-field system. Therefore, it may be useful as a beam expander but not as an imaging instrument.

A four-mirror telescope in a quasi-Cassegrain configuration not only produces an image quality comparable to that of a long-focal-length Cassegrain telescope but does so in a much-desired flat field. Its two additional reflecting surfaces enable a high degree of correction, even with a spherical primary mirror.

A large unitary primary mirror makes a telescope heavy and difficult to manufacture and transport. The difficulties can be alleviated by making the large mirror in segments. This reduces the overall weight because the minimum required thickness of a mirror is roughly proportional to its size; the total weight of segments would be less than that of a unitary primary.

The segments of the primary mirror must be aligned. This is less of a problem for spherical than for aspherical mirrors. An aspherical surface requires four independent motions — one radial and three angular — to correct an image mismatch. A segment of a spherical surface, on the other hand, requires only two angular motions. Thus, a spherical primary mirror may be preferred in some instances, even though a paraboloidal primary mirror would have superior wide-field performance and would be less sensitive to misalignments of the tertiary and quaternary mirrors.

The document includes a section on the point-spread functions of rectangular and multiple circular apertures. Though the point-spread functions of single circular

apertures are well known, a single noncircular aperture or multiple circular or noncircular apertures may be preferable in the large telescope on account of physical contraints on design or operation, to reduce costs, or to obtain the highest possible resolution for a given total area.

The report concludes by giving the major design parameters of an afocal Cassegrain telescope with lag-angle compensation for use in ranging experiments. This telescope would have a paraboloidal primary reflector of 1.25-m diameter and 4.00-m vertex radius. The secondary mirror would be a paraboloid with a diameter of 6.25 cm and a vertex radius of 20 cm.

This work was done by Dietrich Korsch of Korsch Optics, Inc., for **Marshall Space Flight Center**. *To obtain a copy of the report, "An Optical Technology Study on Large Aperture Telescopes," Circle 104 on the TSP Request Card.*
MFS-27143

Formula for Evaluation of Nickel/Hydrogen Cells

Theoretical and empirical results are well correlated.

Part of the standard practice for the evaluation of a battery or group of electrochemical cells is to display complete discharge curves that show the changes in the behavior of each cell during its life as well as the differences among the cells. Changes associated with the discharge curves give insight to the gross properties of the cells. However, when many cells are being investigated, the data-processing and trend-analysis procedures become unmanageable without suitable mathematical techniques. An equation that describes the various characteristics of the discharge shape would make it possible to assign definitive attributes to the discharge curve. This reduces the quantity of information to be assimilated to a manageable amount, and it allows the use of other mathematical procedures to elucidate further the changes in the curves.

To achieve these results, an equation has been developed to give a quantitative relationship among the voltage-versus-time discharge curves. This equation quantifies the initial exponential voltage decay, the rate of decay of voltage, the overall voltage shift of the curve, and the total capacity of the cell at the given discharge current. The equation has been applied to 11 nickel/hydrogen boilerplate cells that have been cycled to an 80-percent depth of discharge, and the results of the equation correlate well with the empirical results.

This work was done by Harold F. Leibecki of **Lewis Research Center**. *Further information may be found in NASA TM-88803 [N86-31680/NSP], "A Mathematical Approach for Evaluating Nickel/Hydrogen Cells."*

Copies may be purchased [prepayment required] from the National Technical Information Service, Springfield, Virginia 22161, Telephone No. (703) 487-4650. Rush orders may be placed for an extra fee by calling (800) 336-4700.
LEW-14537

Impingement of Rocket Exhaust

A computer program calculates forces, heating, and contamination.

A report presents the theoretical basis of the Source Flow Impingement Program (SFPLIMP), a computer program that analyzes the impingement of exhaust from several rocket engines on nearby surfaces in a vacuum. SFPLIMP is designed to calculate quickly the undesired forces, heating, and contamination caused by firing attitude-control jets toward other surfaces of a controlled spacecraft.

To standardize the numerical integration and facilitate changes in the configuration of the rocket engines and the target surfaces to be analyzed, the target surfaces are represented by a simplified geometrical model comprising simple subshapes including right triangles, rectangles, circles, circular cones, circular cylinders, spheres, and polynomials of revolution. Each subshape surface is divided into small areas (integration elements). With the help of three interrelated coordinate systems, the orientation of each element with respect to the local flow field is determined, and the local properties of the flow field and its impingement on the element are calculated.

The limiting angle of divergence of the flow from a rocket nozzle is calculated from the Prandtl-Meyer expansion function, which expresses this angle as a function of the nozzle-exit mach number, the angle of divergence of the nozzle, and the ratio of specific heats of the exhaust gas. The mach number is obtained from another equation that involves the throat and exit cross-sectional areas of the nozzle and the ratio of specific heats.

In the flow field, the exhaust is treated as moving radially outward from a point in the nozzle. The flow field is divided into three regions, in each of which the impingement on a target surface is modeled differently: a high-density continuum region near the nozzle (where the molecular mean free path is less than a tenth of a characteristic length of the region), an intermediate-density transition region (molecular mean free path from one-tenth to ten times a characteristic length), and a far-field free-molecular region (molecular mean free path greater than ten times a characteristic length).

The forces and moments due to impingement are calculated by direct integration of the flow pressure on each element of each subshape. The impinging flow is assumed to turn parallel to the surface. Free-molecular coefficients of pressure and shear model the forces of impingement in the far field. An empirical equation smoothes the transition between the free-molecular and continuum regions.

In the continuum region, normal- and oblique-shock formulations are incorporated into SFPLIMP to model the shock adjacent to the surface. Both the density and velocity of the unperturbed flow are expressed as products of radius- and angle-dependent functions obtained by interpolation in tables of data that originated in a more sophisticated analysis of the continuum flows from reaction-control-thrustor rockets. The dynamic pressure is computed from the density and velocity and used to compute the force of impingement on each subshape.

In the continuum region, convective laminar and turbulent boundary-layer heating rates are computed for each surface element. In the far field, molecular energy fluxes are used to calculate net heating rates. A surface is assumed to be contaminated by a constituent of the exhaust when the partial pressure of that constituent is greater than its critical vapor pressure when the rate of its impingement on the surface exceeds its rate of evaporation from the surface.

This work was done by Bret G. Drake and Kenneth S. Leahy of McDonnell Douglas Corp. for **Johnson Space Center**. *To obtain a copy of the report, "Plume Impingement Analysis," Circle 121 on the TSP Request Card.* *MSC-21352*

Thermal Conductances of Metal Contacts

Data may aid the design of cryogenic instruments.

A report presents the results of measurements of the thermal conductances of aluminum and stainless-steel contacts at temperatures from 1.6 to 6.0 K. The contacts had surface finishes characterized by root-mean-square (rms) roughnesses in the range of 0.1 to 1.6 μm. The measurements provide data for the prediction of the thermal conductances of bolted joints in cryogenic infrared instruments.

The measurement apparatus included a gearmotor assembly connected to a rocker arm by music wire to load the sample pair with forces up to 670 N. A heater was placed above the upper sample. Germanium resistance thermometers in the upper and lower samples measured the temperature difference across the interface over a range of heater powers from 0.1 to 10.0 mW. The thermal conductance was calculated from the temperature difference.

As in earlier measurements of copper and brass samples, the thermal conduct-

ances increased according to a simple power law function of temperature: $k = \alpha T^n$, where k is thermal conductance, T is temperature, and α and n are constants determined empirically with the help of a computer program. Thermal conductances also increased asymptotically with applied contact forces and were found to depend on the surface finishes of the samples. The maximum contact conductance for stainless steel was found in samples having an rms surface roughness of 0.4 μm. For aluminum, the conductance is lowest for this surface finish. The reason for this behavior at this surface finish remains unknown.

This work was done by L. J. Salerno, P. Kittel, and F. E. Scherkenbach of **Ames Research Center** *and A. L. Spivak of Trans-Bay Electronics, Inc. To obtain a copy of the report, "Thermal Conductance of Pressed Aluminum and Stainless Steel Contacts at Liquid Helium Temperatures," Circle 84 on the TSP Request Card.*

Inquiries concerning rights for the commercial use of this invention should be addressed to the Patent Counsel, Ames Research Center [see page 12]. Refer to ARC-11777.

Long-Lived Glass Mirrors for Outer Space

Design criteria for these mirrors are more stringent than for terrestrial mirrors.

A paper summarizes the available knowledge about glass mirrors for use in outer space. The paper draws on terrestrial experience with glass mirrors and on tests in space to provide guidance for the design of long-lived reflectors.

The authors note that considerable terrestrial experience has been gathered over the past decade on the fabrication, handling, environmental exposure, and evaluation of glass mirrors for such applications as solar power generation. The strengths and weaknesses of various types of first and second reflective surfaces have been identified. From this vast technology, criteria have evolved for the design and manufacture of long-lived terrestrial mirrors. Generally, the fabrication and handling techniques for Earth solar mirrors can be used for space mirrors, though additional technology will have to be developed.

Second-surface glass mirrors for use in outer space must be designed to different criteria that are more stringent than those for terrestrial mirrors. Protons, electrons, cosmic rays, meteorites, and orbiting space debris will affect the longevities of the components. Contamination — a major consideration on Earth — may also be a factor in space in many cases.

The primary source of contamination in space will be rocket plumes. To minimize problems, a surface coating should be chosen to provide a low-energy surface and, of course, to be compatible with cleaning agents. The surface coating should also reduce the effects of atomic oxygen and the buildup of electric charge.

Because debris in space can damage mirrors, it is preferable to make each mirror in many small segments that can be replaced individually. For a similar reason and to facilitate construction and alignment, segmented mirrors are also becoming accepted for use on Earth.

This work was done by Frank L. Bouquet and Carl R. Maag of Caltech and Philip M. Heggen of Energy General for **NASA's Jet Propulsion Laboratory**. *To obtain a copy of the report, "Design Considerations for Long-Lived Mirrors for Space," Circle 105 on the TSP Request Card. NPO-17047*

Estimating Electron Content of the Ionosphere

An empirical method is used for local or global monitoring.

A report presents a method for the estimation of the total electron content of the ionosphere. Estimates of the total electron content are important for precise deep-space navigation, since total electron content contributes to the delay experienced by electromagnetic waves traversing the ionosphere. These estimates are also important in evaluating data from radio-science experiments on space missions.

The method is based on measurements of signals transmitted from global positioning satellites (GPS's). Ionospheric delays are obtained by measuring the differential arrival times of signals at two different frequencies. Since the GPS observations cover only certain regions of the sky, the location of a space probe to be calibrated might not overlap the GPS field of view. Therefore certain assumptions are made about the behavior of the ionosphere so that the total electron content can be estimated in any direction from the receiver.

In this report, the ionosphere is modeled as a spherical shell at an altitude of 350 km above mean sea level. The total vertical electron content is modeled locally as a function of lateral distance, and a mapping function converts the vertical to the total line-of-sight electron content.

It is assumed that the electron content is constant in time for the duration of the observation session in a geocentric solar reference frame oriented along the Sun/Earth axis. For that observation session, the electron content is approximated by a six-coefficient, second-order polynomial in Earth-centered solar spherical coordinates. A least-squares fit is applied to all observations to estimate the six coefficients as well as the offset delays of the GPS transmitters.

The report briefly describes the estimation technique and experimental results. It discusses the mathematical model employed in the method. Finally, it suggests possible improvements.

This work was done by G. E. Lanyi of Caltech for **NASA's Jet Propulsion Laboratory**. *To obtain a copy of the report, "Ionospheric Electron Content Prediction From SERIES/GPS Data," Circle 141 on the TSP Request Card. NPO-16923*

Approximations for Predicting Electrostatic Discharges

Electrostatic field strengths are estimated for assorted electrode shapes.

A report provides approximate equations for the capacitances and ratios of maximum electrostatic field strengths to potentials of variously shaped electrodes in the vicinity of ground planes. The maximum-field-strength/potential ratio of a given electrode is used in conjunction with the measured or estimated potential to determine whether a discharge is likely. The capacitance and potential give a measure of the maximum energy that could be released and, therefore, the maximum damage that could be done by a discharge.

For purposes of analysis, the medium between the electrode and the ground plane can be a neutral gas, a vacuum, or an uncharged, homogeneous, isotropic solid insulator. In many practical configurations, the electrode has a radius of curvature R on the tip facing the ground plane, and the tip lies at a distance L from the ground plane. A useful approximation that gives a fairly reliable estimate (typically within 20 percent) of the correct ratio is

$$V/E = LR/[(2L/3) + R]$$

where V is the potential of the electrode with respect to the ground plane and E is the electric field at the apex, where breakdown is likely to start.

Although the strongest field usually occurs at the apex, it is sometimes useful to know the field strength at other points. The report gives approximate equations for the field strength and potential at points on and off the axis of symmetry of the electrode. Approximate integral equations are also given for the capacitance of an electrode that is convex everywhere.

The report discusses the importance of surface deformities and discharge mechanisms. On a microscopic scale, the protuberances of ordinary surface roughness can act as small-radius, field-concentrating electrodes in their own right and may have to be considered as such in the approximate equations.

This work was done by Larry D. Edmonds of Caltech for **NASA's Jet Propulsion Laboratory**. *To obtain a copy of the report, "Approximations Useful for the Prediction of Electrostatic Discharges for Simple Electrode Geometries," Circle 122 on the TSP Request Card. NPO-17065*

Materials

Hardware, Techniques, and Processes

Ceramic Fabric Coated With Silicon Carbide

The material can be used as a high-temperature shell.

Ames Research Center, Moffett Field, California

A ceramic fabric coated with silicon carbide (SiC) serves as a tough, heat-resistant covering for other refractory materials. Developed to protect the reusable insulating tiles on advanced space transportation systems, the covering might also be used on furnace bricks or on insulation for engines.

The new covering makes a protective glaze unnecessary. Because of its brittle character, the glaze affords only minimal protection against impacts and can crack and spall.

The SiC coated fabric adds no more weight to the tile and may withstand temperature up to 3,000 °F (1,650 °C), whereas the glaze can withstand only 2,300 to 2,700 °F (1,260 to 1,480 °C). The coated fabric can be formulated with the required heat-emissivity properties. It is isolated from the tile, and it is fastened to the tile in a way that compensates for the differences in thermal expansion between the two.

The fabric is woven from fibers of alumina/boria/silica composition. It is formed into a top-hat shape (see figure). The SiC is applied to the formed fabric by chemical vapor deposition. The amount of SiC deposited depends on the temperature of the vapor reaction, the time in the reactor, and the nature of the fabric substrate. The finished rigid covering is attached to the tile by integral pins or clips or by pin of a ceramic similar to the tile material.

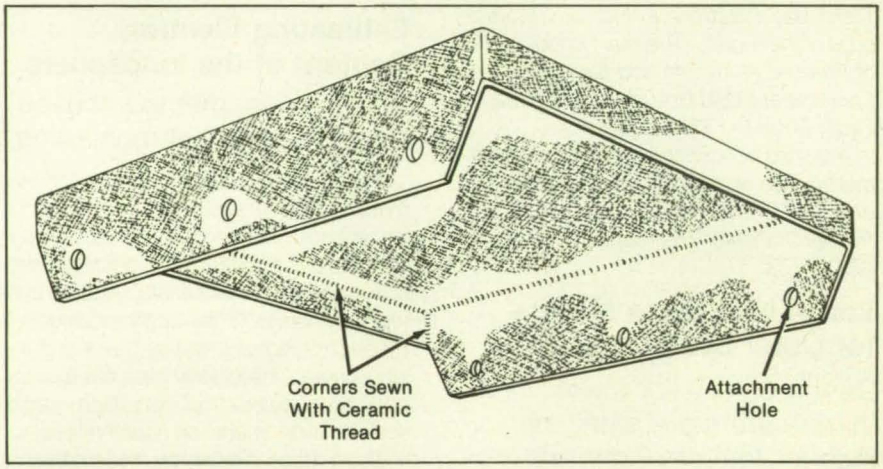

A **Shell of Ceramic Cloth** is sewn together. A coating of SiC is then deposited on the shell. The product has a mass of about 0.4 lbm per square foot of surface area (2 kg/m^2).

This work was done by S. R. Riccitiello, M. Smith, H. Goldstein, and N. Zimmerman of **Ames Research Center**. *For further information, Circle 152 on the TSP Request Card.*

Inquiries concerning rights for the commercial use of this invention should be addressed to the Patent Counsel, Ames Research Center [see page 12]. Refer to ARC-11641.

Improved Zirconia Oxygen-Separation Cell

The cell structure distributes feed gas more evenly for more efficient oxygen production.

NASA's Jet Propulsion Laboratory, Pasadena, California

A new cell configuration promises to raise the efficiency of oxygen production in solid-electrolyte zirconia cells. The new cell structure would ensure a more uniform feed pressure over the electrolyte surface.

Zirconia-membrane electrolytic cells may eventually replace cryogenic equipment in producing oxygen for such industrial applications as steel manufacturing. Some separation processes use refrigeration that typically consumes large amounts of electrical energy for liquefying air and distilling oxygen from it. The zirconia process has no moving parts, requires less electrical energy, and can use waste heat or coal to maintain the operating temperature of 375 to 1,200 °C.

In the basic zirconia cell, the solid-electrolyte membrane is an impervious ceramic disk composed of zirconium oxide and yttrium oxide stabilizer. Both faces of the disk are clad with a pervious layer of platinum or other metal. A voltage is applied to these electrodes while the disk is heated to the operating temperature. The feedstock (usually air, although such other oxygen-rich materials as sulfur trioxide or nitrous oxide may be used) flows along one face of the disk. Under the influence of the electric field across the disk, oxygen ions move through the disk and emerge through its opposite face as gaseous oxygen.

Until now, the efficiency of the zirconia cell has been only about 2 percent. However, the cell efficiency depends critically on the uniformity of the oxygen partial pressure on the input side of the cell. The proposed new cell structure is expected to distribute the feedstock more evenly, thus ensuring a more uniform pressure.

In the new cell structure (see figure), impervious electrodes form the top and bottom layers of a sandwich composed of a feedstock distributor, porous ceramic spacers, and a zirconia membrane. The

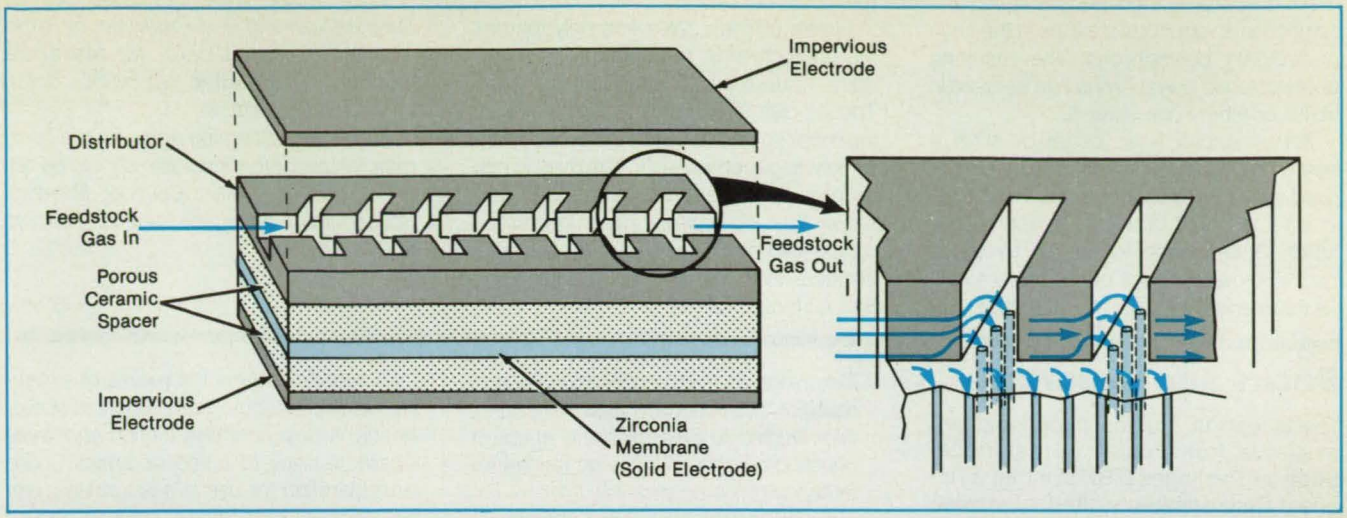

A **Multilayer Cell Structure** containing passages, channels, tubes, and pores will help to distribute pressure evenly over a zirconia electrolytic membrane. The resulting more uniform pressure distribution is expected to improve the efficiency of oxygen production.

spacers are made of mixed metal oxides that are electrically conductive so that they can apply the requisite voltage to the membrane. The distributor is made of a similar material.

The distributor contains a central passage with oblique channels. The channels communicate with the adjacent ceramic spacer through many narrow holes. The porous ceramic spacer contains a multitude of passageways that help to distribute the feedstock more evenly to the zirconia membrane below it.

Oxygen ions migrate through the membrane and, reconstituted as oxygen atoms and molecules, enter the lower ceramic spacer and exit through a port for storage or use. Not all the oxygen in the feedstock is removed through the membrane. The excess feedstock passes from the distributor to an outlet manifold. From the manifold, it may be fed to other cells, exhausted, or recirculated.

This work was done by John V. Walsh and James G. Zwissler of Caltech for **NASA's Jet Propulsion Laboratory**. *For further information, Circle 128 on the TSP Request Card.*

Title to this invention has been waived under the provisions of the National Aeronautics and Space Act [42 U.S.C 2457(f)], to the Caltech/JPL. Inquiries concerning licenses for its commercial development should be addressed to

Edward Ansell
Director of Patents and Licensing
California Institute of Technology
1207 East California Boulevard
Pasadena, CA 91125

Refer to NPO-16161, volume and number of this NASA Tech Briefs *issue, and the page number.*

Rust Inhibitor and Fungicide for Cooling Systems

A mixture of benzotriazole, benzoic acid, and a fungicide prevents the growth of rust and fungus.

Marshall Space Flight Center, Alabama

A water-based cooling mixture made from readily available materials prevents the formation of metallic oxides and the growth of fungi in metallic pipes. The coolant remains clear and does not develop the thick sludge that tends to collect in low points in cooling systems with many commercial rust inhibitors. The coolant is compatible with iron, copper, aluminum, and stainless steel, but it cannot be used with cadmium or cadmium-plated pipes.

The recommended component concentrations and concentration ranges for the coolant are the following:

- Benzotriazole — 0.15 to 0.25 weight percent,
- Benzoic acid — 0.075 to 0.15 weight percent,
- Fungicide —>1 liter per gallon (0.26 parts by volume), and
- Water— balance

Any commercial fungicide can be used. The pH of the mixture is in the range of 2.5 to 4.5; the conductivity is in the range of 200 to 400 μmho/cm.

This work was done by James F. Adams and D. Clay Greer of Rockwell International Corp. for **Marshall Space Flight Center**. *No further documentation is available. MFS-29248*

Photochromic Polyaphrons for Visualization of Flow

Drops of ultraviolet-activated dyes encapsulated in liquid films would reveal flow patterns.

Marshall Space Flight Center, Alabama

A proposed method for the visualization of flow would be nonintrusive and could be applied selectively to regions of special interest. The method would be particularly suitable for turbulent flow.

The method is based on a visualization material composed of polyaphrons containing photochromic dye. Polyaphrons are droplets of organic liquid encapsulated in a thin layer of another liquid, which holds the droplets stably by surface tension. The photochromic dye within a polyaphron acquires color temporarily after exposure to strong ultraviolet light.

Photochromic dyes ordinarily must be dissolved in nonpolar liquids and thus cannot be used directly in water. The few that work in water can be activated only by light of very short wavelength; this is impractical because such light is absorbed by the transparent plastic housings used to contain experimental flows. These obstacles are overcome by dissolving a photochromic dye in a nonpolar solvent suitable for

making aphrons, then encapsulating the solution in an aqueous shell, as in the case of ordinary polyaphrons. The resulting photochromic polyaphrons can be used in water or other polar solvents.

An ultraviolet laser beam or such a beam expanded into a sheet would be used as a light source to activate the dyes in selected flow locations at appropriate times. Other, nonphotochromic, dyes can be incorporated in the polyaphrons to act as permanent tracers or to provide contrast.

Unlike ordinary dyes and polyaphrons, the photochromic polyaphrons do not require strategically-located injection ports. These polyaphrons are always in the flowing medium and need only to be activated by light to become visible. The dyes in photochromic polyaphrons dissipate more slowly than do ordinary dyes. In addition, unlike solid particles, they can be used to visualize flow around rolling- or sliding-contact surfaces.

This work was done by M. R. Subbaraman and B. J. Ostermier of Rockwell International Corp. for **Marshall Space Flight Center**. *No further documentation is available.*

Inquiries concerning rights for the commercial use of this invention should be addressed to the Patent Counsel, Marshall Space Flight Center [see page 12]. Refer to MFS-29259.

Books and Reports

These reports, studies, handbooks are available from NASA as Technical Support Packages (TSP's) when a Request Card number is cited; otherwise they are available from the National Technical Information Service.

Fire-Retardant Decorative Inks for Aircraft Interiors

Seven retardants were investigated.

A report describes the testing of commercial and experimental fire retardants for incorporation into acrylic printing inks used on aircraft-interior sandwich panels. To avoid one of the main problems connected with the use of such fire retardant agents as antimony trioxide — the migration of the agent to the surface — attention was focused on candidate retardants that might not migrate; for example, reactive fire retardants and polymeric fire retardants in which migration or leaching is controlled by diffusion.

The seven following fire-retardant additives were investigated:

1. Brominated polymeric additive (BPA) is available at various molecular weights ranging from 660 to 40,000. Each molecular unit has two glycidyl groups and includes aromatic bromine, which is very thermostable. The BPA investigated (formulation 1) had 50 weight percent bromine.
2. Formulation 2 was BPA/tribromophenol (BPA/TBP), in which the BPA was blocked through its diglycidyl endgroups with the brominated phenols. The bromine content was 58 percent.
3. Formulation 3 — BPA/pentabromophenol (BPA/PBP) — had a bromine content of 63.0 percent.
4. Rubberized BPA/tribromophenol (formulation 4) contained 12 percent of carboxy-terminated butadiene/acrylonitrile (CTBN) rubber and enough TBP to produce a 53-percent bromine content.
5. Rubberized BPA/tribromophenol (formulation 5) was similar to 4, except that the CTBN content was increased to 16.2 percent, and that the bromine content was decreased to 48.6 percent.
6. 2,3-Dibromopropyl acrylate (formulation 6) contains 58.8 percent bromine.
7. Bis(chloroethyl) vinyl phosphonate (formulation 7), a nonbrominated compound, was studied to determine the effect of phosphorous and chlorine on the fire retardancy of the acrylate ink.

The ink formulations were adjusted to contain 10 percent bromine, except when formulation 7 was used. All ink formulations were also adjusted to contain 60 weight percent solids so that the resulting viscosities were approximately the same as those of the acrylic-ink control formulation.

Films of acrylic ink containing the fire-retardant additives were prepared by casting on glass plates. After the solvent was evaporated in a vacuum, the cast films were cured at 80 to 100 °C for 30 minutes in an air-circulating oven.

The thermochemical properties of these films were examined by thermogravimetric analysis and differential scanning calorimetry (DSC). Similarly, samples of the inks were cast on sheets of polyvinyl floride (PVF), and their limiting oxygen indices and smoke evolution were measured. The most effective fire retardant proved to be formulation 5, followed by formulations 3 and 4, which showed the highest limiting oxygen indices and the highest thermal stabilities in terms of the lowest weight losses at 280 °C.

This work was done by D. A. Kourtides of **Ames Research Center**, *Z. Nir of Makhteshim, Ltd., and J. A. Mikroyannidis of the University of Patras. Further information may be found in NASA TM-88198 [N86-18441/NSP], "Fire-Retardant Decorative Inks for Aircraft Interiors."*

Copies may be purchased [prepayment required] from the National Technical Information Service, Springfield, Virginia 22161, Telephone No. (703) 487-4650. Rush orders may be placed for an extra fee by calling (800) 336-4700.

Inquiries concerning rights for the commercial use of this invention should be addressed to the Patent Counsel, Ames Research Center [see page 12]. Refer to ARC-11729.

Lubrication and Wear of Hot Ceramics

Properties of materials for engine parts are studied.

A report presents the results of experiments on the tribological properties of ceramics. It describes the friction and wear characteristics of some ceramics under consideration for use in gas turbines, diesel engines, and Stirling engines. It also discusses the formulation of composite plasma-sprayed ceramics that contain solid lubricant additives, and data for carbide-and oxide-based composite coatings for use at temperatures up to at least 900 °C.

Ceramics do not have inherently-useful tribological properties, and surfaces must therefore be modified to achieve acceptable levels of friction and wear. Lubrication is a major challenge because the operating temperatures of ceramic engine parts are often higher than the thermal oxidation limits of oils and even of such conventional solid lubricants as graphite and molybdenum disulfide. Nevertheless, lubrication is needed not only for ceramic/ceramic contacts but also for ceramic/metal contacts.

The study includes measurements of friction and wear of selected ceramics sliding on a precipitation-hardened nickel-base superalloy at room temperature and at 800 °C to determine the lubricating effects of the oxidation of the metal. The results of a more-detailed parametric study of the effects of temperature and sliding velocity on friction and surface characteristics are also included.

None of the ceramics evaluated in unlubricated sliding contact had acceptable characteristics at room temperature. However, at 800 °C in air, the metal oxides formed on the metal provided a degree of lubrication.

Attempts to improve the tribological properties of plasma-sprayed zirconia by the addition of calcium fluoride to the coating composition were unsuccessful. Calcium fluoride additions up to 10 percent reduced friction, but increased the wear of the coating.

A composite plasma-sprayed coating based on chromium carbide with solid-lubricant additions of metallic silver and a eutectic of barium fluoride and calcium fluoride was very resistant to wear at temperatures from 25 to 760 °C in air, helium, and hydrogen. The coefficients of friction did not exceed 0.25 in hydrogen. These results suggest that the coating may be a

good candidate for a cylinder-liner material for Stirling engines that use hydrogen as the working fluid.

This work was done by H. E. Sliney, T. P. Jacobson, D. Deadmore, and K. Miyoshi of **Lewis Research Center**. *Further information may be found in NASA TM-87267 [N86-25476/NSP], "Tribology of Selected Ceramics at Temperatures to 900 °C."*

Copies may be purchased [prepayment required] from the National Technical Information Service, Springfield, Virginia 22161, Telephone No. (703) 487-4650. Rush orders may be placed for an extra fee by calling (800) 336-4700.
LEW-14595

Adhesives for Use in Vacuum, Radiation, and Cold

Data on mechanical and optical properties are compiled.

A report presents results of literature searches and tests of eight adhesives for use in the high-radiation, low-temperature, vacuum environment of the Galileo spacecraft mission to Jupiter. The adhesives, intended for use as bonding agents for thermal blankets, instruments, structural members, and coatings, were exposed to protons and electrons.

The adhesives were tested for contamination, reflectance, bond integrity, color, transmittance, outgassing, dielectric constant, coefficient of thermal expansion, optical interference, peel strength, and shear strength. Some of the tests were conducted at the temperature of liquid nitrogen (−150 °C).

In various degrees, all the adhesives performed satisfactorily. On the basis of tensile strength, the one used on an embossed aluminum tape (3M-1267 or equivalent) proved superior to the one used on copper tape (3M–X1245). Although the 3M adhesives lose their strengths at radiation doses orders of magnitude below the external Jovian dose, the metals in the tapes shield the adhesives sufficiently to reduce the internal doses to acceptable values.

The results of the investigation are given in tables and graphs. Suggestions for improving characteristics of adhesive bonds with new materials and treatments by ultraviolet irradiation and ion implantation are offered.

This work was done by Frank L. Bouquet of Caltech for **NASA's Jet Propulsion Laboratory**. *To obtain a copy of the report, "Adhesive Systems for Long Term Use at Low Temperatures," Circle 66 on the TSP Request Card.*
NPO-17034

Designing Ceramic Coatings

Design criteria are based on thermomechanical considerations.

A report summarizes the state of the art in the design of ceramic coats for metal parts in heat engines. A ceramic coat is typically used to reduce the transfer of heat from a hot gas to a cylinder wall, piston, turbine blade, or other internally-cooled metal part. This enables the use of the higher gas temperatures needed for higher efficiencies, permits the use of less cooling air, or extends the life of the metal part by reducing its temperature.

A ceramic coat can fail from a combination of differential-thermal-expansion stresses caused by the coating process and by changes of temperature during use. Tensile loads — like those caused by expansion of the substrate — give rise to cracks. Compressive loads — like those caused by excessive heating of the coat or excessive cooling of the substrate — cause the ceramic to spall in large sections.

The report describes a finite-element simulation of the elastic and plastic thermomechanical behavior of the multilayer ceramic coat on the outer-gas-path seal of a gas turbine. The main thrust of the simulation was to determine the creep and plastic strains and to superpose them to yield residual thermomechanical-stress and thermomechanical-strain fields. The numerical results showed the following:

- Severe stresses were generated in the interface zone between the metal substrate and the first ceramic layer.
- Plasticity appeared to dominate creep in the ceramic laminae closest to the substrate.
- The effects of creep and plasticity tended to combine to reduce the surface stress in the ceramic layer exposed to the hot gas.
- Significant residual thermomechanical fields were generated by the inelastic behavior.

A finite-element simulation was also done to investigate the initial stresses in a multilayer ceramic coat due to the coating process. The simulated bending moment was about 67 percent of the bending moment calculated from the warp of the experimental version of the coat, which had been removed by chemical etching.

The report discusses design analysis, design criteria, testing, fabrication, and materials. The basic criteria are the following:

- low thermal conductivity,
- substrate cooling,
- noncatalytic surfaces,
- strain-relief mechanism,
- adhesive and cohesive bonding, and
- smooth exterior surface.

Loading considerations include thermal cycling, the effects of contamination on swelling and long-term inelastic behavior, and mechanical erosion. Geometrical considerations arise in fabrication: ceramic coats are often applied by plasma spraying, which is limited to the line of sight. Geometrical considerations also affect adhesion and endurance.

The foregoing and other design and analysis criteria were applied as rules of thumb to the testing of shroud seals in a turboshaft engine. The analysis predicted that the seals would work, and the prediction was confirmed by tests. Designers will likely continue to work by such rules of thumb, pending the completion of more-detailed thermomechanical studies.

This work was done by G. McDonald and R. C. Hendricks of **Lewis Research Center**; *R. L. Mullen of Case Western Reserve University; and J. Padovan, M. J. Braun, and B. T. F. Chung of the University of Akron. Further information may be found in NASA TM-87328 [N86-25726/NSP], "Thermomechanical Design Criteria for Ceramic-Coated Surfaces."*

Copies may be purchased [prepayment required] from the National Technical Information Service, Springfield, Virginia 22161, Telephone No. (703) 487-4650. Rush orders may be placed for an extra fee by calling (800) 336-4700.
LEW-14545

Ceramic Thermal Barriers for Dirty-Fuel Turbines

Coatings like those in aircraft turbines quickly deteriorate, but alternatives are on the horizon.

A report discusses the performances of ceramic thermal-barrier coating materials for use in electric-utility gas-turbine engines. Studies show that ceramic coatings insulate metal components in turbines and allow cooling schemes to be simplified and cooling airflows to be reduced. This in turn allows the use of higher gas temperatures while decreasing the temperatures of metal components. Efficiency is thereby increased.

Such coatings have been developed for aircraft turbines. However, these ceramics are not suited to electrical utility turbines that burn "dirty" fuel. Unlike clean aircraft fuels, dirty fuels may produce condensates of sodium sulfate and vanadium salts. These compounds can rapidly attack the standard thermal barrier composed of zirconia with 6 to 8 percent yttria.

Many variations of the standard coating have been evaluated in the search for a coating resistant to dirty fuel. The variations have included alterations of the level of yttria, replacement of yttria by other stabilizers, controlling surface density (by plasma spray processing, infiltration, laser glazing, or sputtering), and interface treatments. Of these variations, laser glazing is particularly promising. The laser-melted surface of the coat is 100 percent dense, with some cracks. Such coats protect the underlying porous ceramics, enabling them to survive longer in the presence of salt condensates than do unglazed ceramic coats.

In addition, many alternatives to zirconia-based thermal-barrier coatings have been evaluated. Two promising ceramics are calcium silicate and calcium titanate. Also promising is a ceramic/metal combination composed of magnesia with an alloy of nickel, chromium, aluminum, and yttrium.

This work was done by Robert A. Miller of **Lewis Research Center**. *Further information may be found in NASA TM-87288 [N86-22687/NSP], "Ceramic Thermal Barrier Coatings for Electric Utility Gas Turbine Engines."*

Copies may be purchased [prepayment required] from the National Technical Information Service, Springfield, Virginia 22161, Telephone No. (703) 487-4650. Rush orders may be placed for an extra fee by calling (800) 336-4700.
LEW-14596

Silicones as Connector-Potting Compounds

Low outgassing is just one of the benefits of silicones.

A report evaluates silicone potting materials for electrical connectors. Silicones, the report states, offer important advantages over conventional polyurethane potting compounds: low outgassing, low flammability, and low toxicity.

The report describes tests of connector specimens made with CV-2510 and DC-6-1104 silicones with dibutyl tin dilaurate catalyst and evaluates the test results in the light of previously published test results for polyurethanes. The report discusses the requirements for connector-potting materials, the methods used to evaluate the silicones, the techniques for preparing specimens, and the results of the tests. It identifies commercial sources of silicone potting materials.

The authors emphasize the importance of correct preparation and processing of the potting materials and the parts to be potted. To obtain the best results, it is necessary to attend scrupulously to such details as cleaning and drying the parts, mixing the ingredients thoroughly in the correct proportions, removing bubbles in a vacuum, and using the proper curing times and temperatures.

This work was done by Frank L. Bouquet and Marjorie S. Bickler of Caltech for **NASA's Jet Propulsion Laboratory**. *To obtain a copy of the report, "Techniques for Fabrication of Improved Pottants for Space Electrical Connectors," Circle 120 on the TSP Request Card. NPO-17251*

The Janus/Ada Difference... More Than Just the Price!

Contrary to what you may believe, all Ada compilers are not equal. The popular misconception is that all Ada compilers are the same for any machine, just differently priced. But the price is just one of the differences. Compilation speed, the ability to emulate floating point, usability on all of the Intel 80 X 86 family, as well as support of networking sites, can make a big difference to your project. That big difference is the Janus/Ada difference!!!

Janus/Ada is substantially different from other Ada compilers. It was developed on the microcomputer, for the microcomputer, and was bootstrapped version by version. The resulting compiler is faster, more robust and more flexible than other Ada compilers. Minimizing the expenses of add-on hardware, run-time library fees and tutorials also makes Janus/Ada different. Take a look at the charts below and see what we mean when we say we're different.

Product Features:	Janus/Ada 2.0	Compiler A 3.2*	Compiler M 2.0*
80 X 87 emulation	YES	NO	NO
Royalty free run time libraries	YES	NO	NO
Site licensing	YES	NO	NO
All 80 X 86 covered	YES	NO	NO
Tutorial included with all Paks	YES	NO	NO
Ada applications for only $12	YES	NO	NO
Runs on floppy disks	YES**	NO	NO
Validation Suite	ACVC 1.9	ACVC 1.8	ACVC 1.8
Validated compiler cost	$99.00	$3,000.00	$795.00

*Comparisons made on product information obtained on 12/11/87.
**3½", 720K Floppies and 5¼", 1.2M Floppies only.

The differences don't end with the facts above; the performance issues, which make or break a production compiler, demonstrate why Janus/Ada is not just different, but better!

Compile and Link Timings:**	Janus/Ada	Compiler A	Compiler M
Sieve	0:50	1:39	1:25
Calculation	0:43	2:14	1:00
Disk Write	0:45	1:33	1:25
Disk Read	0:43	1:34	1:23
Integer Sort	0:47	2:13	1:34
Dynamic Allocation	0:47	2:02	1:32
Matrix Inversion	0:46	2:24	1:39
Recursion	0:47	2:10	1:34

**(These results are from BYTE Magazine, July 1987 issue; full details on the tests, as well as the standard equipment used, can be found in that issue.)

Our seven years of providing quality Ada software to over ten thousand users reflects the commitment we have to your programming needs. Our policy has always put you, the customer, first and foremost. We think it's a difference you can appreciate! You can order our **"JET SET" (Ada compiler and tutorial) for only $99.** Please call our toll free number **1-800-722-3248 (1-800-PC ADA 4 U)** to place your order or request our products brochure.

R.R. SOFTWARE, INC.

specialists in state of the art programming

P.O. Box 1512 Madison, Wisconsin 53701
(608) 244-6436 TELEX 4998168

1-800-722-3248

Circle Reader Action No. 467

Computer Programs

48 Molecular-Beam-Epitaxy Program
48 General-Purpose Image-Data Program
50 Mapper of FORTRAN Programs

COSMIC: Transferring NASA Software

COSMIC, NASA's Computer Software Management and Information Center, distributes software developed with NASA funding to industry, other government agencies and academia.

COSMIC's inventory is updated regularly; new programs are reported in *Tech Briefs*. For additional information on any of the programs described here, circle the appropriate TSP number.

If you don't find a program in this issue that meets your needs, call COSMIC directly for a free review of programs in your area of interest. You can also purchase the 1988 *COSMIC Software Catalog*, containing descriptions and ordering information for available software.

COSMIC is part of NASA's Technology Utilization Network.

COSMIC® — *John A. Gibson, Director,* (404) 542-3265
The University of Georgia, 382 East Broad Street, Athens, Georgia 30602

Computer Programs

These programs may be obtained at a very reasonable cost from COSMIC, a facility sponsored by NASA to make computer programs available to the public. For information on program price, size, and availability, circle the reference number on the TSP and COSMIC Request Card in this issue.

Electronic Components and Circuits

Molecular-Beam-Epitaxy Program

Performances of solar cells are predicted from manufacturing parameters.

The Molecular Beam Epitaxy (MBE) computer program was developed to aid in the design of single- and double-junction cascade cells made of silicon. The process of molecular-beam epitaxy offers the potential of growing complex and arbitrary doping profiles in devices, with accurate depth resolution on both front- and back-surface fields.

The MBE program can be used to calculate optimum doping profiles and to predict the resulting performances of solar cells. Analysis by the use of the MBE program has shown that a cascade cell has an efficiency 1 or 2 percent higher than that of a single cell, with twice the open-circuit voltage. The input parameters include the doping density, diffusion lengths, thicknesses of regions, the solar spectrum, the absorption coefficients of silicon (data are included for 101 wavelengths), and surface recombination velocities. The results include the maximum power, short-circuit current, and open-circuit voltage.

The MBE program is written in FORTRAN IV for batch execution and has been implemented on an IBM 370-series computer operating under OS. The program requires the commercial IMSL subroutine package and includes sample SAS procedures for plotting results. This program was developed in 1984.

The program was written by Patricia D. Sparks of the University of California, Los Angeles, for **NASA's Jet Propulsion Laboratory**. *For further information, Circle 11 on the TSP Request Card.*
NPO-16706

Mathematics and Information Sciences

General-Purpose Image-Data Program

Files of image data are easily retrieved and analyzed.

The Image Database computer program, IBASE, is a general-purpose imagery-information system. The system includes functions for cataloging and managing files of digital images and for conducting analyses of these images. Use of the system may be accomplished either by commands or through a hierarchy of menus. The analytical capabilities of IBASE include contigency tables, image filtering (low-, high-, and band-pass), proximity maps, clustering, histograms, regression, slope calculations, scaling, and Boolean manipulations. IBASE also has an interface to the Cheshire Image Classification expert system.

All information stored by IBASE is considered part of a GeoCube. A GeoCube is a rectangular region defined by the coordinates of two opposite corners and can store many images called layers. Each layer contains information such as the name, date, and layer type. An IBASE layer can contain a report or data: as used here, "report" denotes text or the results of an IBASE analysis, and "data" denotes such image specifications as the pixel size, the number of samples, and the actual continuous/discrete, integer/byte image-data

Interactive math with your IBM/XT/AT

IAS
INTERACTIVE ANALYSIS SYSTEM

Over 40 preprogrammed functions are grouped into 7 menus for direct selection.

Powerful math options such as differentiate, integrate and FFT are executed in a couple of seconds with simple menu picks.

You can list data, edit, operate on, plot and store to disk. The function file directory allows easy access to stored data.

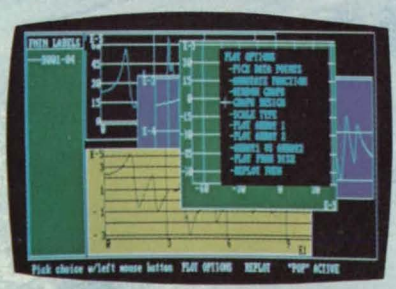

Select plot options in pop-up window using MOUSE or keyboard.

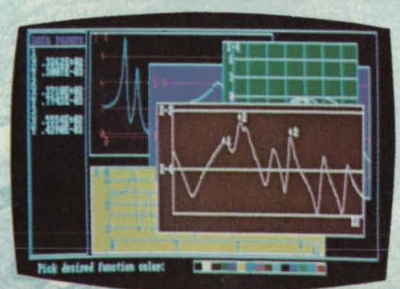

Pick desired colors directly from color bar.

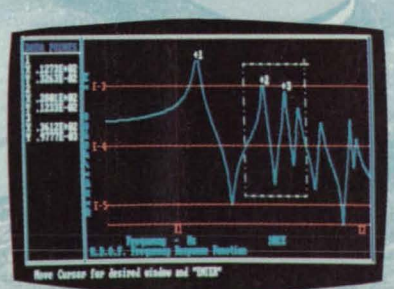

Rubber-banding box zooms on data you wish to magnify. Use MOUSE or keyboard.

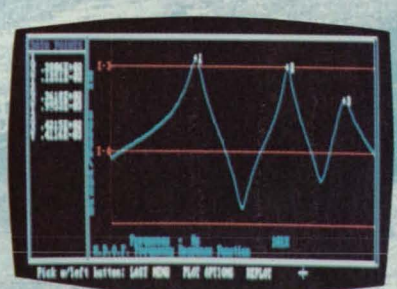

Redisplayed data from zoom box. Data points are cursored for x-y values.

From the NASA Johnson Space Center environment comes breadth and depth of math functionality you've not seen on a Personal Computer.

Now, you have IAS, a main frame grade advanced menu driven system at a price accessable to everyone.

- Your choice: mouse, FNTN key, arrow key cursor pick, or type two-character commands
- New lookahead window and stacked menus with command trail
- More ways to generate math functions
- Pick preprogrammed functions directly from menu
- Keyboard x-y data entry
- Type algebraic equations
- Differential Equations. 1st, 2nd and 3rd order.
- Interpolation
- Curve fitting
- EQN, parameter and variable tables
- Extensive operations on functions, including FFT, differentiation, integration
- The other guys are eating their hearts out over IAS plot capability. No hoops to jump through, either.
- Matrix analysis
- Wireframe object eigenvector animation (vibration simulation)
- Breakthrough: User menu puts your program inside IAS
- External data interface menu
- Special picks for SDRC I-DEAS, Univ. of Cincinnati Universal Files and Lotus 1-2-3.
- EE's: Build your data acquisition system inside IAS
- Menu driven file management
- DOS command menu
- IBM XT/AT. 512K. 8087. CGA or EGA. Screen copy.
- 30 day moneyback guarantee

$149.00

VISA master charge

ATC ANALYSIS TECHNOLOGY COMPANY

3914 Miami Road
Cincinnati, Ohio 45227

(513) 561-1100

Circle Reader Action No. 546

samples.

The various analyses are performed by specifying input data layers and output report layers. Typical IBASE operations include listing GeoCubes, printing data or report layers, mapping data layers using a line-printer gray scale, editing data, and routine management of files with such procedures as copy, delete, list, print, and summarize.

IBASE is written in FORTRAN 77 for interactive execution and has been implemented on a DEC VAX 11/780-series computer operating under VMS 2.4. The program was developed in 1986.

This program was written by Steven W. Engle of Informatics for **Ames Research Center**. *For further information, Circle 130 on the TSP Request Card.*

Inquiries concerning rights for the commercial use of this invention should be addressed to the Patent Counsel, Ames Research Center [see page 12]. Refer to ARC-11712.

Mapper of FORTRAN Programs

Relationships among various parts of a program are shown graphically.

The SUPERMAP computer program was designed to produce a map of all components and attributes of a FORTRAN program. Unlike the maps produced by the CRAY FORTRAN compiler, which relate only to a single module, SUPERMAP relates to the entire program unit.

SUPERMAP maps the usage of all variables and all COMMONs used in a FORTRAN program. It also maps the alignment of subprograms CALLed with the arguments and dummy arguments of the CALLed subprogram. SUPERMAP tallies the externals called by each module. The tabular output can be directed to either 132-character printer paper or to a cathode-ray-tube display. SUPERMAP can accommodate up to 20,000 unique variable names and 100 undefined variables.

The input to SUPERMAP is a compiled, error-free, FORTRAN program unit with the CFT option ON = CNPQRSTX, OFF = ABDEFHIJLMOV. It reads the listing of source to obtain the calling statements with the name and arguments for these calls. The source code is used to obtain names of PROGRAM, FUNCTION, BLOCK DATA, SUBROUTINE, and ENTRY statements and any argument list associated with one of these statements. Statement line numbers are saved when any of these statements is found. These numbers will be used to associate this information with information obtained from the maps. Once an END statement is read within the source program, it switches to reading the CFT map that follows the source listing.

The CFT map is cracked for information relating to variables, externals, and COMMONs. The main information obtained shows how a variable is used within the module and its type and length if dimensioned. The length of COMMONs is extracted from the map. Also, references to externals are gleaned from the map. When the end of the map is encountered, it loops back to read the FORTRAN source again and continues the above process until the end of all FORTRAN and map data have been obtained.

Once all information is stored, the program prepares tables by sorting the information into required form. It then prepares information extracted about external calls into a meaningful form for printing. Then it generates maps and tables of externals, modules, COMMONs, and variables.

SUPERMAP is written in FORTRAN 77 for batch execution and has been implemented on a CRAY X-MP 22 (dual CPU) computer operating under COS with a central-memory requirement of approximately 63K (octal) words. The program was developed in 1985.

This program was written by Clayton J. Guest of Informatics for **Ames Research Center**. *For further information, Circle 82 on the TSP Request Card.*

ARC-11708

Where do you find good Ada programmers?

Free Poster: see coupon.

You could spend and spend trying to hire good Ada programmers and still not find what you need. Big demand; short supply. The irony is, your best Ada people may be the programmers you already have; all they need is good training.

Alsys offers a full range of quality Ada training products for growing your own programmers. For example . . .

■ A 27 video tape seminar covering the entire Ada language – 18 hours of authoritative instruction by the principal designer of the language itself. Benefit? Understanding Ada's architecture and scope should be the foundation for all further work or study. It will help develop that most elusive skill: the Ada programming intuition to guess right.

■ For programmers ready for hands-on skills development, a comprehensive CAI course on a PC, running 50–60 hours, with exercises and progress tracking. Multiple users. Licenses for 5 machines. The course is also excellent for brushing up, or extra work on one subject, or for new employees.

■ For practicing, and then moving directly to serious Ada programming, Alsys offers a full-featured, production quality Ada compiler, with tools, for the PC AT. This same compiler is used to build some of the largest Ada programs in existence!

Alsys offers more training products. A CAI course for programmers familiar with Fortran . . . a searchable, on-line version of the Reference Manual . . . a (limited) offering of live training courses.

Good Ada training for your own people. For Ada now. Write or call.

alsys

Ada Programmers Are Made – Not Hired.

In the US: Alsys Inc., 1432 Main St., Waltham, MA 02154 Tel: (617) 890-0030
In the UK: Alsys Ltd., Partridge House, Newtown Rd., Henley-on-Thames, Oxon RG9 1EN Tel: 44 (491) 579090
In the rest of the world: Alsys SA, 29 Avenue de Versailles, 78170 La Celle St., Cloud, France Tel: 33 (1) 3918.12.44

Send me POSTER and more information on:

_____ *Ichbiah, Barnes & Firth on Ada* 27-tape Video Series.
_____ *Lessons on Ada* CAI Course. _____ Live Training.
_____ *PC AT Compiler and Tools.* _____ *AdaQuery* On-Line Reference.
_____ *You Know Fortran, Ada is Simple* CAI Course.
_____ *Ada Immersion* Combination Package.

Name _____
Company _____
Address _____
City _____ State _____ Zip _____
Phone ( ) _____ Ext. _____
Mail to: Alsys, Inc. 1432 Main St., Waltham, MA 02154

NTB 4/88

*Ada is a registered trademark of the U.S. Government (AJPO).

Circle Reader Action No. 341

Mechanics

Hardware, Techniques, and Processes

Books and Reports

Sizing Dye-Penetrant Indications of Defects

Sizes of cracks and holes viewed through a borescope can be measured.

Marshall Space Flight Center, Alabama

A reference chart makes it possible to estimate the sizes of borescope-observed defects that are on the inner walls of tubes or are otherwise hidden. The chart can be used both for round defects like pits or pores and for elongated ones like cracks.

Intended for use in dye-penetrant inspection, the chart contains pictures of 14 cracks and 7 round defects as they appear after a penetrant dye has been applied to them (see figure). The linear defects range in size from 0.031 to 2 inches (0.787 to 50.8 millimeters) and the round ones from 0.031 to 0.5 inch (0.787 to 12.7 millimeters).

To use the chart, an inspector focuses the borescope on a defect so that the defect image fills the borescope window or, if that is not possible, so that it fills half the window. Keeping the instrument at the same focus, the user withdraws it from the part and places its objective lens facing the chart at the same angle at which the defect was viewed. The inspector moves the borescope from picture to picture, looking for the image that most nearly fills the borescope window (or half the window). The size of that picture, as indicated on the chart, is approximately the size of the internal defect.

For added realism, the color of the penetrant dye is duplicated on the chart. On the original chart, for example, the pictures were red to match the Accu-Pen P&R (or equivalent) penetrant dye used to inspect hidden surfaces in rocket-engine parts. Any other color, including that of fluorescent yellow-green penetrants, can be duplicated.

This work was done by Orlando G. Molina of Rockwell International Corp. for **Marshall Space Flight Center**. *No further documentation is available.*

Inquiries concerning rights for the commercial use of this invention should be addressed to the Patent Counsel, Marshall Space Flight Center [see page 12]. Refer to MFS-29216.

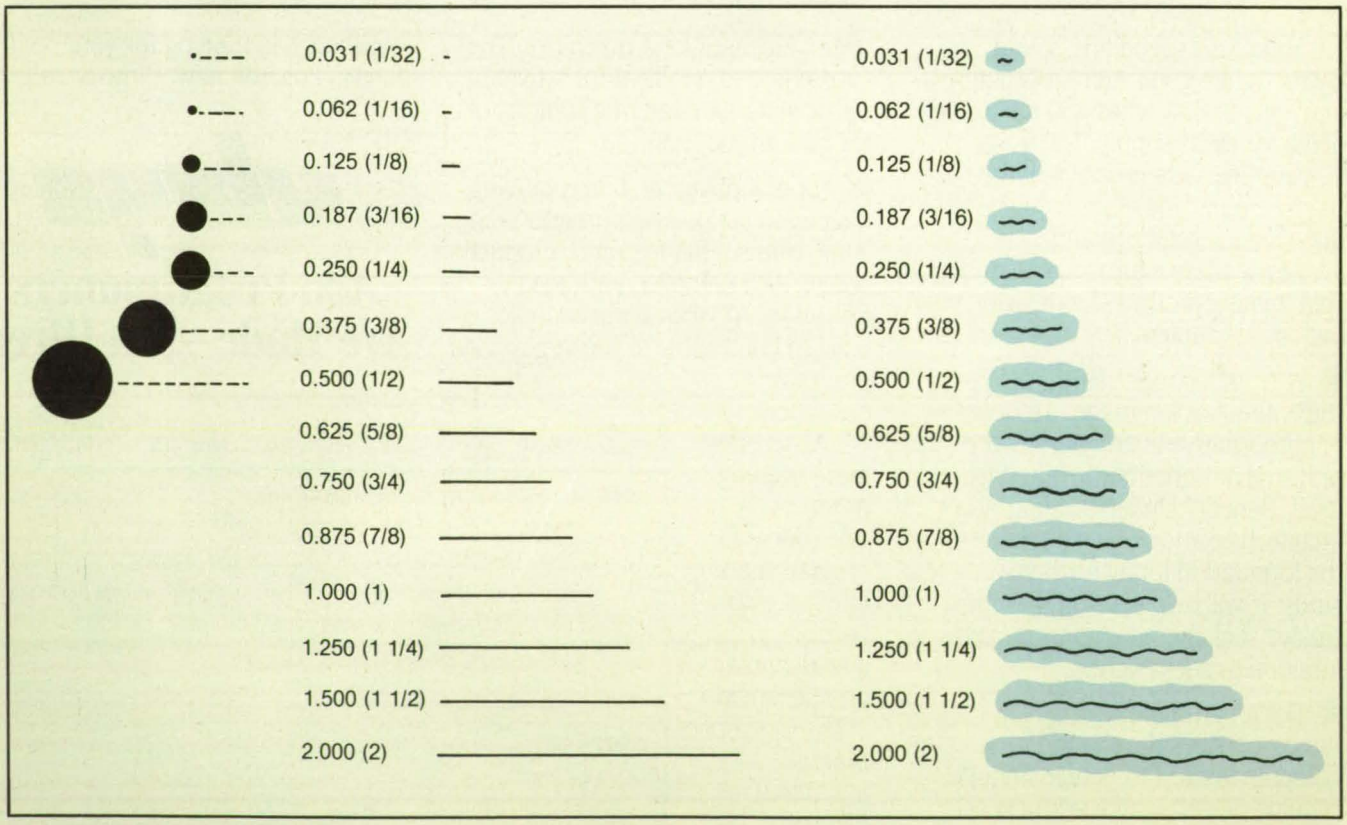

Pictures of Defects as they appear after treatment with a penetrating dye can be used to determine the sizes of real defects viewed through a borescope. The pictures let the inspector take the viewing angle into account.

Low-Heat-Transfer Tank Mount

A supporting element adapts to high or low side loads.

Ames Research Center, Moffett Field, California

A Passive Orbital Disconnect Strut (PODS) for a cryogenic tank engages an extra-strong member only during peak side or axial loads like those from vibrations, accelerations, and shocks. Most of the time, when the side loads are low, support is provided by the lower-strength, lower-thermal-conductance, passive disconnect.

The strut provides primarily axial support; however, a filament ring and collar were added to the end of the strut to increase side-stiffness (see figure). A bicycle-spoke arrangement of graphite filaments is assembled between the ring and the collar with the help of a whiffle-tree set of pulleys, ball joints, and sliders. The filaments, which conduct little heat, resist ordinary side loads on the strut. If, however, loads are great enough to stretch the filaments elastically, then the collar presses against the stem of the strut and takes up the load.

This work was done by R. T. Parmley and I. E. Spradley of Lockheed Missiles & Space Co., Inc., for **Ames Research Center**. *For further information, Circle 107 on the TSP Request Card.*

Inquiries concerning rights for the commercial use of this invention should be addressed to the Patent Counsel, Ames Research Center [see page 12]. Refer to ARC-11779.

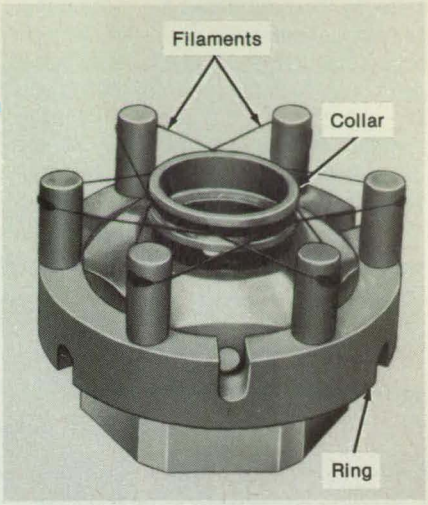

Graphite Filaments Arranged Like Bicycle Spokes at the end of the strut resist ordinary side loads. The filaments transfer high loads to the heavy-duty member.

Multispan-Beam Shear Test for Composite Laminates

This test probes failure modes unattainable in the three-point-beam test.

Langley Research Center, Hampton, Virginia

Laminated composites have unique failure mechanisms much different from those of homogeneous materials. One such failure mechanism is cracking in the weaker plies caused by transverse shear deformation and local bending. A new approach for studying this type of failure is the use of the multispan-beam shear test, which puts some regions of the specimen in almost pure shear and enables the observation of the location of the initial failure and the way in which the damage propagates. The test can be stopped at any time, such as when the first failure event occurs, for study of a phenomenon or for taking photographs of a failure event. Individual plies can be studied easily with a long-distance microscope or from photographs taken during the test.

A five-point load fixture (Figure 1) is used while a lateral load is slowly applied to simulate a static loading condition. To impose significant transverse shear stresses, the specimen size is selected to provide a ratio of distance between the line loads to the specimen thickness of approximately 4:1. The dimensions of the specimen in Figure 1 are 4 by 1 by 0.25 in. (10.2 by 2.5 by 0.64 cm), and the spacing between the line loads is 1 in. (2.5 cm).

As the load is applied, the progression of the failure can be observed. Frequently, the first failure event is a crack in a single layer; for example, a 45° or 90° ply. Subsequent failure events may involve cracks and/or delaminations, depending on the material and the ply orientations. For example, the initial failure (Figure 2) of a $[(\pm 45°/0°_2)_2(\pm 45°/0°/90°)]_{2s}$ laminate is the cracking of the two centrally-located 90° plies in a region of high shear in the specimen.

One use for this test procedure is to study the effects of interleaving of adhesive layers in composites. In a laminate without interleaving, the 45° and 90° plies can withstand little transverse shear before cracking. However, adhesive layers placed between plies can delay the cracking until a higher load level or higher transverse displacement is reached because the adhesive layers can deform in shear more than the graphite/epoxy plies can. The multispan-beam shear test allows the failure to be seen easily so that the effect of the interleaving on the failure mechanism can be studied.

The second use of this test procedure is the study of the deformations related to the reduction of strength of a composite panel after an impact. A laminated panel undergoes local transient bending deformation immediately after impact and subsequently transforms to its final global deformation

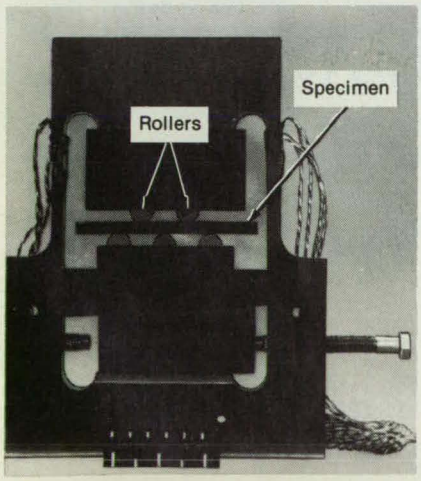

Figure 1. This **Five-Point Load Fixture** is used in shear testing.

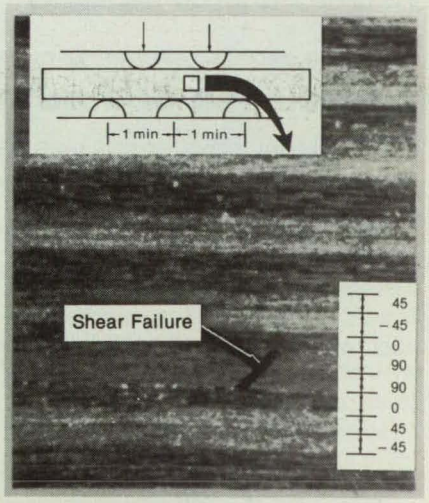

Figure 2. **Shear Failure** is evident in 90° plies.

state. In the brief time before the panel takes on its final shape, significant damage occurs due to the extreme local deformation gradients in the region of the impact. The multispan-beam shear test forces the test specimen to assume, in two dimensions, approximately the same deformation shape that occurs in the impacted section of the panel. Failure results from the multispan-beam shear test correlate well with failure results from impact tests on panels in axial compression. Since small beam specimens can be used in place of larger panels for these tests, this test procedure provides a simple, economical way of evaluating the strengths of composite materials after impacts.

This work was done by Dawn C. Jegley and Jerry G. Williams of **Langley Research Center**. *No further documentation is available.*
LAR-13605

Door Opens Four Ways

A concept is based on poppable hinges.

NASA's Jet Propulsion Laboratory, Pasadena, California

A proposed hinge system would allow a door to swing open on any of its four edges. The proposed system consists of four separable ball joints that resemble "pop-it" beads, one at each corner of the door (see figure). Made of molded plastic, the joints would be cheap to make and install.

The socket part of a hinge would be attached to the door frame and the plug part to the door. When one edge of the door is pulled, the joints at that edge would pop apart, and the door would swing open on the intact joints on the opposite edge. Pushing the door shut would re-engage the separated plugs and sockets, and the door could then immediately be swung open on any other edge. The entire door could be popped off when full access to the door opening is needed. A four-arm deadlock, like that on a garage door, could be used to prevent the door from being opened.

For heavy doors, stiff plugs and socket stems could be used. The plugs and sockets could be engaged and disengaged with latching handles, which would provide the required leverage.

This work was done by Andrew D. Morrison of Caltech for **NASA's Jet Propulsion Laboratory**. *For further information, Circle 31 on the TSP Request Card.*
NPO-16801

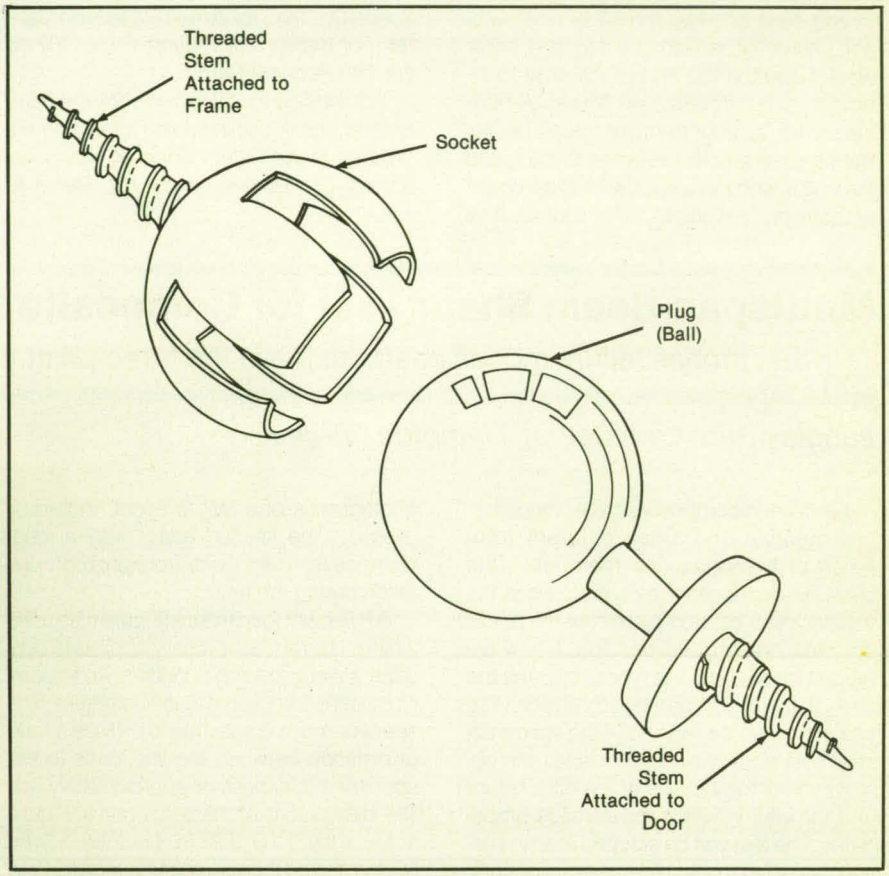

Four **Separable Ball Joints**, one of which is shown, join a door to its frame. The socket and plug members can be disengaged and re-engaged readily.

Aeroelastic Computations for Wings With Loaded Tips

External fuel tanks or missiles can degrade stability because of unsteady aerodynamics.

Ames Research Center, Moffett Field, California

The transonic aeroelasticity of wings with tip stores (missiles, fuel tanks, or other objects at the wing tips) can now be simulated with an improved version of the ATRAN3S computer code, which had previously been used to study the behavior of clean wings only. According to preliminary tests, the output of the code agrees well with wind-tunnel data.

The computer code is derived from a coupling of the unsteady/small-disturbance transonic aerodynamic equations with the equations of structural motion. The tip store is incorporated into the mathematical model via a small-disturbance flow-tangency boundary condition and the distribution of the tip-store mass.

The overall aeroelastic equations of motion are obtained by the Rayleigh-Ritz method, in which the aeroelastic displacements are expressed as a function of a finite set of assumed vibrational modes. It is assumed that the deformation of a continuous wing structure can be represented by deflections at a set of discrete points; this facilitates the use of such discrete structural data as the modal vector, the modal stiffness matrix, and the modal mass matrix. In a study based on a physical model, the modal data could be obtained by influence-coefficient measurements. In a study based on a mathematical model, modal data are obtained by the finite-element method.

The resulting matrix equations of motion are solved by numerical integration in time,

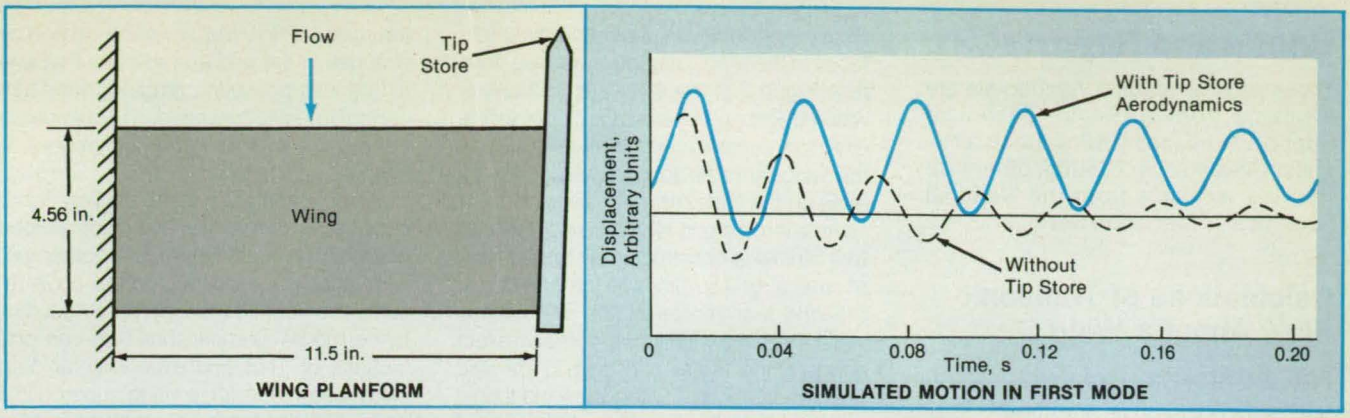

The **Aeroelastic Behavior of the Rectangular-Planform Wing** was simulated with the help of the improved computer program. The simulated motion in the fundamental vibrational mode was calculated with a speed of mach 0.715.

using the linear-acceleration method, which is equivalent to the explicit finite-difference Euler method. The aerodynamic forces are calculated starting from assumed initial freestream and wing-boundary conditions on displacements and velocities. The resulting accelerations, displacements, and velocities are used to compute the boundary conditions for the next time step. The process is repeated for as many time steps as are needed to carry the results forward in time for the required interval or to obtain the desired response.

The computational technique was applied to a uniform rectangular wing having a parabolic-arc airfoil section (see figure) and to a wing similar to that of the F-5 fighter. Both cases were analyzed with and without missile-shaped tip stores having masses about 10 percent of those of the respective wings. For the rectangular wing without the tip store, the predicted flutter agreed well with wind-tunnel flutter measurements. For both wings, the addition of the tip stores decreased the vibrational frequencies, as one would intuitively expect as a result of the increased vibrating mass. In both cases, the addition of the tip store decreases the aeroelastic damping by increasing the unsteady lift. These changes in aeroelastic response indicate that a wing with a tip store can be aeroelastically less stable even though the same wing without the tip store is stable.

A typical analysis for the rectangular wing requires about 1 hour of central-processor time on a high-speed computer (CRAY-XMP or equivalent). The augmented ATRAN3S code can be an efficient compliment to wind-tunnel and flight tests and can thereby reduce the costs of aerodynamic designs.

This work was done by Peter M. Goorjian and Eugene L. Tu of **Ames Research Center** *and Guru P. Guruswamy of Sterling Software. For further information, Circle 136 on the TSP Request Card.*

Inquiries concerning rights for the commercial use of this invention should be addressed to the Patent Counsel, Ames Research Center [see page 12]. Refer to ARC-11753.

Toolmaker's Microscope With Video Monitor

Display accessories increase resolution and flexibility of use.

Marshall Space Flight Center, Alabama

A toolmaker's microscope equipped with a video monitor, auxiliary lighting, and high-resolution readout devices enables noncontacting measurements of tiny slots, indentations, and similar features on parts. The microscope can measure in places that are difficult or impossible to reach by mechanical means.

The microscope (see figure) is easy to set up and position. The user can select from a variety of light sources to illuminate the workpiece and can choose a magnification according to the size and nature of the feature. With the video display, more than one observer can evaluate a feature.

This work was done by Arif S. Ahmed of Rockwell International Corp. for **Marshall Space Flight Center**. *No further documentation is available.*
MFS-29227

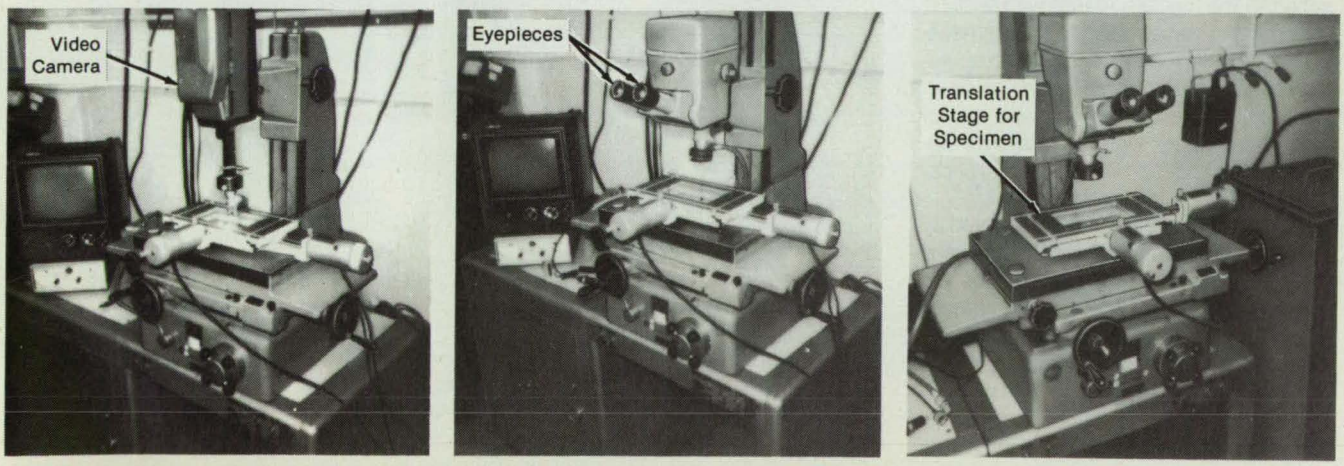

A **Workpiece on an x-y Table** is observed through the microscope above it. A video camera in the microscope head produces an image of the workpiece on the video monitor at the left.

Books and Reports

These reports, studies, handbooks are available from NASA as Technical Support Packages (TSP's) when a Request Card number is cited; otherwise they are available from the National Technical Information Service.

Calculations of Transonic Flow About a Wing

Navier-Stokes and Euler formulations are applied on zonal grids.

A report describes calculations of transonic airflows about a wing in a wind tunnel by the use of an Euler/Navier-Stokes approach in which the flow field is divided into several grid zones. The numerical solutions agree well with experimental results, even in cases that include significant effects of the wind-tunnel walls and shock-induced separations of flow on the upper wing surface.

The basic equations of flow used in this study are the Reynolds-averaged Navier-Stokes equations in strong conservation-law form. Two simplifications increase the efficiency of the calculation procedure: (1) in the zones near body surfaces, where viscous effects are important, the standard thin-layer approximation of viscous terms is used; and (2) in the zones where viscous effects are not important, the Euler (inviscid-flow) equations are used. Because the Euler equations are applicable over a considerable portion of the flow field, this reduces the computational load significantly.

The equations of flow are incorporated into a finite-difference computer code called TNS (Transonic Navier-Stokes). The code applies a standard second-order-accurate, central differencing scheme to the governing equations. A fourth-order-accurate smoothing operator is used on the right and left sides of the iteration scheme. The time step varies with position according to the Jacobian scaling (a measure of the local mesh size of the computational grid). The code also incorporates an easy-to-use algebraic turbulence model that is consistent with the thin-layer approximation and can be used to treat separated flows.

The computational grid is generated by the solution of partial differential equations that yield smooth meshes that conform to the surfaces of the wing and wind tunnel. The grid is divided into four zones: Grid 1 is the basic grid that occupies most of the volume, excepting a small volume that surrounds the wing. Grid 2 occupies most of the volume around the wing that is not included in grid 1 and is about twice as fine (along each coordinate axis) as grid 1. Grids 3 and 4 hug the upper and lower surfaces of the wing, respectively; these grids match grid 2 in the spanwise and chordwise directions but are much finer in the direction perpendicular to the surface of the wing, in order to capture viscous effects on the surfaces of the wing.

An alternate grid for the computation of free airflow is constructed by the addition of several grid surfaces to the portions of the grid that represent the wind-tunnel walls. Thus, the wind-tunnel grid is an exact subset of the free-air grid; grids 2, 3, 4, and the portion of grid 1 within the wind tunnel are the same in the free-air and wind-tunnel cases. This suppresses the spurious perturbations of flow that would be caused by changes in the grid and assures that any differences between computed wind-tunnel and free-air flows are due to changes in the outer grid zone and to differences in boundary conditions.

When applied to a mach-0.5 flow about a nonlifting airfoil, the TNS code yielded boundary-layer profiles in close agreement with established boundary-layer code results: this verified the incorporated turbulence model. Comparisons between predictions of TNS and experimental data were also made for a lifting supercritical case, with good to excellent agreement of data points. When applied to a case of

massive shock-induced boundary-layer separation, the code predicted some interesting flow-field features for the first time, including a separation saddle point, a node, a reattachment saddle point, and a focus.

This work was done by Terry L. Holst, Karen L. Gundy, Jolen Flores, and Neal Chaderjian of **Ames Research Center**, *and Univer Kaynak of Stanford University and Scott D. Thomas of Sterling Software. To obtain a copy of the report, "Transonic Wing Flows Using an Euler/Navier-Stokes Zonal Approach," Circle 20 on the TSP Request Card.*

Inquiries concerning rights for the commercial use of this invention should be addressed to the Patent Counsel, Ames Research Center [see page 12]. Refer to ARC-11803.

Piezoviscosity in Lubrication of Nonconformal Contacts

Developments in the theory of lubrication are reported.

A NASA technical memorandum presents an analysis of the piezoviscous-rigid regime of lubrication of two ellipsoidal contacts. Earlier studies have yielded incorrect estimates of the minimum thickness of the film of lubricating fluid, either because they have not considered the effect of the perpendicular force between the contacts or because they used an oversimplified equation for the dependence of the viscosity of the lubricant upon the pressure.

The analysis begins with the Reynolds equation for point contact. The Reynolds equation is nondimensionalized using the Roelands empirical formula for the viscosity of a general lubricant as a function of the pressure and the Dowson and Higginson formula for the dimensionless density of mineral oil as a function of the pressure. Subject to the Reynolds cavitation boundary condition, the Reynolds equation is solved numerically.

Solutions are obtained for a full spectrum of conditions to find the effects of the dimensionless load, the speed, the parameters of the lubricated and lubricating materials, and the angle between the direction of rolling and the direction of entrainment of lubricant. The dimensionless speed parameter is varied over a range 5.6 times its lowest value. The dimensionless load parameter is varied over an order of magnitude. To obtain the exponent in the dimensionless material parameter, conditions representative of the use of contacts of steel, bronze, and silicon nitride and of lubricants of paraffinic and naphthenic mineral oils are considered.

Altogether, 41 cases are used to obtain a formula for the minimum thickness of the lubricating film:

$$H_0 = 178G^{0.386}U^{1.266}W^{-0.880}[1-\exp(-0.0387\alpha)]$$

where H_0 is the dimensionless central film thickness, G is a dimensionless material parameter related to the elastic moduli of the contacts and the asymptotic isoviscous pressure, U is the dimensionless speed parameter, W is the dimensionless load (that is, perpendicular contact force) parameter, and α is a ratio of equivalent contact radii. In addition, contour plots show the pressure in the lubricating film between the contacts.

This work was done by Yeau-Ren Jeng and Bernard J. Hamrock of **Lewis Research Center** *and David E. Brewe of the U.S. Army Aviation Research and Technology Activity — AVSCOM. Further information may be found in NASA TM-87141 [N86-21797/NSP], "Piezoviscous Effects in Nonconformal Contacts Lubricated Hydrodynamically."*

Copies may be purchased [prepayment required] from the National Technical Information Service, Springfield, Virginia 22161, Telephone No. (703) 487-4650. Rush orders may be placed for an extra fee by calling (800) 336-4700.
LEW-14589

Machinery

Hardware, Techniques, and Processes

Books and Reports

Dovetail Rotor Construction for Permanent-Magnet Motors

Rotor/stator-gap and eddy-current losses are reduced.

Lyndon B. Johnson Space Center, Houston, Texas

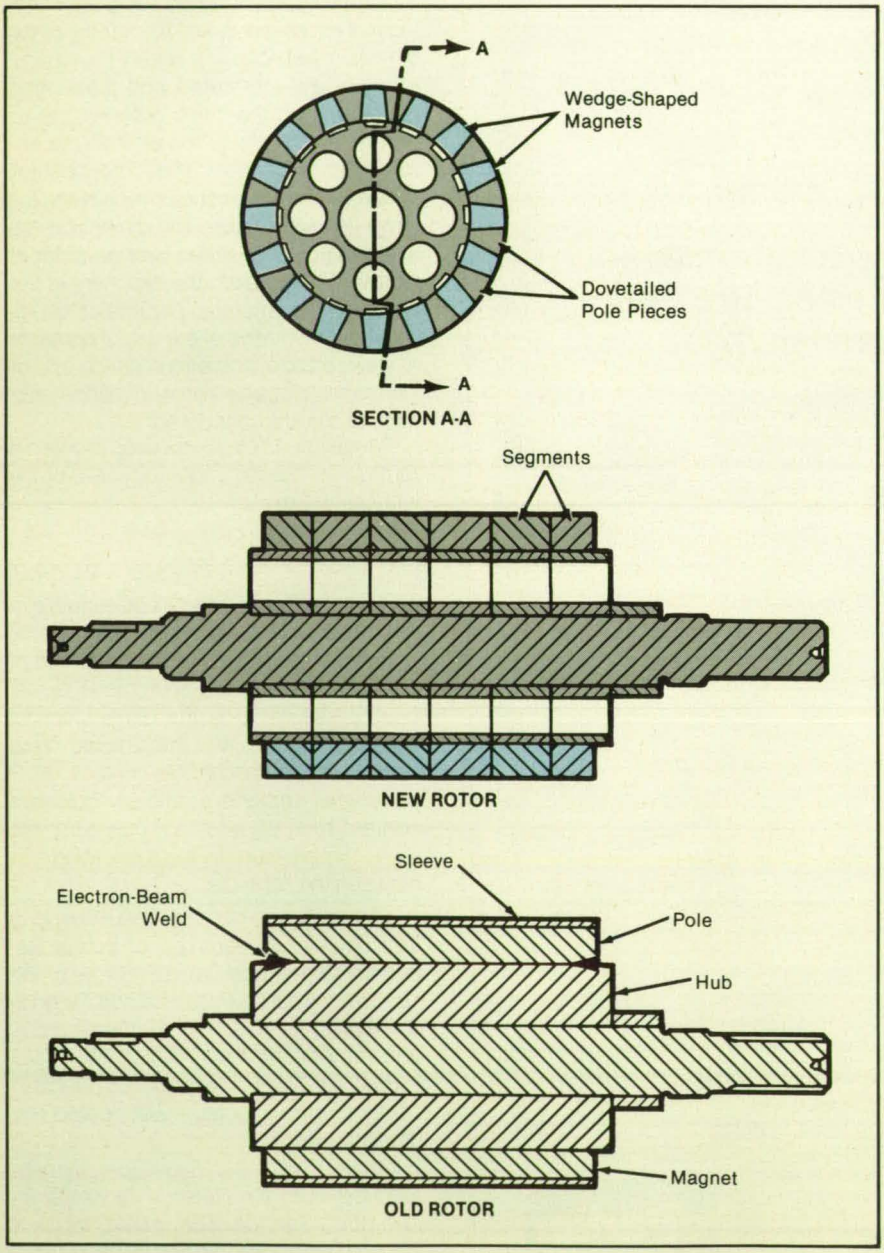

Dovetailed With Pole Pieces, rare-earth magnets are securely held on a rotor. Pole pieces are segmented for ease in welding. In an older construction, a metal sleeve retained the pole pieces and magnets.

A new way of mounting magnets in permanent-magnet, electronically commutated, brushless dc motors makes it possible to exploit the high torque and fast response characteristic of rare-earth-magnet motors. In the new mounting scheme, the magnets are wedge shaped, tapering toward the center of the rotor. Oppositely tapered pole pieces, electron-beam welded to the rotor hub, retain the magnets against the centrifugal force generated by the spinning rotor (see figure). To avoid excessively long electron-beam welds, the pole pieces are assembled in segments rather than as single long bars.

Previously, the magnets were retained by a metal sleeve around the rotor. However, the sleeve increased the effective gap between the rotor and the stator and provided a conductive path for eddy currents. Both effects reduced the efficiency of the motor. Although using a nonconductive material such as a fiber-reinforced composite would eliminate the eddy currents, the relatively large gap would still exist. The new mounting method does not introduce either of these sources of energy loss.

This work was done by Lawrence J. Kintz, Jr., and William J. Puskas of Sundstrand Corp. for **Johnson Space Center**. *No further documentation is available.*

Title to this invention has been waived under the provisions of the National Aeronautics and Space Act [42 U.S.C 2457(f)], to the Sundstrand Energy Systems. Inquiries concerning licenses for its commercial development should be addressed to

Sundstrand Energy Systems
4747 Harrison Ave.
Rockford, IL 61125-7002

Refer to MSC-20942, volume and number of this NASA Tech Briefs *issue, and the page number.*

Calculating Turbine-Blade Loads

Rotor/stator interactions are analyzed with the help of approximations.

Marshall Space Flight Center, Alabama

An analytical procedure assists designers of turbomachinery in calculating the dynamic loads on blades and vanes. The procedure involves approximations that simplify the calculation of the phase angles and amplitudes of the pressure fields throughout the blade and vane rows at each disturbance frequency.

A row of blades (all remarks apply equally to vanes) is approximated as a planar cascade (see figure). The unsteady inlet-velocity field approaching the cascade must be defined: this can be done by measurements or by a theoretical estimate based on a Navier-Stokes or potential-flow solution for the flow field coming from the upstream cascade (if any). The inlet-velocity field is then decomposed into harmonics of the rotational frequency and into components perpendicular and parallel to the chord of the blade for which the dynamics are to be analyzed.

The next step is to calculate the steady-state lift of the cascade by use of any of a number of standard computer programs for flow about a cascade. One then defines an equivalent cascade. Although the blades of interest may have a complicated shape, they are replaced by thin, circular-arc blades in a cascade that has the same solidity and produces the same steady-state lift as those of the cascade of interest. Using the harmonic inlet-velocity components, the dynamic loads on the circular-arc blades are then found by Henderson's method for computing the unsteady response of such a cascade to a disturbance that originates upstream. The validity of this approach depends on the assumption that the blade/flow interactions of the circular-arc blades adequately approximate those of the blades of interest.

This procedure has been tested by comparing its results to those of a flat-plate analysis and of experiments conducted to determine the dynamic pressure as a function of chordwise position along a blade in a compressor stator. Both analytical methods yielded adequate approximations for the magnitudes of the first and second harmonics of the pressure, but the new procedure gave more-accurate phase angles. This is important because the phase angles are critical in determining the dynamics at the resonant frequencies of the blades; for example, if the load distribution acts out of phase with the resonant mode of the blade, it might be exploited to damp the resonance; or if the load distribution acts in phase with the blade vibration, it could increase the vibration to an unacceptable level.

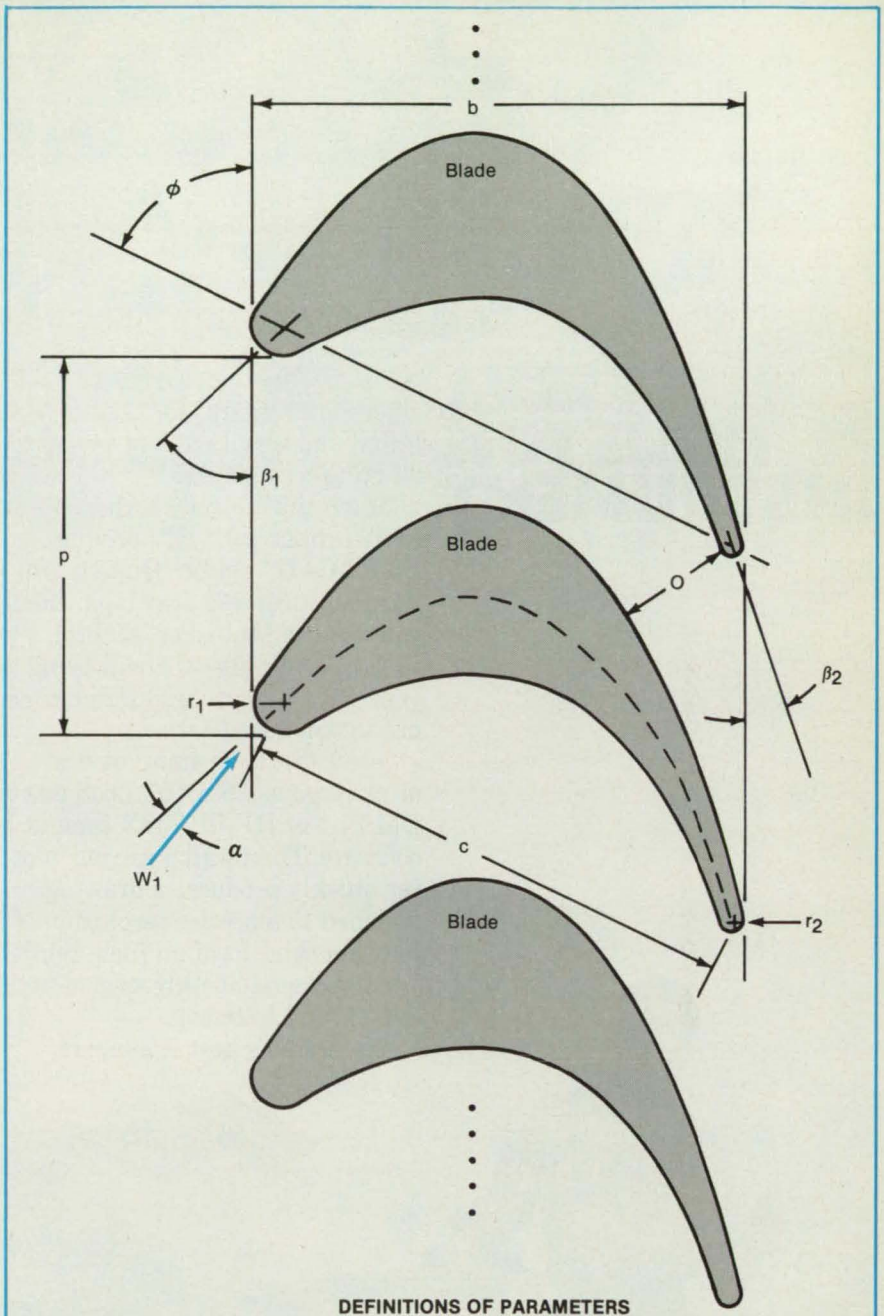

DEFINITIONS OF PARAMETERS

P	Pitch	W_1	Velocity of Approaching Fluid
b	Axial Width	α	Angle of Incidence
O	Throat Opening	θ	Camber Angle = $180° - (\beta_1 + \beta_2)$
r_1	Leading-Edge Radius	β_2	Blade-Discharge Angle
r_2	Trailing-Edge Radius	c	Chord Length of Blade
ϕ_1	Chord Angle	σ	Solidity = c/p
β_1	Blade-Inlet Angle		

A **Planar Cascade**, consisting of an infinitely long row of blades, is used to approximate a row of blades (or vanes) on the rotor (or stator) of a turbomachine. The parameters shown here are important in calculations of the flow about the blades.

This work was done by Sen Yih Meng, Eugene D. Jackson III, and Raymond B. Furst of Rockwell International Corp. for **Marshall Space Flight Center**. *For further information, Circle 99 on the TSP Request Card.*
MFS-29165

MOVE UP TO A NEW LINE

FROM HOUSTON INSTRUMENT

Prepare to be impressed. Meet the new line of high-performance plotters from Houston Instrument.™ HI's sleek new DMP-60 series is designed to impress even the most demanding CAD professional.

Discover unprecedented flexibility—blended with ultra-fine resolution, speed, and software compatibility. Benefit from HI's rigorous standards for quality, reliability, and service. All at prices starting from $4,695.*

Watch the DMP-60 series double as a scanner with HI's unique SCAN-CAD™ option. Quickly produce multicolored drawings when you use the Multi-Pen adaptor. Plot several originals—without tying up your PC when you add HI's buffer expansion board.

Select media as small as 8½"×11" or as large as 36"×48". Load either DM/PL™ or HP-GL 758X-compatible software. Then watch as your plotter quickly produces a drawing polished to a precise resolution of 5 ten-thousandths of an inch. Smile when you see smoothly formed circles, curves, and lettering.

Explore HI's host of support programs including an overnight plotter-replacement service. And then relax, knowing that HI's new plotters rest on 27 years of engineering excellence.

Move up. To a fine, new line. From Houston Instrument. Begin by calling 1-800-444-3425 or 512-835-0900 or writing Houston Instrument, 8500 Cameron Road, Austin, TX 78753. **U.S. suggested retail price.*

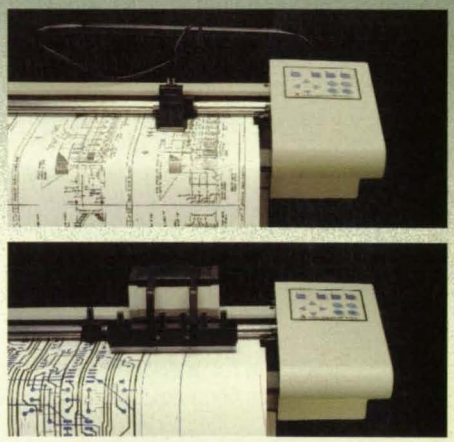

HOUSTON INSTRUMENT
A DIVISION OF AMETEK

Houston Instrument, SCAN-CAD, and DM/PL are trademarks of AMETEK, Inc.

Circle Reader Action No. 550

Books and Reports

These reports, studies, handbooks are available from NASA as Technical Support Packages (TSP's) when a Request Card number is cited; otherwise they are available from the National Technical Information Service.

High-Capacity, Portable Firefighting Pump

An improved unit is evaluated.

A report describes an evaluation of a firefighting module that can deliver water at 5,000 gal/min (320 L/s). The module is a compact, self-contained, portable water pump. Designed for fighting fires in and around seaports, it can be carried by helicopter to fight fires in remote places. Besides firefighting, the module can be used for flood control and for pumping water into large vessels, especially those brought into port on short notice. It can also pump water from sinking ships.

The evaluation was conducted to verify the performance of the module and to determine whether the module could safely be returned to service after major improvements. The modifications included the installation of a larger pump, a larger gas-turbine engine, a new electronic control system, and an electrically-driven lubricating-oil pump for the main water pump.

The tests included measurements of the loads in the tiedown lines and of vibrations of the pump and engine during operation. Other measurements were made to establish graphs of flow versus head at the back pressures created by nozzles of various sizes from 2 to 4 in. (5 to 10 cm) and at various pump speeds from 45 to 100 percent of the maximum available.

The evaluation showed that the module can be returned to service. The module satisfied two of three flow specifications: it pumped water at 5,000 gal/min (320 L/s) at a total pump pressure rise of 150 lb/in.^{2} (1.0 MPa) and pumped 3,000 gal/min (190 L/s) at 200 lb/in.^{2} (1.4 MPa). It could not, however, pump 2,500 gal/min (160 L/s) at 250 lb/in.^{2} (1.7 MPa) because of inadequate engine power.

At first, the time required to prime the pump was found to be excessive: priming took 295 seconds for a lift of only 12 ft (3.7 m), whereas a maximum of 120 seconds at 20 ft (6.1 m) is specified. To correct this deficiency, the area of the flow passage in the prime suction line was increased. As a result, the main pump can now be primed within 2 minutes.

The tiedown loads during normal operation were well within allowable limits. In a simulation of sudden failure of a discharge hose or coupling, however, loads and vibration increased tiedown loads sharply. Because such sudden increases could be hazardous (possibly overturning the module), discharge hoses should therefore be pressure-tested frequently.

This work was done by Ralph A. Burns of **Marshall Space Flight Center**. *Further information may be found in NASA TM-86560 [N87-16919/NSP], "5000 GPM Firefighting Module Evaluation Test."*

Copies may be purchased [prepayment required] from the National Technical Information Service, Springfield, Virginia 22161, Telephone No. (703) 487-4650. Rush orders may be placed for an extra fee by calling (800) 336-4700. The report is also available on microfiche at no charge. To obtain a microfiche copy, Circle 74 on the TSP Request Card. MFS-27177

Fabrication Technology

Hardware, Techniques, and Processes

Growing Wider Silicon Ribbons

A new lid design would make a larger withdrawal opening feasible.

NASA's Jet Propulsion Laboratory, Pasadena, California

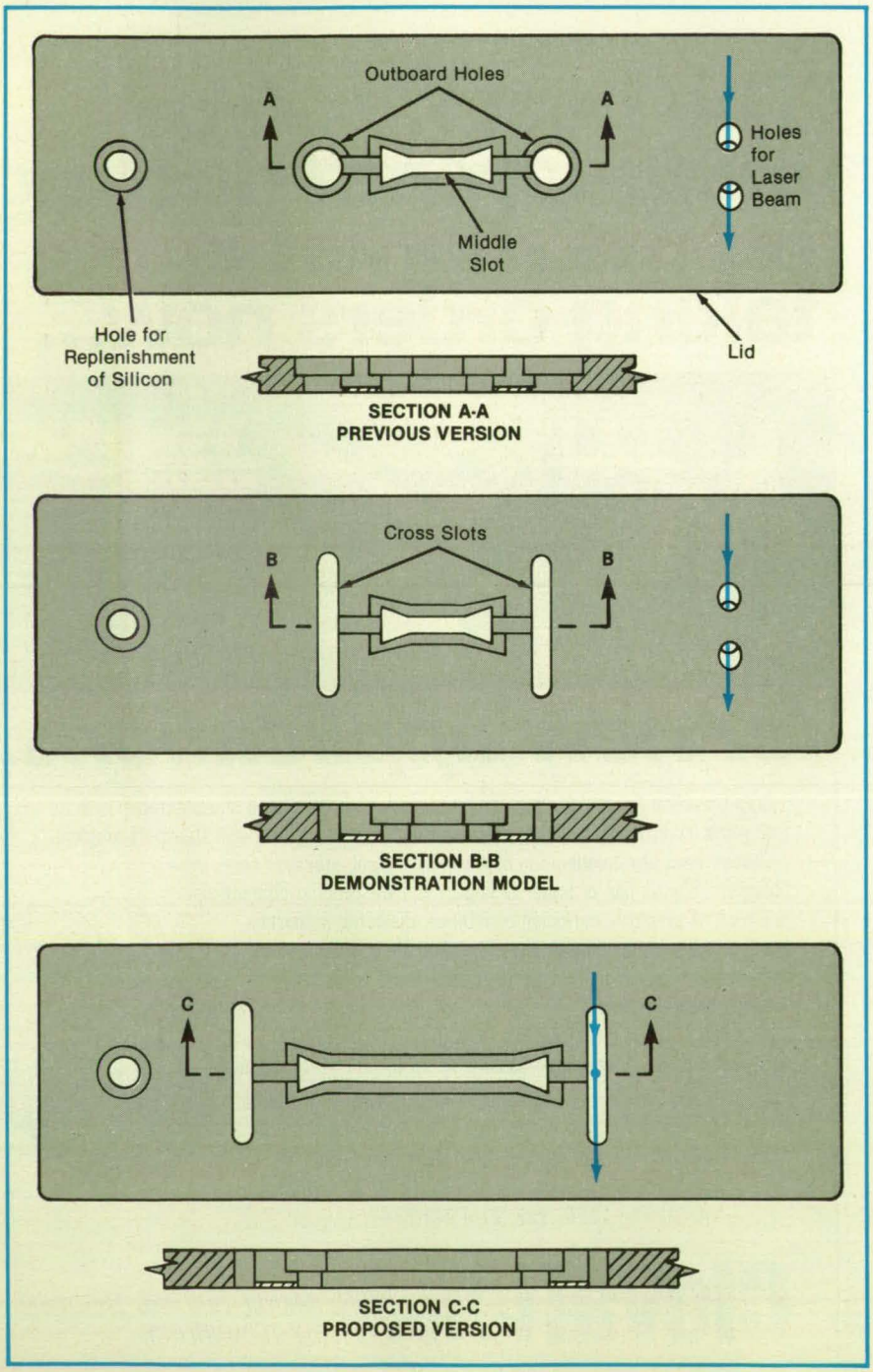

Wider silicon ribbons can be grown by the dendritic-web method with a proposed modification of the furnace lid. The modification would increase by about 22 percent the size of the portion of the lid that limits the ribbon width, thereby potentially increasing the area of single-crystal silicon ribbon and the productivity of the furnace.

The modification consists of adding cross slots at the ends of the middle slot through which the ribbon is pulled. The cross slots would provide openings for cooling at the edges of the web, a function formerly provided in part by two round outboard holes (see figure). The cross slots would also be used for the entry and exit of the laser beam used to sense the melt level. The separate holes for the laser beam are no longer needed, and the middle slot can therefore be elongated to occupy a greater portion of the width of the crucible.

The concept has been demonstrated with a lid and shield having cross slots at the end of a middle slot of standard length. The demonstration showed that ribbon growth was equivalent to that for the middle slot with circular holes at its ends. Thus, it appears feasible to lengthen the middle slot to accommodate a wider ribbon.

This work was done by C. S. Duncan and P. A. Piotrowski of Westinghouse Electric Corp. for **NASA's Jet Propulsion Laboratory**. *For further information, Circle 33 on TSP Request Card.*
NPO-17054

In a **Demonstration Model of the New Lid**, cross slots were added to the ends of the middle slot through which the silicon ribbon passes as it is pulled from the melt. The hole at left is replenishing the melt. In the proposed version of the lid, the holes for the laser beam would be eliminated, and the middle slot and cross slots could then be extended almost to the edges of the lid.

Modified Withdrawal Slot Increases Silicon Production

A new shape reduces ribbon breakage and resulting idle time.

NASA's Jet Propulsion Laboratory, Pasadena, California

A new shape for the slot through which single-crystal silicon ribbon is pulled from a melt increases productivity. Previously, the slot in the furnace lid widened into circular notches at its ends. In the redesigned lid, the end notches are triangular rather than circular (see figure).

The new shape reduces the tendency of the emerging ribbon to grow too thin and break. Such thinning is apparently connected with the degradation of crystalline quality in the vicinities of the dendrites at the edges of the ribbon. When the ribbon breaks, a new one must be started — a time-consuming operation that reduces productivity. The triangular notches increase the loss of heat from the liquid/solid interface in the previously thinned region, so that the ribbon grows with more nearly uniform thickness.

Whereas the weekly production rate per furnace was previously about 40,000 cm^2 of ribbon, it is now 47,000 cm^2 — a 17.5-percent boost. The number of restarts dropped from 50 to 30 per week. Moreover, a 17-m-long ribbon was grown — a new record for a single pull.

The new slot configuration makes it easier to grow ribbons of greater width while maintaining uniform thickness. The first version of the triangular slot was used to grow ribbons 4 cm wide. Another version yielded a ribbon 5.5 cm wide, so that productivity was further increased.

This work was done by P. A. Piotrowsky and C. S. Duncan of Westinghouse Electric Corp. for **NASA's Jet Propulsion Laboratory**. *For further information, Circle 62 on the TSP Request Card.*
NPO-17055

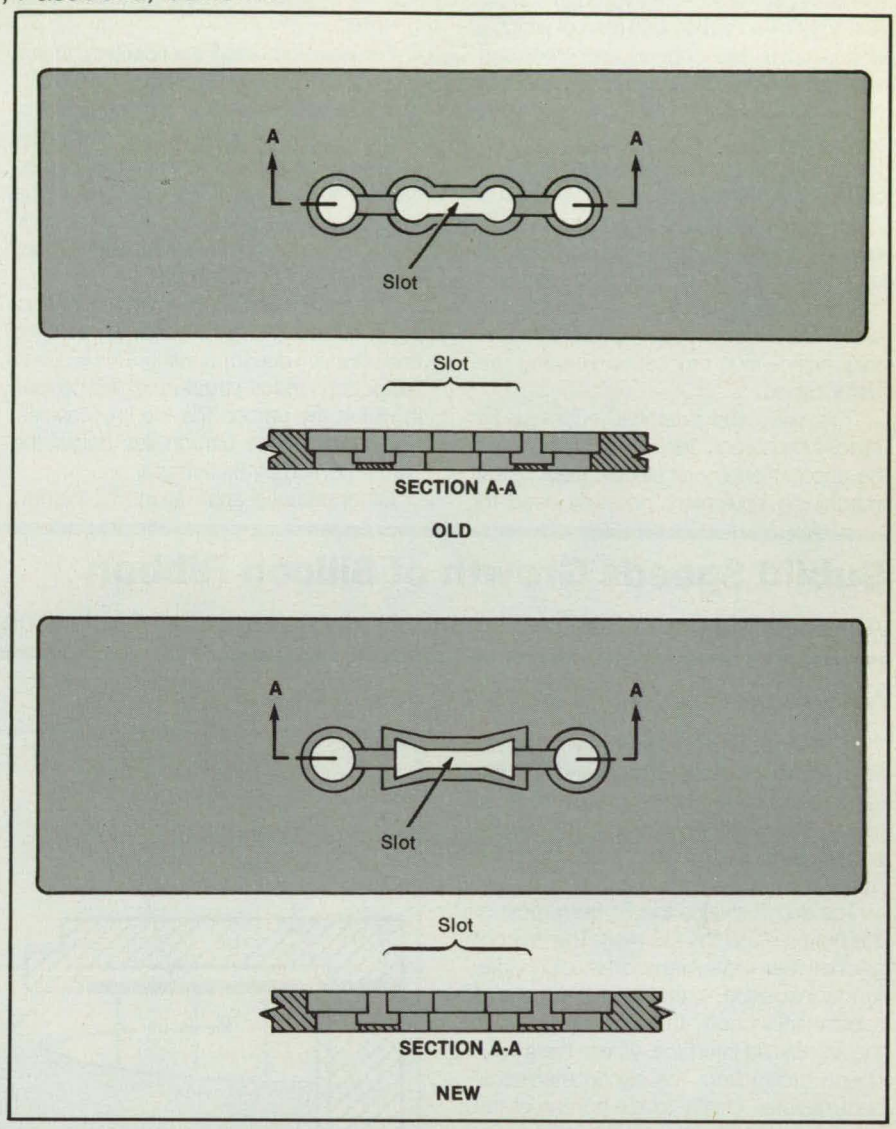

The **Bow-Tie-Shaped Slot** replaces the dumbbell-shaped slot in the lid over the silicon-growing crucible. The new slot cools the liquid/solid interface in a pattern that produces a ribbon with fewer defects.

Carbon Coating of Copper by Arc-Discharge Pyrolysis

An adherent, abrasion-resistant coat is deposited with existing equipment.

Lewis Research Center, Cleveland, Ohio

Carbon is a material that has an intrinsic ability to suppress the emission of secondary electrons and to reduce reflections of primary electrons. Such electron-beam devices as multistage depressed collectors have electrodes that are commonly made of copper, a material that has secondary emission much higher than that of carbon. If a practical method can be found to apply an adherent carbon coating on such copper electrodes, the overall efficiencies of microwave traveling-wave-tube amplifiers with multistage depressed collectors can be increased by approximately 10 percent. Since carbon is also very efficient in absorbing and emitting radiant energy, there also may be thermal applications for such carbon-coated copper.

Carbon can be formed and deposited as a coating on a copper substrate by the pyrolysis of hydrocarbon oil in electrical-arc discharges. The following description is a simplified explanation of the process: The workpiece, which is the copper material to be coated with carbon, serves as the anode. A carbon cathode shaped to the same contours as those of the workpiece is placed in close proximity to the workpiece to provide the necessary spark gap. Both electrodes are submerged in a dielectric oil, which fills the spark gap. Repetitive pulses of sufficient voltage to cause dielectric breakdown of the oil are applied at a

rate of about 10,000/s.

The intensity of the arc energy released in the dielectric breakdown causes localized heating of the oil to temperatures believed to be in the range of 15,000 to 20,000 °F (8,000 to 11,000 °C). As a result, the oil is pyrolyzed. The byproducts of the decomposition are carbon (part of which is deposited on the copper) and other substances, including hydrogen and gaseous hydrocarbons. The electrical discharge also superficially melts the copper and forms a lightly eroded or pitted surface that serves the useful function of anchoring or firmly holding the deposited carbon. The copper is subjected to localized heating only in the vicinity of the arc discharges. The entire copper workpiece may get warm but is not likely to reach a temperature high enough to cause warping and deformation.

This easy and practical technique for producing carbon deposits on copper can be accomplished with electrical-discharge-machining equipment normally used for cutting metals. However, for the generation of a carbon coating, the operating parameters must be changed and optimized to deposit an adherent carbon film while removing the least amount of the copper. Excluding the setup time, a typical copper electrode can be coated in a few minutes.

For electron-beam applications, which require extreme cleanliness, high-purity carbon electrodes and a purified grade of dielectric oil were used in a test of the new coating technique. In addition, the coated hardware was cleaned by repeated rinsing in an ultrasonically agitated bath of solvent, then purified and degassed at 550 °C in an ultra-high-vacuum chamber.

The carbon film adheres well to the copper substrate and resists ordinary scuffing and abrasion due to handling. This is due to the pitted surface structure of the copper, in which the carbon fills the tiny cavities, and much of the carbon lies below the planar portion of the surface.

Other potential applications for the new coating technique include the following: solar-energy-collecting devices, the coating of metals other than copper with carbon, and the carburization of metal surfaces. In addition, the concentrated energy of the arc might be used in combination with a suitable catalyst to bring about not only decomposition but also chemical changes to various inorganic and organic compounds. Applications may be found for the manufacture of unusual chemicals or for the detoxification of dangerous chemicals by the production of temperatures not reachable by ordinary means.

This work was done by Ben T. Ebihara and Stanley Jopek of **Lewis Research Center**. *No further documentation is available.*

This invention is owned by NASA, and a patent application has been filed. Inquiries concerning nonexclusive or exclusive license for its commercial development should be addressed to the Patent Counsel, Lewis Research Center [see page 12]. Refer to LEW-14454.

Sublid Speeds Growth of Silicon Ribbon

A heat shield permits enhancement of exit cooling without formation of unwanted crystals.

NASA's Jet Propulsion Laboratory, Pasadena, California

A thermal barrier between the molten silicon and the lid of a susceptor and crucible (see figure) allows a solidifying ribbon of silicon to be withdrawn faster. The barrier, or sublid, thus increases the production rate.

The sublid shields the lid from most of the heat radiated by the melt. The layer of gas between the sublid and the lid provides further insulation, so that the lid can be kept substantially cooler than the sublid. Near the liquid/solid interface, where the silicon ribbon grows from the silicon meniscus, heat radiates chiefly to the portion of the relatively cool lid in the vicinity of the slot. The silicon at the interface thus loses heat faster, solidifies faster, and can be withdrawn as ribbon faster. Moreover, the speed increase does not introduce excessive thermal stress in the solidified material.

Because the sublid still provides a hot environment for the melt, it does not allow spontaneously frozen silicon crystallites to form in the melt. Such crystallites can interfere with ribbon growth, and thereby inhibit production, if the melt is exposed to a relatively cool lid without an intervening thermal barrier.

In one experimental system, the growth speed of a ribbon of 100- to 125-μm thickness is increased from 1.6 cm/min without the sublid to 2.3 cm/min with the sublid. At the current maximum practical ribbon width of about 6 cm, the increase in growth speed yields 13.8 cm^2 of ribbon per minute — within 12- to 15-cm^2/min throughput required to establish commercial feasibility of the dendritic-web growth process. By increasing the growth rate, the sublid circumvents the formidable problems of increasing the ribbon width to increase production.

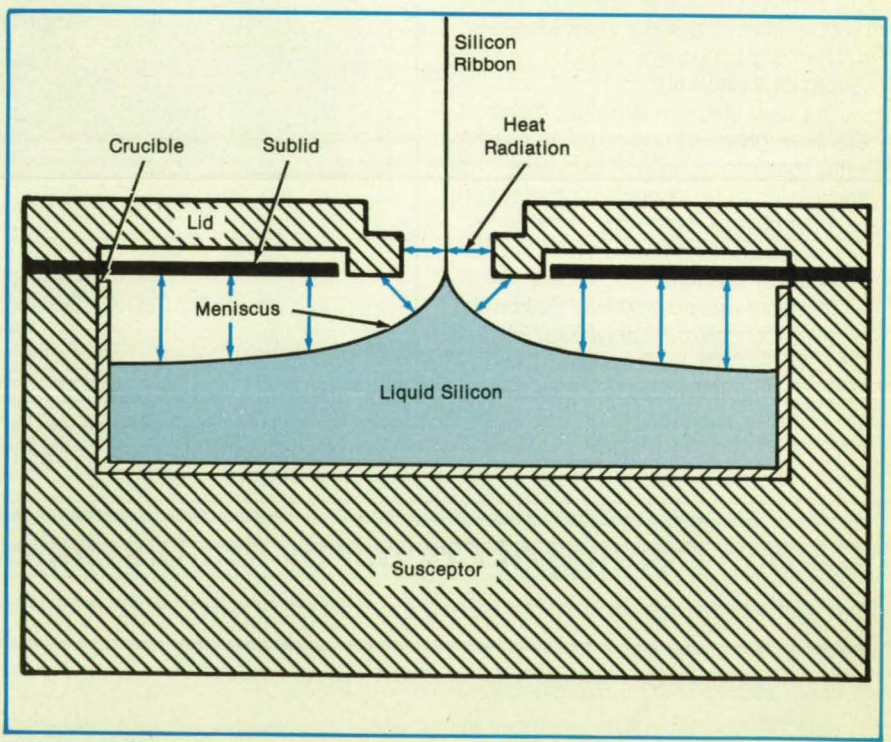

A **Ribbon of Silicon** is pulled from the melt through a slot in the susceptor lid. Heat from the solidifying silicon at the meniscus is absorbed by the lid more rapidly than by the hotter sublid.

This work was done by R. G. Seidensticker and J. P. McHugh of Westinghouse Electric Corp. for **NASA's Jet Propulsion Laboratory**. *For further information, Circle 35 on the TSP Request Card.*
NPO-17056

New on the Market

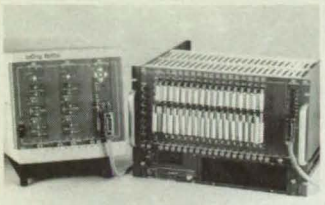

LeCroy Corp., Chestnut Ridge, NY, has introduced a high performance line of automated single channel **waveform digitizers,** called the Century™ Series. The new digitizing systems offer extended memory-length waveform recording, high resolution transient capture, digital signal processing and analysis, and total program mobility. A modular design allows for channel expansion. Additional channels can either operate independently, with different timebase and trigger setups, or can be synchronized for simultaneous multi-channel capture.
Circle Reader Action Number 786.

A new digital plotter from RDK, Inc., Austin, TX, features four pen capability for precision plotting of B, C, and D size drawings. The Model RY-5214 offers plotting velocity up to 400mm/second using standard ceramic or ball-point pens. Seven programmable settings allow pen pressure adjustment from 10 to 180g.
Circle Reader Action Number 796.

Project management tasks are made easier with the VIS1ONmicro PC **software package**, marketed by Systonetics, Fullerton, CA. VIS1ONmicro displays a project as a time scaled network of activities, dependencies, events, lags, and hammocks. During the planning stages, the network can be sketched on the screen and then modified with simple movements of the mouse-controlled cursor. Pop-up menus offering CUT/PASTE, COPY/PASTE or MOVE/PASTE options allow project elements to be moved and connected. These changes are immediately reflected on the screen. VIS1ONmicro also features a one-touch zoom control for more detailed activity information.
Circle Reader Action Number 778.

A new eight page brochure from Teledyne Taber, North Tonawanda, NY, describes a variety of applications for the company's line of **pressure transducers and transmitters.** Major features and specifications are highlighted for 25 standard models. The brochure also reviews the transducer production process, from research and development through engineering and assembly.
Circle Reader Action Number 798.

A four-color brochure from Watlow Electric, St. Louis, MO, illustrates the advantages of the FIREBAR™ **heating element** over tubular heating methods. Detailed are the FIREBAR element's higher watt density, longer heat life, lower sheath temperature, greater buoyancy force and faster response time. The eight page brochure also contains a breakdown of the FIREBAR element's construction materials and marketing advantages.
Circle Reader Action Number 788.

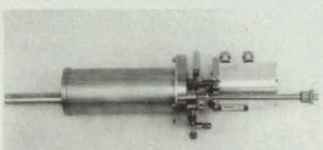

The Superconductor Characterization Cryostat (SCC) manufactured by APD Cryogenics Inc., Allentown, PA, provides a cryogenic atmosphere for **testing high-temperature superconductors.** Applications include basic material characterizations, superconducting electronic studies, and power applications studies. The SCC features an operating range of 12K to 350K. Cryogenic liquids or operator experience with cryogenics are not required.
Circle Reader Action Number 784.

RR Software Inc., Madison, WI, has released a **videotape series** featuring Geoff Gilpin, an Ada author, teaching Ada programming. The ten hour series is offered alone or with the Janus/Ada "JET SET" package, which includes an **Ada compiler**, linker, and tutorial. RR Software is the first Ada vendor to offer validated compilers for all current Intel 80X86/MS DOS computers.
Circle Reader Action Number 782.

The Logic Analyzer Division of Tektronix, Inc. (Beaverton, OR) has introduced the DAS 9200 Personal ASIC Verification System, a **benchtop tester** for "first silicon" prototypes. The system offers data conversion packages for popular simulators, automative setup and interactive menu-driven display, and reliable test fixturing at 50 MHz. Simple tester resource allocation and mapping of simulator signal names to tester resources can be accomplished in just a few key strokes. Tests are programmed on a simple run control screen via menu selections, thereby eliminating the need for a test language. Interchangeable device adaptor cards optimize setup times for testing other parts.
Circle Reader Action Number 776.

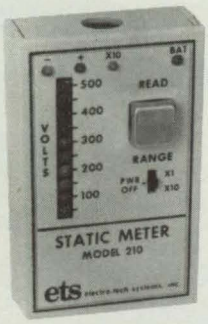

The Model 210 **Electrostatic Field Meter** from Electro-Tech Systems Inc., Glenside, PA, accurately measures the magnitude and polarity of any electrostatic field. The noncontacting, hand-held meter utilizes a four color array of light emitting diodes for high resolution and easy measurement reading. 500 or 5000 volt ranges are selected at a flip of the unit's range selector switch.
Circle Reader Action Number 794.

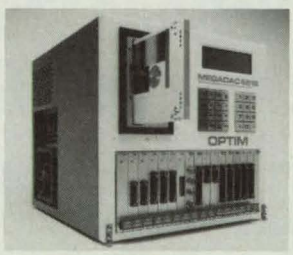

The MEGADAC 6516, the first portable **data acquisition system** using laser disk technology for its on-line mass storage, is now available from Optim Electronics Corp., Germantown, MD. In addition to its 400 megabyte laser storage capacity, the system offers 128 channels of differential inputs, four simultaneous scanning rates, and 250,000 samples-per-second scanning. Using data input levels to trigger recording, the 6516 captures only data pertinent to the experiment, significantly reducing subsequent data reduction and analysis tasking.
Circle Reader Action 792.

The Night Hawk family of **supermicrocomputer systems,** developed by Harris Computer Systems Division, Ft. Lauderdale, FL, are the first systems that combine advanced microprocessor technology, high-performance multiprocessing, and a real-time Ada environment. Designed for trainers and simulators, the Night Hawk computers feature up to eight tightly-coupled MC68030 CPUs (each rated at six million instructions per second) in a single cabinet, context switch times of less than 60 microseconds, and interrupt response times of less than five microseconds. The Harris Ada compiler, validated by the U.S. Department of Defense, is being cross-targeted to the Night Hawk systems.
Circle Reader Action Number 790.

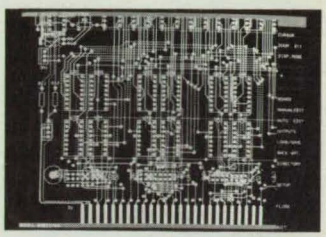

Visionics Corporation, Sunnyvale, CA, has introduced the EE Designer III, a new **CAE/CAD integrated software package** for end-to-end circuit design, simulation, PCB layout, and circuit board fabrication. EE Designer III accomodates up to two megabytes of above-board memory using the Lotus/Intel/Microsoft specification, and offers 1284 x 960 graphics resolution (with Visionics' graphics board) for workstation performance on a PC hardware platform. Full simulation capability provides for both analog and digital circuitry.
Circle Reader Action Number 800.

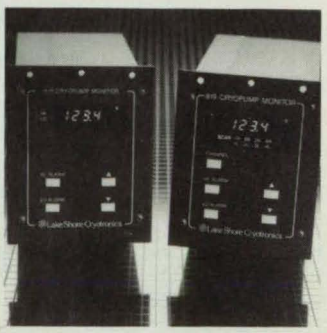

Two new **cryopump monitors** from Lake Shore Cryotronics, Westerville, OH, provide continuous monitoring of cryopump operating temperatures from 4K to 475K. The Models 818 (single-channel) and 819 (four-channel) monitors offer four-digit temperature display in K, °C, °F, or sensor voltage. Multiple standard sensor response curves are stored in each unit and can be independently assigned to any input channel. Input range is 0 to 3 volts with a resolution of 0.1 millivolts.
Circle Reader Action Number 780.

Subject Index

Advertiser's Index

*RAC stands for **Reader Action Card.** For further information on these advertisers, please circle the RAC number on the Reader Action Card elsewhere in this issue. This index has been compiled as a service to our readers and advertisers. Every precaution is taken to ensure its accuracy, but the publisher assumes no liability for errors or omissions.

NASA Tech Briefs, ISSN 0145-319X, USPS 750-070, copyright © 1988 in U.S., is published monthly except July/August and November/December (10x per year) by Associated Business Publications Co., Ltd. 41 E. 42nd St., New York, NY 10017-5391. The copyrighted information does not include the individual Tech Briefs which are supplied by NASA. Editorial, sales, production and circulation offices at 41 E. 42nd Street, New York, NY 10017-5391. Subscriptions for non-qualified subscribers in the U.S., Panama Canal Zone, and Puerto Rico, $75.00 for 1 year; $125.00 for 2 years; $200 for 3 years. Single copies $15.00. Remit by check, draft, postal or express orders. Other remittances at sender's risk. Address all communications for subscriptions or circulation to NASA Tech Briefs, 41 E. 42nd Street, New York, NY 10017-5391. Second-class postage paid at New York, NY and additional mailing offices.

POSTMASTER: please send address changes to NASA Tech Briefs, 41 E. 42nd Street, Suite 921, New York, NY 10017-5391.

Grumman's best-designed aircraft are tested by Gould's best-designed recorders.

Flight testing is the most critical method by which Grumman Aircraft Systems evaluates tactical aircraft designs for both its planes and those from other aerospace companies. So, when Grumman puts these jets through series of strenuous test points, a recording system they rely on is from Gould.

Gould's 3000 Series programmable recorders permit Grumman flight test engineers to make real-time analysis of critical flight parameters with split-second timing. This allows decisions to be made that increase the productivity and safety of each test flight.

That's because Grumman's ATS (Automated Telemetry System) controls each Gould 3000 recorder with an entire series of planned test points for a specific flight. This way, while the plane and its pilot are in the air, everything is automatic. It allows the test engineers to get answers quickly, reducing both hazardous and costly flight time.

"The programmability of the Gould 3000 recorder provides greater productivity in a number of ways," says Tom Kastner, Grumman corporate manager of automated telemetry. "First, it allows faster, easier test setup with computer control of all parameter settings. "Second, it allows us to tie more resources together on-line. And, third, we can make fast changes to meet modifications in the flight plan. We're now able to make accurate value judgments and technical decisions to continue with our established flight plan or to modify it," concludes Kastner.

With the Gould 3000 recorder, Grumman has been able to expand its flight testing capabilities, speed development and delivery of aircraft, and reduce test costs. When Grumman relies on Gould to help them make a better airplane, it's not just a flight of fancy.

To get more information on this application or on the Gould 3000 Series recorders, call **1-800-GOULD-10**, or write Gould Inc., Test and Measurement, 3631 Perkins Avenue, Cleveland, OH 44114.

Gould: making its mark in Test and Measurement Instrumentation.

GOULD
Electronics

Circle Reader Action No. 486

THE X-30 IS KID STUFF.

To soar with ease on swift, strong wings—farther, higher and faster than ever before. For a kid, that's the stuff dreams are made of.

Kid stuff, because it's your kids, and ours, who will benefit most from the advances in computational fluid dynamics required to build the X-30 National AeroSpace Plane (NASP).

With supercomputers, we're simulating the effects of air pressure, speed and heat on proposed X-30 airframes. This wind-tunnel-in-a-computer technology allows us to test-fly numerous airfoil shapes and configurations—rapidly, and without building models.

The X-30 is kid stuff, because it is our children who will move from Earth to space and back at far less cost than we do today. And one day fly from Los Angeles to Tokyo in two hours aboard an Orient Express.

And it is they who will have—or not have—world leadership in aerospace as a result of our nation's resolve now.

Let's not let them down.

MCDONNELL DOUGLAS

Circle Reader Action No. 501